Practical determination of heat loads for existing deep level gold mines

D Nell

orcid.org / 0000-0002-2817-9343

Thesis accepted in fulfilment of the requirements for the degree *Doctor of Philosophy in Mechanical Engineering* at the North-West University

Promoter: Prof EH Mathews

Graduation: May 2020

Student number: 23351209

ACKNOWLEDGEMENTS

I would like to start by expressing my sincere gratitude to the following people for their support and guidance throughout the completion of my thesis:

- First and foremost, I would like to give thanks to my heavenly Father for the privilege of having the opportunity to pursue post-graduate studies. May all the work done and yet to be pursued be for the glory of Your name. Thank you for your love and undeserving mercy.
- I would like to thank my study leader prof. Eddie Matthews for all the advice and guidance during this study. I have learned a lot throughout this process. Also, thanks to prof. Marius Kleingeld for the unique opportunity of completing my post-graduate studies. Special thanks to Enermanage (Pty) Ltd and its sister companies for the financial support throughout this study.
- A big thank you to my study mentor, Dr Philip Maré, for always being willing to listen and assist. I have learned and immense amount from you as an engineer as well as a person. Thanks for the role model you were during this thesis.
- I would like to thank my family. Thank you for your continuous support and motivation throughout this endeavour. I appreciate the fact that you understood the stringent time schedule accompanying this pursuit. I was truly blessed by such support.
- I would like to thank my friends for their patience and understanding. I look forward in making up for the lost time in the days to come.
- I special thanks for the investment made by industry in my development as an engineer as well as a person. Thank you very much for assisting me with the required information to enable my study and constantly challenging me as an engineer.
- I would also like to thank my co-workers for their valued inputs and time, especially Dr. Deon Arndt. I appreciate your willingness to always hear my view on a matter and share your much-valued experience.
- Finally, I would like to give a special thanks to my wife, Dr. Kristy Nell. Your support throughout this process was unparallel. For all you have assisted me with, a thank you seems so small. I would not have been able to complete this study without your love, support and understanding.

ABSTRACT

Title: Practical determination of heat loads for existing deep-level gold mines

Author: D. Nell

Promotor: Prof. E.H. Mathews

Degree: Doctor of Philosophy in Engineering (Mechanical)

Keywords: Deep-level gold mines, heat load, energy balance

Deep-level gold mines in South Africa (SA) are faced with immense challenges regarding profitability. Optimising these mines is a pivotal step to prolong the current lifespan of the gold-mining sector in SA. As these mines constantly reach new depths, the challenge of increased working temperatures arises as a result of the geothermal gradient. Excessive heat exposure leads to production loss, directly reducing the industry's profit margins. To ensure that adequate cooling is supplied, with the aim of reducing production losses, heat load studies are conducted.

Various approaches have been developed over the past seven decades to assist in determining the actual heat load of a mine. Most of these methods were developed to assist mines during their initial planning phase. Many of these approaches consist of empirical data sets developed in the late 1980s. However, deep-level gold mines are constantly changing, and over the past two decades, have reached record depths and have also seen an increase in mine mechanisation.

This study focuses on developing a new approach to determine mine heat loads by using an energy balance. This approach aims to determine all the various heat sinks, heat sources and the geothermal heat source from an energy balance.

Two case studies were evaluated using this energy balance approach through simulation and compared to well-known heat-prediction graphs commonly used by industry. From these studies, it was shown that in mines not adhering to the typical mine layout and mining strategy, as was used for developing these heat-prediction graphs, large errors can be made when determining heat loads through using such approaches. Alternatively, it was proven that the energy balance approach can easily be applied to various cases studies.

Focus was also placed on the industry application of such an energy balance approach through evaluating an Industry 4.0 roll-out strategy. This strategy is aimed at evaluating the dynamic nature of mine heat loads with greater accuracy and increased frequency. This has also led to the SAJIE publication titled *"Industry 4.0 roll-out strategy for dynamic mine heat load management"*.

TABLE OF CONTENTS

ACKNOWLEDGEMENTS ..... **I**

ABSTRACT ..... **II**

TABLE OF CONTENTS ..... **III**

LIST OF FIGURES ..... **V**

LIST OF TABLES ..... **VII**

LIST OF EQUATIONS ..... **IX**

NOMENCLATURE ..... **X**

STUDY OUTLINE ..... **XIII**

1. INTRODUCTION TO MINE HEAT LOADS **2**

1.1. Background 2

1.2. Deep-level mine heat loads 5

1.3. Problem statement 11

1.4. Novel contributions 12

1.5. Conclusion 15

2. A NEW METHOD TO DETERMINE MINE HEAT LOADS **17**

2.1. Preamble 17

2.2. Energy balances 17

2.3. Heat load component review 20

2.4. Conclusion 38

3. RESULTS AND DISCUSSIONS **41**

3.1. Preamble 41

3.2. Case study 1: Mine A 41

3.3. Case study 2: Mine B 61

3.4. Conclusion 70

4. INDUSTRY APPLICATION **72**

4.1. Preamble 72

4.2. Methodology 73

4.3. Results and discussion 78

4.4. Conclusion 80

5. CONCLUSIONS AND RECOMMENDATIONS 82

5.1. Summary 82

5.2. Novel contributions 82

5.3. Recommendations for future work 83

5.4. Final conclusion 84

BIBLIOGRAPHY 85

APPENDIX A CRITICAL LITERATURE STUDY 92

APPENDIX B HEAT PRODUCTION GRAPHS 97

APPENDIX C INPUTS FOR ENERGY BALANCE APPROACH 100

APPENDIX D MODELLING FUNDAMANETALS 102

APPENDIX E CALCULATED ENERGY BALANCE RESULTS 105

APPENDIX F SAJIE PUBLICATION 107

APPENDIX G PROCESS TOOLBOX 117

APPENDIX H SENSITIVITY ANALYSIS 120

LIST OF FIGURES

Figure 1-1: Global gold reserves....2
Figure 1-2: Historical gold production [6]....2
Figure 1-3: Number of heat exhaustion cases by month [15]....3
Figure 1-4: Percentage exposure to thermal stress/heat per regional classification [20]....4
Figure 1-5: Heat load source breakdown of previous studies....6
Figure 1-6: Chronological critical literature review of heat load calculation (A) 7
Figure 1-7: Chronological critical literature review of heat load calculation (B)....8
Figure 2-1: Energy sources in mines 17
Figure 2-2: Heat load calculation methodology....19
Figure 2-3: Mine boundary definition....20
Figure 2-4: Summary of heat-sink calculation steps in deep-level mines 21
Figure 2-5: Air-cooling power (ACP) approach....22
Figure 2-6: Major components of a vapour compression cycle [14] 23
Figure 2-7: Secondary cooling evaluation scenarios 24
Figure 2-8: Combined water balance....25
Figure 2-9: Heat sources summary 27
Figure 2-10: Potential gain of multiple water streams pumped to the surface 29
Figure 2-11: Excluded electrical consumers....30
Figure 2-12: Fissure water source illustration 33
Figure 2-13: Detailed heat load calculation methodology....39
Figure 3-1: Mine A orebody layout 41
Figure 3-2: Mine A layout (Process toolbox) 43
Figure 3-3: Mine A simplified boundary side view layout....45
Figure 3-4: Heat load graph of Mine A 53
Figure 3-5: Screenshot of a portion of the discretised model (Case study 1)....55

Figure 3-6: Underground seasonal effect at refrigeration complex (Case study 1) 58
Figure 3-7: Required versus actual refrigeration demand (Case study 1) 59
Figure 3-8: Mine B model layout (Process toolbox) 61
Figure 3-9: Mine B simplified boundary side view layout 62
Figure 3-10: Heat load graph of Mine B 65
Figure 3-11: Screenshot of a portion of the discretised model (Case study 2) 67
Figure 3-12: Secondary cooling required at Mine B 68
Figure 4-1: DIKW Model [62, 63] 72
Figure 4-2: Basic mine ventilation flow diagram [14] 73
Figure 4-3: Detailed heat load calculation methodology 76
Figure 4-4: Dynamic heat load – Current conditions 78
Figure 4-5: Dynamic heat load breakdown 79
Figure 4-6: Dynamic surface fan system characteristic curve 79
Figure B-1: Heat flow rate prediction in the Free State gold mines [23] 97
Figure B-2: Extrapolated heat production graph 98
Figure B-3: Method for estimating refrigeration requirements [23] 99
Figure G-1: PTB 3D Graphical User Interface 117
Figure G-2: PTB heat transfer solver schematic 119
Figure H-1: Case study 1 sensitivity analysis 120
Figure H-2: Case study 2 sensitivity analysis 120

LIST OF TABLES

Table 1-1: Legal thermal stress limits [16] 4
Table 1-2: Literature review criteria 9
Table 1-3: Critical literature study summary 10
Table 2-1: Auto-compression air mass flow distribution impact 28
Table 2-2: Metabolic heat rate per activity [25, 34, 48, 49] 35
Table 2-3: Computer model ventilation software evaluation 37
Table 3-1: Air-cooling power (Case study 1) 46
Table 3-2: Secondary cooling (Case study 1) 47
Table 3-3: Summary of heat sinks (Case study 1) 47
Table 3-4: Auto-compression (Case study 1) 48
Table 3-5: Potential gain from electrical equipment (Case study 1) 49
Table 3-6: Equipment to be excluded from effective electrical heat load (Case study 1) 49
Table 3-7: Effective electrical heat load (Case study 1) 50
Table 3-8: Potential gain from mechanised equipment (Case study 1) 50
Table 3-9: Mechanised heat load (Case study 1) 51
Table 3-10: Diesel machinery utilisation breakdown (Case study 1) 51
Table 3-11: Effective mechanised heat load (Case study 1) 52
Table 3-12: Metabolic heat rate (Case study 1) 52
Table 3-13: Explosives heat load (Case study 1) 52
Table 3-14: Geothermal heat load balance 53
Table 3-15: Industry approach results (Case study 1) 54
Table 3-16: Rock properties used for simulation [14, 34, 56, 57] 55
Table 3-17: Simulation results (Case study 1) 56
Table 3-18: Cooling shortage/surplus (Case study 1) 57
Table 3-19: Monthly ambient seasonal weather conditions (@ 86.5 kPa) 57

Table 3-20: Energy cost comparison – Required vs achieved cooling (Case study 1) 59
Table 3-21: Case study 1 results summary 60
Table 3-22: Air-cooling power (Case study 2) 63
Table 3-23: Secondary cooling (Case study 2) 63
Table 3-24: Summary of heat sinks (Case study 2) 64
Table 3-25: Fissure water (Case study 2) 64
Table 3-26: Summary of heat sources (Case study 2) 64
Table 3-27: Geothermal heat load balance (Case study 2) 65
Table 3-28: Industry approach results (Case study 2) 66
Table 3-29: Simulation results (Case study 2) 67
Table 3-30: Energy cost comparison - Required vs achieved cooling (Case study 2) 68
Table 3-31: Case study 2 results summary 69
Table 4-1: Data acquisition detail level 74
Table A-1: Comprehensive literature review 92
Table C-1: Energy balance heat load approach input parameters 100
Table E-1: Auto-compression (Case study 2) 105
Table E-2: Potential gain from electrical equipment (Case study 2) 105
Table E-3: Equipment to be excluded from effective electrical heat load (Case study 2) 105
Table E-4: Effective electrical heat load (Case study 2) 106
Table E-5: Mechanised heat load (Case study 2) 106
Table E-6: Metabolic heat rate (Case study 2) 106
Table E-7: Explosives heat load (Case study 2) 106
Table E-8: Rock properties used for simulation [14, 56, 57] 106
Table G-1: Process ToolBox (PTB) - Available components 119

LIST OF EQUATIONS

Equation 2-1: Steady flow energy equation [14] 17
Equation 2-2: Combined air mass flow-weighted enthalpy 21
Equation 2-3: Air-cooling power [34] 22
Equation 2-4: Induced cooling through surface BAC 24
Equation 2-5: Induced cooling through underground refrigeration 25
Equation 2-6: Flow-weighted water inlet temperature 26
Equation 2-7: Cooling duty of liquid water [14] 26
Equation 2-8: Total heat sinks [14, 23] 26
Equation 2-9: Adiabatic 'pure' auto-compression [14, 34] 27
Equation 2-10: Auto-compression [14, 34] 28
Equation 2-11: Potential energy [14] 29
Equation 2-12: Effective electrical heat load 30
Equation 2-13: Mechanised heat [14] 31
Equation 2-14: Ratio of water produced per fuel consumed [14] 32
Equation 2-15: Mechanised heat (latent) [14] 32
Equation 2-16: Mechanised heat (sensible) 32
Equation 2-17: Effective mechanised heat load 32
Equation 2-18: Steady flow energy equation for compressed air nett heat/cooling [14] 34
Equation 2-19: Metabolic heat load [14] 35
Equation 2-20: Explosive heat load [14] 36
Equation 2-21: Geothermal heat load balance 37
Equation 2-22: Cooling shortage 38

NOMENCLATURE

Abbreviations

Abbreviation	Description
ACP	*Air-cooling power*
BAC	*Bulk air cooler*
BTUs	*British thermal unit*
COP	*Coefficient of power*
CV	*Calorific value*
DIKW	*Data-information-knowledge-wisdom*
KPI	*Key performance indicator*
P.E.	*Potential energy*
RAW	*Return airway*
SA	*South Africa*
SCADA	*Supervisory control and data acquisition*
VRT	*Virgin rock temperature*

List of symbols

Symbol	Description	*Units*
ACP	Air-cooling power	*kW*
C_p	Specific heat of water	*J/kg°C*
C_p	Specific heat of air	*J/kg°C*
CV	Calorific value of diesel	*kJ/l*
dP	Pressure	*kPa*
EHL	Explosive heat load	*W*
F	Frictional force	*N*
g	Gravitational acceleration	m/s^2
g	Gravitational constant	m/s^2
h	Enthalpy	*J/kg*
H	Height	*m*
H.P	Heat produced by the explosive type	*kJ/kg*
h_{comp}	Enthalpy of compressed air	*J/kg*
h_{vent}	Enthalpy of ambient air	*J/kg*

L_V	Latent heat of evaporation of water	*kJ/kg*
$\dot{m}$	Mass flow	*kg/s*
$\dot{m}_{comp}$	Mass flow of compressed air	*kg/s*
MHL	Metabolic heat load	*W*
MHR	Metabolic heat rate p.p.	*W*
N.E.	Number of employees	-
η_{Com}	Combustion efficiency	*%*
Θ_1	Compressed air inlet temperature	*kPa*
Θ_2	Compressed air outlet temperature	*N*
Θ_{amb}	Ambient ventilation air temperature	*N*
P	Barometric pressure	*kPa*
q	Heat transfer/duty	*J/kg*
R.P.	Release period	*s*
RH	Relative humidity	*%*
T_{db}	Dry-bulb temperature	*°C*
T_{wb}	Wet-bulb temperature	*°C*
T_{in}	Inlet temperature	*°C*
T_{out}	Outlet temperature	*°C*
u	Velocity	*m/s*
V	Specific volume	m^3/kg
VF	Vapour factor	-
w	Mechanical energy (work)	*J/kg*
Z	Elevation	*m*

Glossary

Blasting	Activity concerning setting-off explosive charges
Conventional mining	Typical narrow reef, track bound mining techniques
Cross-cut	Split from the main haulage towards a raise-line
Foot wall	Floor of the mine haulage
Fridge plant complex	Numerous fridge plants grouped together
Geothermal	Refers to the surrounding rock body and related heat from it
Hanging	Roof of a mine haulage
Haulage	Mine tunnel
Hoisting	Activity of extracting (bringing out) ore from the mine to surface
Intake airway	Mine haulage where fresh air flows towards to workings
Level	Mine haulage located at a specific depth below surface
Massive	Refers to wide open cavities blasted
Mean rock breaking depth	Average mining depth
Mechanised mining	Mining technique involving mechanised equipment (trackless)
Ore	Refers to the gold (rock) deposits being mined
Raise-line	Inclined access connecting the cross-cut and the stopes
Re-entry period	Period after blasting during which entry is prohibited.
Reject temperature	Air temperature leaving the working area
Return airway	Mine haulage where return air flow from the workings to surface
Shaft	Vertical access to the respective depth used for travelling/hoisting
Side wall	Sides of a mine haulage
Stope	Working area of a narrow reef mine

STUDY OUTLINE

Chapter 1: Introduction and critical literature review

The first chapter of this study gives context to the heat-related challenges faced by the deep-level gold-mining industry in South Africa. Research conducted with regards to these challenges is explored in more depth through a comprehensive critical literature study. From this study a clear problem is identified and consequently addressed through the novel contributions of this study.

Chapter 2: Development of methodology

During this chapter, a detailed new heat load determination methodology is developed with the aim of addressing the shortcomings identified in Chapter 1. This methodology is thoroughly explained and serves as a road map to address the problem defined in Chapter 1.

Chapter 3: Results and discussions

In Chapter 3 the developed methodology is applied to a number of case studies. Each case study, unique in nature, is readily evaluated using the developed methodology and is also compared to results obtained through applying the typical industry approach, as well as results derived from using simulation models.

Chapter 4: Industry application

Chapter 4 highlights the need to adapt Industry 4.0 technologies in the deep-level gold-mining industry. This chapter highlights the benefits and possibilities to be gained by discussing a roll-out strategy with regards to Industry 4.0 technologies.

Chapter 5: Conclusion

The final chapter of this study concludes the main findings and also serves as a platform for recommendations to be addressed in future studies.

1

CHAPTER 1

Introduction to mine heat loads

"The definition of insanity is doing the same thing over and over again and expecting different results."

Albert Einstein[1]

[1] History, https://www.history.com/news/here-are-6-things-albert-einstein-never-said, [2019/11/10]

1. INTRODUCTION TO MINE HEAT LOADS

1.1. Background

South Africa (SA) is a country well known for the vast number of commodities it holds, specifically precious metals such as gold [1, 2]. This has led to the development of an extensive gold-mining sector from as early on as 1886 and features some of the world's deepest mines and most challenging mining conditions [3]. Figure 1-1 illustrates the top ten countries' gold reserve ranking at a mineable depth.

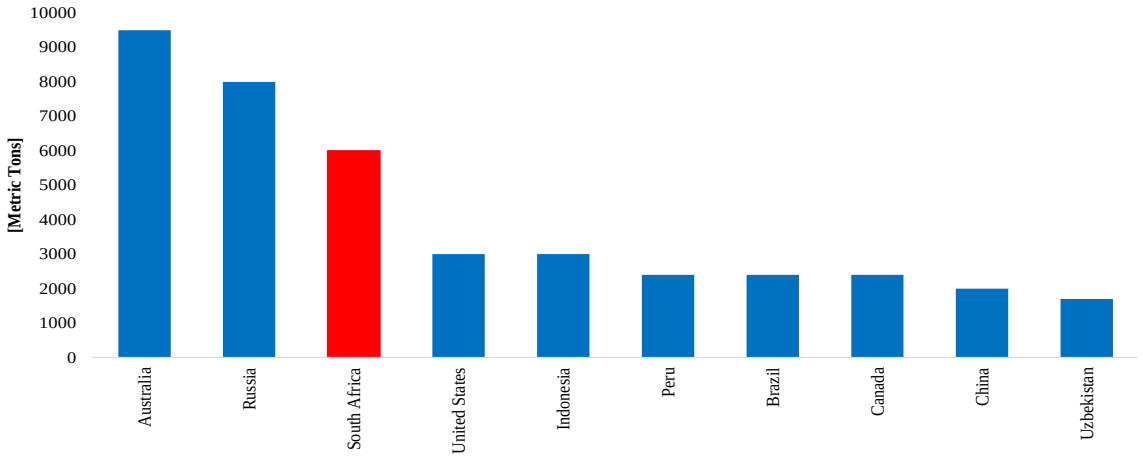

Figure 1-1: Global gold reserves

Figure 1-1 highlights that SA still holds a considerable amount of gold to be mined. To date, the South African gold-mining sector has contributed significantly to the local economy through job creation and exports, amounting to a 7.3% contribution to the country's GDP in 2018 [4]. However, this is an industry under severe pressure [5]. Figure 1-2 illustrates South Africa's gold production in tonnes from 1960 to 2018.

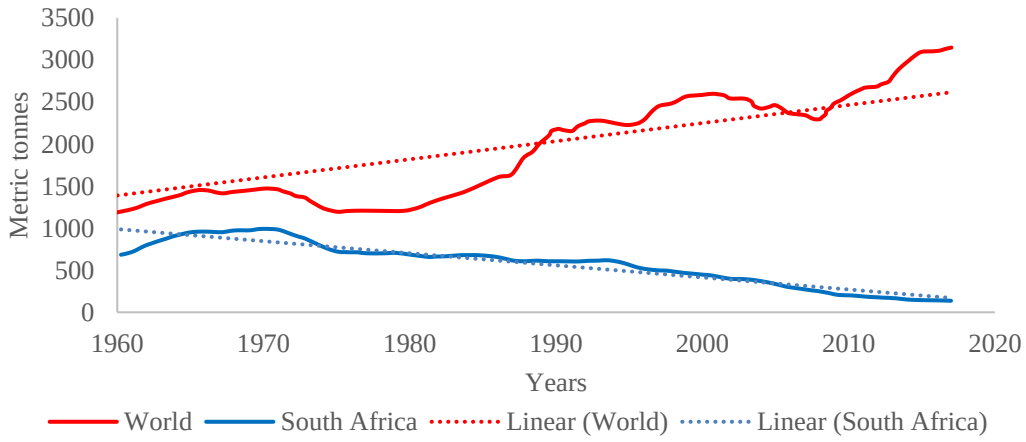

Figure 1-2: Historical gold production [6]

Figure 1-2 shows the declining production trend faced by the South African gold-mining industry. For the financial year of 2017/2018, the local gold-mining industry contracted by as much as 4%, based on market capitalisation [7]. In a recent report released by Stats SA, the gold-mining sector has shown a decline in production for the 19th consecutive month. This decline can be attributed to numerous challenges, ranging from technical to socio-economical, and is further negatively impacted by political instability [8].

One such challenge is that of creating a safe working environment at the extreme depths most established gold mines operate in SA [9]. Even though South African deep-level gold mines are known for a low geothermal gradient (virgin rock temperatures {VRT} increase at increased depth), some of the mines operate beyond depths of 4 km, resulting in excessive heat at the working face, which can lead to heat-related illnesses [3, 10–12].

Heat-related illnesses can be divided between heat exhaustion and heatstroke. Heatstroke is more severe and causes central nervous system dysfunction and, consequently, death [13, 14]. In a study done on 106 cases it was found that there exists a strong correlation between heat-related illness and an increase in mining depth [15]. The study also noted that there is a distinctive seasonal impact on heat-related illness cases. Figure 1-3 shows heat exhaustion cases recorded monthly at Mt Isa mine, Australia to illustrate a typical heat exhaustion distribution. Comparable data was limited for South African mines although a similar distribution is expected.

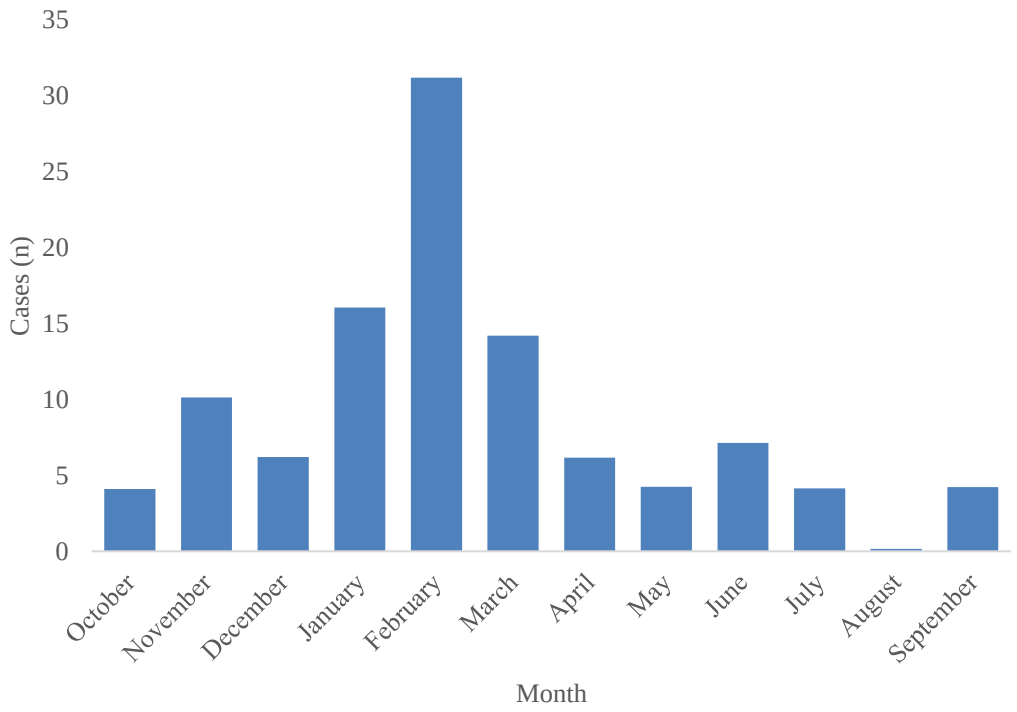

Figure 1-3: Number of heat exhaustion cases by month [15]

In Figure 1-3 an increase in heat exhaustion is evident during the warmer months. As a safety precaution against heat-related illnesses, clear environmental limits have been defined and legally enforced to help prevent such thermal stress conducive environments [16]. Table 1-1 highlights the legal limits for ensuring that an acceptable working environment is maintained in South African deep-level gold mines.

Table 1-1: Legal thermal stress limits [16]

Parameter	Limit
Maximum allowable dry-bulb temperature	37.0℃
Maximum allowable wet-bulb temperature	32.5℃
Maximum allowable mean radiant temperature	37.0℃

There are also various guidelines for when working in high-temperature environments to ensure an acceptable work rate for the given environmental conditions [17–19].

Despite these clear limits, there are still a number of mines struggling to adhere. Figure 1-4 illustrates the thermal stress exposure as a percentage for the various provinces in SA, as was recorded in the annual mining report of 2017/2018 [20].

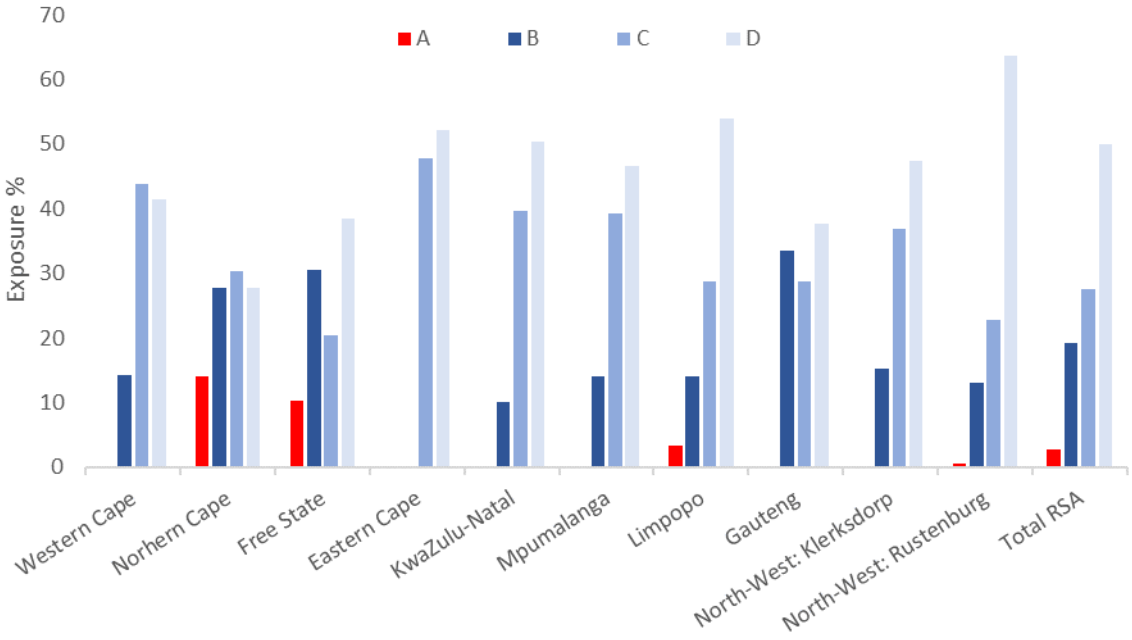

Heat stress exposure classification band:
Range A = WB > 32.5℃ or DB > 37℃ or globe temperature > 37℃
Range B = 29.0℃ < WB ≤ 32.5℃ and DB ≤ 37℃ globe temperature as for dry-bulb
Range C = 27.5℃ < WB ≤ 29.0℃ and DB ≤ 37℃ globe temperature as for dry-bulb
Range D = WB ≤ 27.5℃ and DB ≤ 32.5℃ globe temperature as for dry-bulb

Figure 1-4: Percentage exposure to thermal stress/heat per regional classification [20]

From Figure 1-4, it is clear that several mines across SA are faced with working area temperatures exceeding the legal limits, as set out in Table 1-1. In cases where the working conditions exceed

acceptable environmental ranges, these workings can be stopped under a Section 54 instruction [16]. This leads to a complete standstill of production in the specific working area or even the mine and negatively impacts production [16].

In 2015 it was estimated that these stoppages amounted to R4.84 billion in production losses across the South African mining sector [21]. From practical experience, it was observed that a large portion of these stoppages in deep-level mines are heat-related. Ensuring these working areas comply with the minimum standards are the daily challenges faced by the responsible ventilation engineer.

1.2. Deep-level mine heat loads

To ensure all working areas in a mine are supplied with adequate ventilation and cooling, it is essential to conduct a heat load study [22]. A heat load study focuses on identifying heat sources and accurately quantifying each source [14, 22, 23]. It is important that the cooling supplied is adequate to mitigate these identified heat sources.

Heat load studies are conducted at various phases during the mining life-cycle. These studies serve as a design tool during the initial planning phase of a mine and supply rough estimates for various heat sources [23]. As the mine progresses, these studies are conducted more frequently and in more detail. As a rule of thumb, heat load studies are conducted on a yearly basis, and revised bi-annually, to ensure the planned cooling infrastructure is still sufficient [24].

Today the most common method for estimating mine heat loads consists of heat-prediction graphs. These graphs were developed through more than 30 years of empirical data collected in the 1980s [23]. However, it raises the question of whether these methods are still relevant, especially considering the changes faced by the mining industry, such as unprecedented depths.

One argument is that these heat load prediction methods only serve as a planning tool during the initial phases of a mine's life-cycle. They should therefore not be used as an accurate heat load evaluation tool. The question is whether the safety margins included in the design parameters of these methods should not be more aggressively contended by a marginal industry, such as the gold-mining sector.

Another more substantial argument would be if these methods, which are based on data sets excluding today's mine mechanisation trends, can be used to evaluate heavily mechanised mines. Older mines utilised only a few diesel locomotives, whereas mechanised mines of today can easily exceed a fleet of more than 100 pieces of mechanised machinery.

To better understand these arguments, several methods were reviewed, which range in complexity and approach. South Africa has been celebrated to be one of the leading countries with regards to contributing to this research field [25]. Figure 1-5 illustrates the reference distribution of all studies evaluated, whereas Figure 1-6 and Figure 1-7 shows the studies pertaining to mine heat loads in chronological order, conducted over more than six decades.

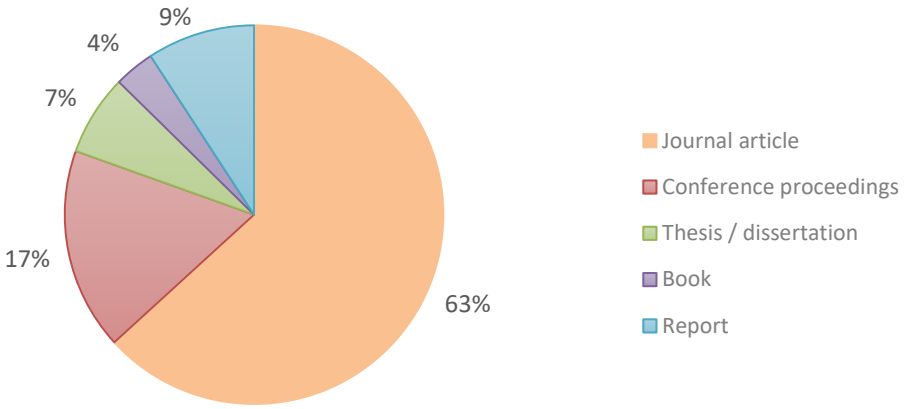

Figure 1-5: Heat load source breakdown of previous studies

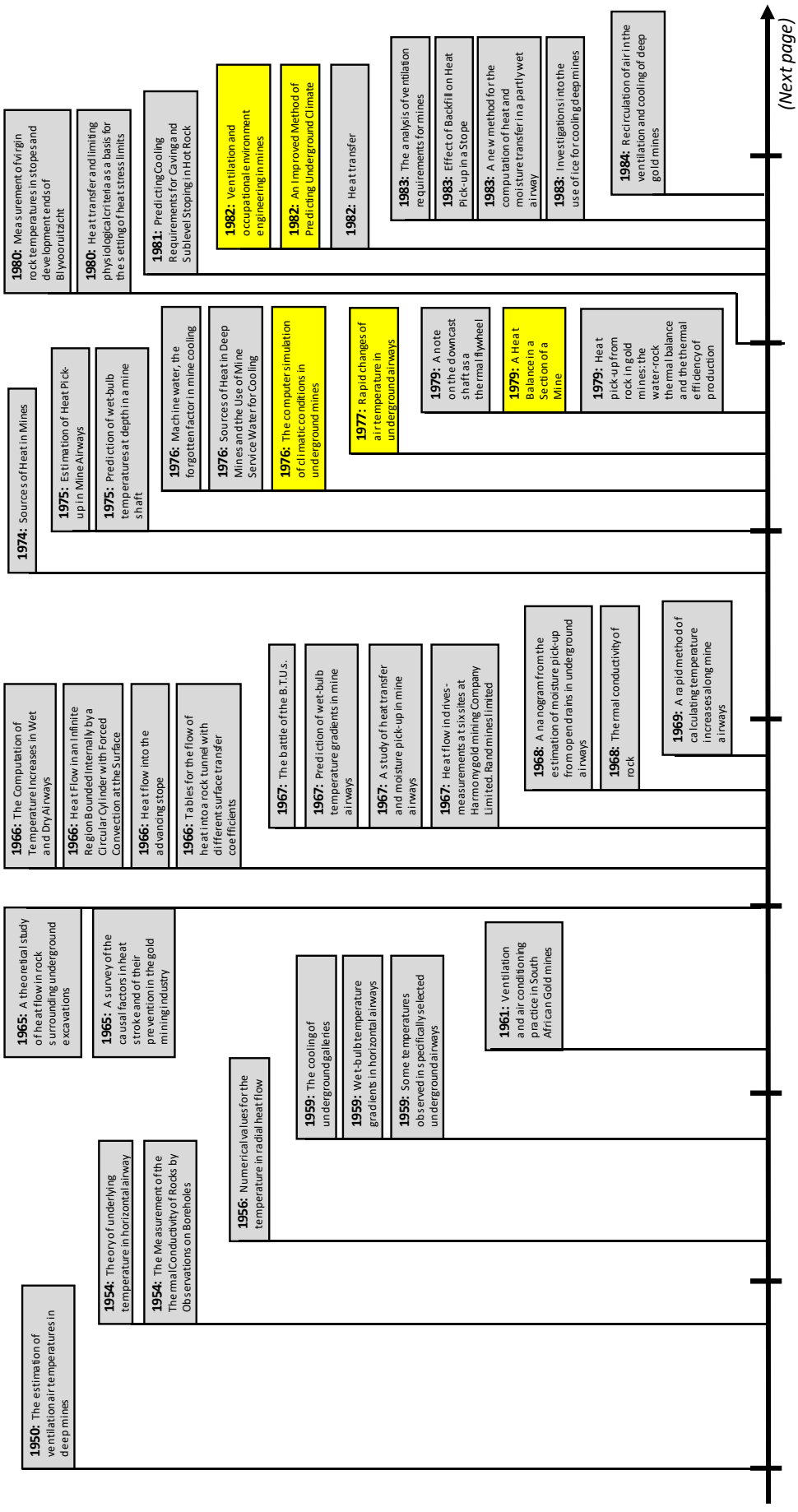

Figure 1-6: Chronological critical literature review of heat load calculation (A)

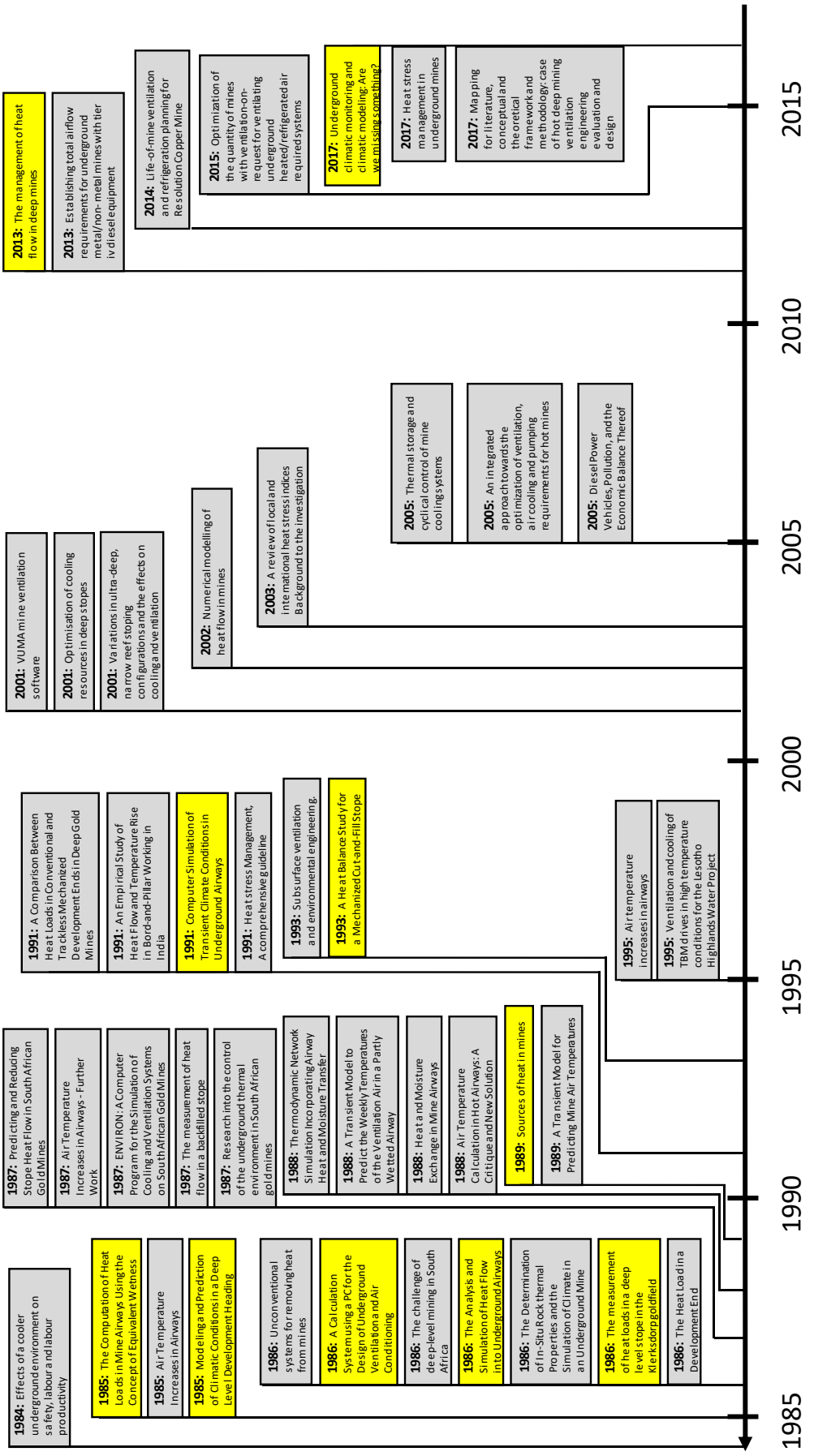

Figure 1-7: Chronological critical literature review of heat load calculation (B)

From the studies shown in Figure 1-6 and Figure 1-7, unique insight is obtained as to how the mining industry has progressed over the past number of years with regards to mine ventilation and heat load determination. These studies are discussed in more detail in Table A-1, which can be viewed under Appendix A.

In Figure 1-6 and Figure 1-7 the research titles, marked in yellow, indicate studies conducted which directly relate to the development of methods used to determine heat loads. These highlighted studies play a critical role in the determination of mine heat loads and were evaluated in more depth. Table 1-2 illustrates the criteria which were used to evaluate each of these studies in more depth. The criteria shown in Table 1-2 become the column headings in Table 1-3.

Table 1-2: Literature review criteria

Criteria	Description
Valid for all mining depths and distances	This criterion was selected to evaluate which approach can be applied at current mining depths and distances from the main shaft.
Applicable to mechanised mines	Ensuring the heat load determination method can be applied, irrespective of the mechanisation trends adopted at a mine.
Evaluates seasonal impact	Highlights which studies evaluated the impact of seasonal changes and how this affects mine heat loads.
Design or planning tool	This criterion evaluates which heat load methods were developed for planning and design purposes.
Localised area	Looked at studies which focus on a specific workplace in question, and developed a heat load determination method for such workplace.
Holistic mine	Heat load studies conducted on a complete mine, accounting for all relevant factors.
Simulations software	Highlights studies which used simulation software to evaluate mine heat loads in greater depths.
Industry 4.0	Studies focusing on ways to conduct heat load studies with higher accuracy at a higher frequency, using Industry 4.0 technology.
Ease of application	Evaluates studies which delivered an easily-reproducible methodology which is practical for everyday use.
Energy balance	Studies adhering to the principle of energy balances.

From the criteria discussed in Table 1-2, the highlighted studies in Figure 1-6 and Figure 1-7 were evaluated and are shown in Table 1-3.

Table 1-3: Critical literature study summary

Reference	Study	Valid for all mining depths	Applicable to mechanised mines	Evaluates seasonal impact	Design / planning tool	Localised area	Holistic mine	Simulation software	Empirical study	Industry 4.0	Ease of application	Energy balance
[25]	The computer simulation of climatic conditions in underground mines.	■	■	■	■	■	■	■	■	■	■	■
[26]	Rapid changes of air temperature in underground airways.	■	■	■	■	■	■	■	■	■	■	■
[27]	A heat balance in a section of a mine.	■	■	■	■	■	■	■	■	■	■	■
[11]	Ventilation and occupational environment engineering in mines: Planning refrigeration and ventilation requirements.	■	■	■	■	■	■	■	■	■	■	■
[28]	An improved method of predicting underground climate.	■	■	■	■	■	■	■	■	■	■	■
[29]	The computation of heat loads in mine airways using the concept of equivalent wetness.	■	■	■	■	■	■	■	■	■	■	■
[30]	Modelling and prediction of climatic conditions in a deep-level development heading.	■	■	■	■	■	■	■	■	■	■	■
[31]	A calculation system using a computer for the design of underground ventilation and air conditioning.	■	■	■	■	■	■	■	■	■	■	■
[32]	The analysis and simulation of heat flow into underground airways.	■	■	■	■	■	■	■	■	■	■	■
[33]	The measurement of heat loads in a deep-level stope in the Klerksdorp goldfield.	■	■	■	■	■	■	■	■	■	■	■
[34]	Sources of heat in mines.	■	■	■	■	■	■	■	■	■	■	■
[35]	Computer simulation of transient climate conditions in underground airways.	■	■	■	■	■	■	■	■	■	■	■
[25]	A heat balance study for a mechanised cut-and-fill stope.	■	■	■	■	■	■	■	■	■	■	■
[36]	The management of heat flow in deep mines.	■	■	■	■	■	■	■	■	■	■	■
[37]	Underground climatic monitoring and modelling: Are we missing something?	■	■	■	■	■	■	■	■	■	■	■

From Table 1-3, limited focus has been placed on evaluating the holistic heat load of a mine through conducting an energy balance. Doing this will give a clear indication of the heat contributed by each heat source whilst ensuring all forms of energy are accounted for. However, focus should be kept on developing a practical way of determining mine heat loads.

There is also a clear need, as shown in Table 1-3, to apply an energy balance approach in conjunction with a real-time monitoring (Industry 4.0 technologies) system. With most mines established, and with the sinking of new shafts becoming less frequent, the current heat load can be a daily measurement rather than an approximation from previous empirical data sets, or purely theoretical methods. This will enable the ventilation engineer to evaluate the thermodynamic balance of the entire mine continuously.

Table 1-3 also highlights the fact that the studies focusing on mine mechanisation trends focus on the specific heat source, as opposed to the part it plays in a heat load determination methodology. However, some of the more frequently used heat load determination methods are empirical in

nature and do not account for the scalability in mine mechanisation. These studies also did not focus on evaluating a holistic energy balance.

These shortcomings led to the development of a problem statement which can be viewed in the following section.

1.3. Problem statement

The key shortcomings of previous studies have been highlighted in Table 1-3. The four key problems were identified, and the focus of this study can, therefore, be summarised as follows:

- Mining depth and distances have exceeded the boundaries of previously developed design estimates, leading to possible misalignment between actual measurements and predicted heat loads. Focus needs to be placed on developing a scalable heat load determination approach to conduct a holistic heat load study for a mine at any depth whilst maintaining an energy balance.
- Previously developed heat production graphs do not account for the ever-growing mechanisation of a mine. The studies evaluating the heat contribution of mechanised equipment does not allow for a holistic heat load determination.
- Although various separate seasonal impact studies have been conducted, the interaction between such studies and the actual mine heat loads needs to be more clearly defined.
- There is a need to implement a real-time heat load determination approach to identify optimisation boundaries in a marginal mining industry.

Hypothesis – From the reviewed literature and defined problem statement, it is expected that there will be a misalignment between these currently used planning methodologies and the actual mine heat load.

The identified problems serve as the basis for the novel contributions made in this study, as discussed in the next section.

1.4. Novel contributions

This study will aim to deliver various novel contributions. These contributions are discussed in more detail below and highlights how this study will address key shortcomings identified in literature.

1.4.1. Heat load determination using an energy balance

Industry approach:

The most common industry approach to determine mine heat loads entails using heat flow rate prediction graphs, as can be seen in Figure B-1 in Appendix B [14]. The data comprising the graphs is based on conventional mining methods of nearly 30 years ago and comprises of empirical data [23]. These graphs assist the ventilation engineer to determine the heat load, based on the planned number of production tonnes. As input, the user specifies the mining distance from the main shaft, as well as the virgin rock temperature (VRT) at the specific depth. The estimated heat load is then adjusted in accordance with the planned reject temperature which yields the final heat load, excluding the effect of auto-compression and fissure water.

Since the heat flow rate prediction graphs are specific to a region, a more generalised approach is that of using another graphical method to determine refrigeration requirements, as can be seen in Figure B-3. This graph assists the user in determining the required refrigeration from mine VRT and depth below the surface.

As previously stated, these studies are broadly conducted during the initial planning phases of a mine and further performed in more depth for specific levels as the mine progresses.

Shortcomings:

The initial intent of developing the heat-prediction graphs was to guide mine developers during the planning phases of a new mine and consist of various rules of thumb. Currently there are various mines operating beyond the initial limits shown in the graphs, with mining distances increasing and new depths constantly being reached. Without a clear indication of how these graphs were developed, it causes a direct problem to extrapolate such methods to suit current mining conditions in various regions.

This study will:

This study will focus on the fundamentals of determining an holistic mine heat loads using the well-known approach of an energy balance. This approach will use current measured values to

quantify the mine heat load. From these calculations, the study will highlight the shortcomings of current approaches in terms of practicality and aim to quantify the impact of these shortcomings.

The aim of this study will also be to simplify the process of mine heat load determination to ensure its more frequent use in the deep-level mining industry.

How will it address the shortcomings?

The heat load in the form of energy balances will give instant heat load source breakdowns, which will allow the approach to be easily applied to other mining operations, irrespective of the mining method. This approach will minimise the large uncertainty, regarding heat load determination, specifically in operations not adhering to conventional mining. This will result in more accurate heat load determination.

1.4.2. Current and future increase in mine mechanisation

Industry approach:

The initial heat load prediction graphs are based on data sets which mainly comprises of conventional mining methods. These methods had a small portion of mechanised equipment forming part of the empirical results.

Shortcomings:

Various mines currently operate with a much larger mechanised fleet to assist with modern supply demands. Consequently, the empirical data used to compile the heat-prediction graphs does not account for increased mechanisation.

This study will:

This study will investigate the alternatives to using heat-prediction graphs to determine the mine heat load and quantify the error when using such graphs.

How will it address the shortcomings?

Understanding how mining has changed in terms of mechanisation or mechanised fleets will improve heat load calculations, as well as the effective management thereof. From a planning point of view this will ensure that capital expenditure regarding cooling is more accurately planned.

1.4.3. Impact of seasonal changes on mine heat loads

Industry approach:

Industry currently determines heat loads based on a worst-case scenario with regards to seasonal impact [23].

Shortcomings:

It is not clear under which seasonal circumstances the heat-prediction graphs were developed, which might lead to large over/under determination of mine heat loads. This negatively impacts the refrigeration systems, either through oversupply, constraining the current system and leading to limited time for critical maintenance, or undersupply resulting in excess heat.

This study will:

The seasonal impact will be dynamically evaluated using the energy balances and provide optimised heat load profiles from such balances. This study will aim to develop a dynamic cooling approach and quantify the effect of the overdesign when using present methodologies. This quantification will serve as a feasibility study for optimising the actual cooling requirements to match a seasonal heat load demand.

How will it address the shortcomings?

Approaching the heat load as a dynamic demand profile will not just result in large energy-saving scope but will also assist mines in planning actual cooling requirements. These requirements will ensure that effective maintenance schedules can be developed and upheld. It will also point to operational improvements that can realise capital expenditure savings on cooling and ventilation systems.

1.4.4. Industry 4.0 adoption in mine ventilation

Industry approach:

In many mines, ventilation data is still predominantly obtained by taking manual measurements. These measurements form part of routine audits with the available workforce. From such audits, data is captured in reports and distributed to various entities.

Shortcomings:

One of the biggest shortfalls in these manual approaches is the frequency of retrieving data. With data only obtained every other day, it leads to difficulty when wanting to analyse the

thermodynamics of a mine. The monitoring of key performance indicators of critical ventilation components becomes resource-intensive due to the result of the scale and complexity of all the thermodynamic processes in a mine.

Beyond collecting data, there is a need to have real-time analyses performed to evaluate the current and future performance of such a complex system.

This study will:

This study will also serve as a clear roll-out strategy to apply new Industry 4.0 technologies in mine ventilation to enable real-time heat load monitoring. It will also explore the potential of real-time monitoring of the various heat sources as part of an implementation strategy. These findings have also led to the publishing of the peer-reviewed article titled "Industry 4.0 roll-out strategy for dynamic mine heat load management" by Nell *et al.*[38].

How will it address the shortcomings?

Doing this will enable effective management of mine heat loads and ensure that adequate cooling planning is done in advance. This study will focus on the benefits of using Industry 4.0 technologies, as well as highlight the optimisation scope when doing so.

1.5. Conclusion

It is evident that the South African deep-level gold-mining industry is under severe pressure due to a decline in production. The decline is partially due to technical challenges, as these mines push the boundaries on mining at extreme depths, which leads to high working area temperatures. To ensure a safe working area is maintained, the heat in a mine needs to be effectively quantified and managed.

Although various techniques regarding mine heat load predictions have been developed over the years, many of these techniques are outdated. The most commonly used method is that of heat-prediction graphs which, in some instances, cannot be applied at the new depths/distances at which mining commences, and specifically falls short in heavily mechanised mines.

This study will aim to address this shortfall by evaluating mine heat loads based on energy balances. It will also present a roll-out strategy to successfully implement this method of evaluation on mines to achieve real-time heat load monitoring and enable the active management thereof.

2

CHAPTER 2

A new method to determine mine heat loads

"Give me six hours to chop down a tree and I will spend the first four sharpening the axe."

Abraham Lincoln[2]

[2] Brainy Quote, https://www.brainyquote.com/quotes/abraham_lincoln_109275, [2019/11/10]

2. A NEW METHOD TO DETERMINE MINE HEAT LOADS

2.1. Preamble

This chapter focuses on the development of a methodology to calculate the heat load for a deep-level gold mine. This methodology will aim to address the shortcomings discussed during the first chapter of this study by using the principles of an energy balance.

2.2. Energy balances

A vast number of energy sources can be identified in deep-level gold mining. These energy sources form part of a complex thermodynamic cycle, which, as the name states, is dynamic in nature. A fundamental principle to be applied in these studies is the first law of thermodynamics, also known as the law of conservation of energy, which states that energy cannot be created or destroyed, but can only change from one form to another [39]. Figure 2-1 illustrates the various sources of energy entering and leaving a deep-level mine.

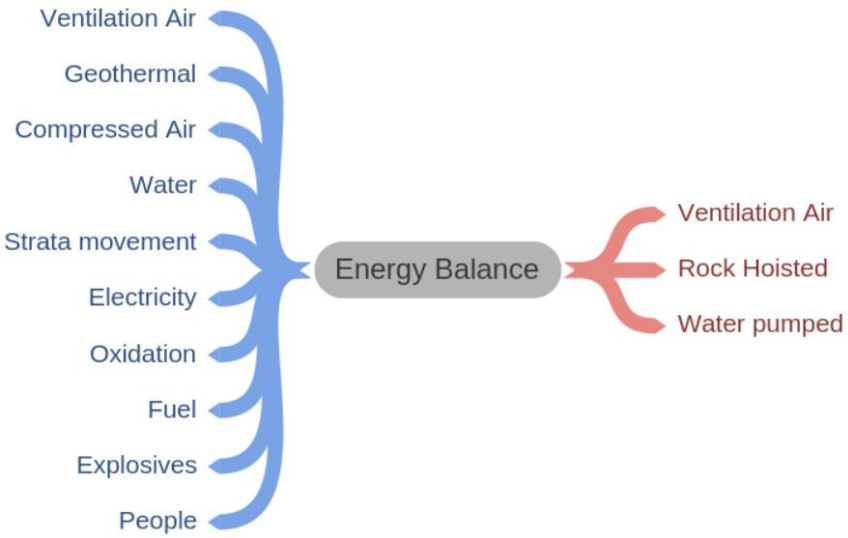

Figure 2-1: Energy sources in mines

In Figure 2-1 it is shown that there is a variety of energy sources in deep-level mines, and it is important to account for each one of these energy sources when conducting an energy balance. Due to the dynamic nature of constant change from one form to another, an energy balance is conducted on a steady-state basis. Equation 2-1 shows the steady-flow energy equation which accounts for all the forms of energy in a deep-level gold mine.

Equation 2-1: Steady flow energy equation [14]

$$\frac{u_1^2 - u_2^2}{2} + (Z_1 - Z_2)g + w_{in} = (h_2 - h_1) - q_{in}$$

Where

u	=	Velocity	m/s
Z	=	Elevation	m
g	=	Gravitational acceleration	m/s^2
w	=	Mechanical energy	J/kg
V	=	Specific volume	m^3/kg
h	=	Enthalpy	J/kg
q	=	Heat transfer	J/kg

Through applying Equation 2-1, all the energy sources in a mine can be easily evaluated. Heat energy is the primary form of energy, which most other forms of energy transfer to before leaving a deep-level mine [36]. The exception is that of useful work, which leaves the mine as a nett potential gain. However, since the potential gain can be easily calculated, an energy balance can be treated as a heat balance.

Previous studies support this theory and have shown that an energy balance does exist between the supplied cooling and the measured heat sources [25, 33]. These studies focused on a specific workplace, such as a stope area, and measured all the relevant heat sources. Clear results were obtained from these studies so that an energy balance could be constructed.

There are, however, challenges regarding evaluating the energy transfer from the surrounding rock, known as geothermal heat. This has been an extensively debated topic and extensive research has been published [14, 34, 40–43]. In the methodology to follow, the geothermal heat will be calculated as the heat balance to allow for steady-state conditions. Figure 2-2 illustrates the heat load calculation methodology that was applied during this study.

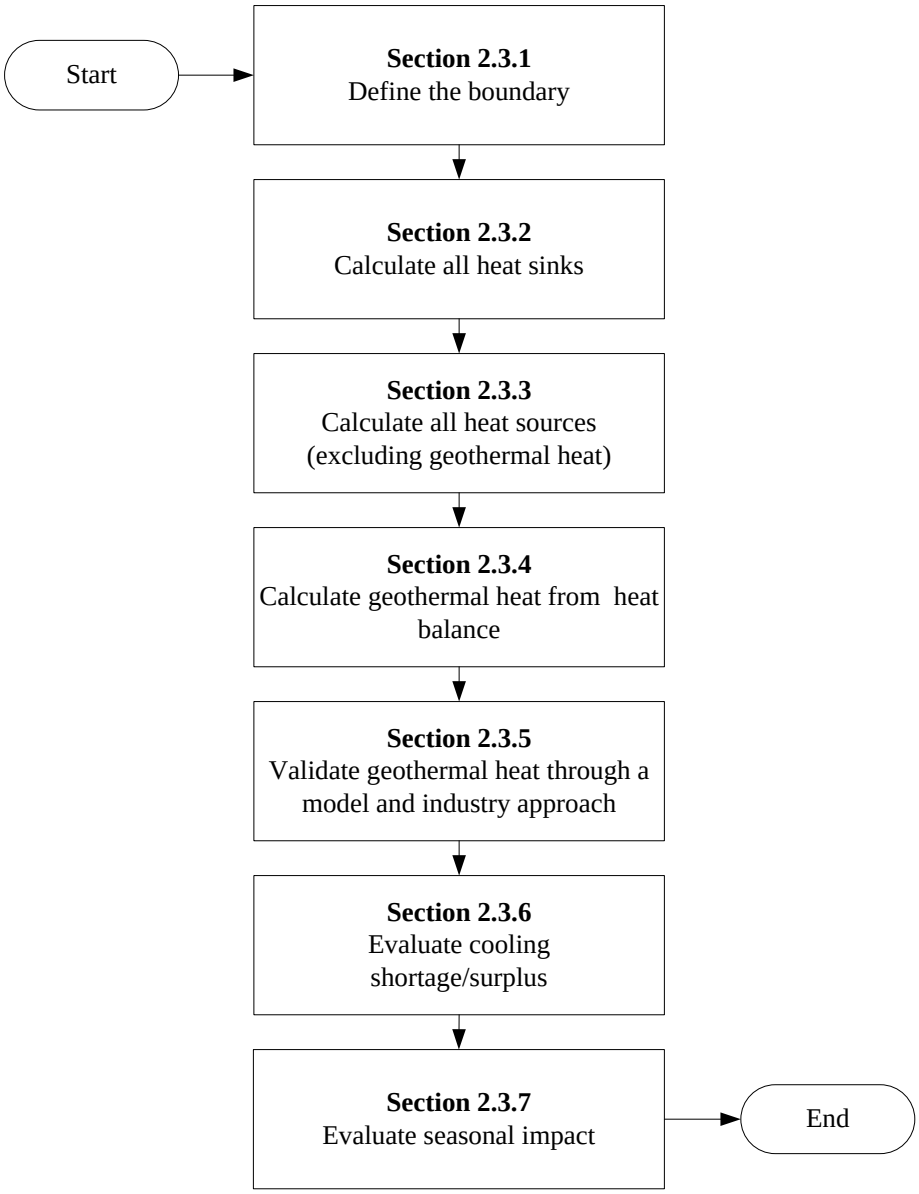

Figure 2-2: Heat load calculation methodology

Figure 2-2 shows all the steps to be taken to conduct a heat load study using energy balances. Each step is numbered in accordance with the headings to follow and will serve as a road map for each component's respective calculation.

Although this study focuses on a steady-state approach, the benefit and impact of transient modelling software will be explored later in this study. Such tools will be applied to validate the results obtained by using a heat-balance approach.

2.3. Heat load component review

2.3.1. Define the boundary

The first essential step is to clearly define the boundary of the specific heat load study. This can range from a workplace to the whole mine. This boundary is essential to account for all the energy forms entering and exiting the boundary perimeter for any given point in time. The boundary selected should be of a nature to encapsulate the appropriate activities, equipment and working areas of concern. Figure 2-3 illustrates a typical boundary selection when calculating the heat load for a complete mine.

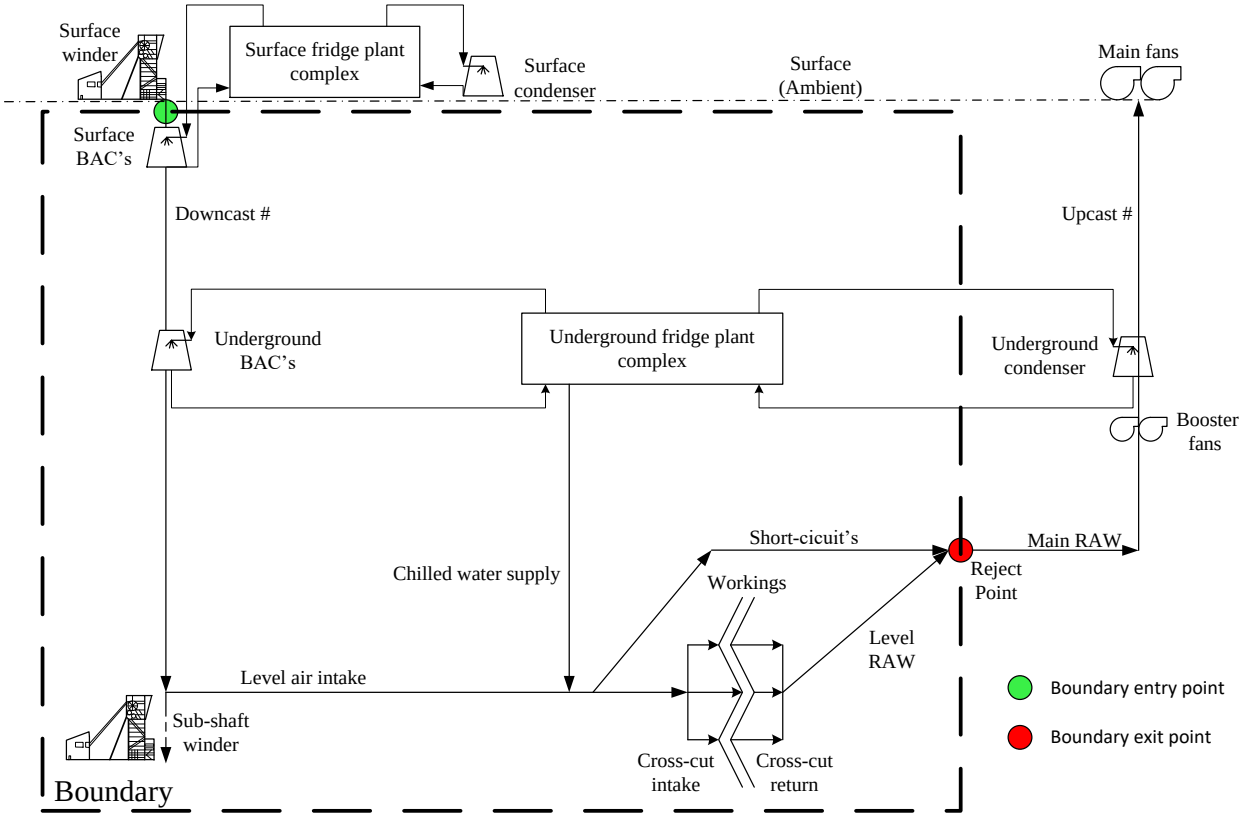

Figure 2-3: Mine boundary definition

In Figure 2-3, some components have been deliberately excluded from the boundary perimeter. Such components include condenser circuits, booster fans situated after working areas, surface fans and return haulages. It is essential to exclude these components from the heat load study since the heat contributed by each will not affect mine employees on a day-to-day basis. However, special arrangements will have to be made to conduct maintenance on these components.

2.3.2. Heat sinks in mines

Heat sinks can be defined as phenomena which extract heat from the environment [14]. Figure 2-4 illustrates the steps to be taken to calculate the three major heat sinks in a mine. Each step is discussed in more detail in the section to follow.

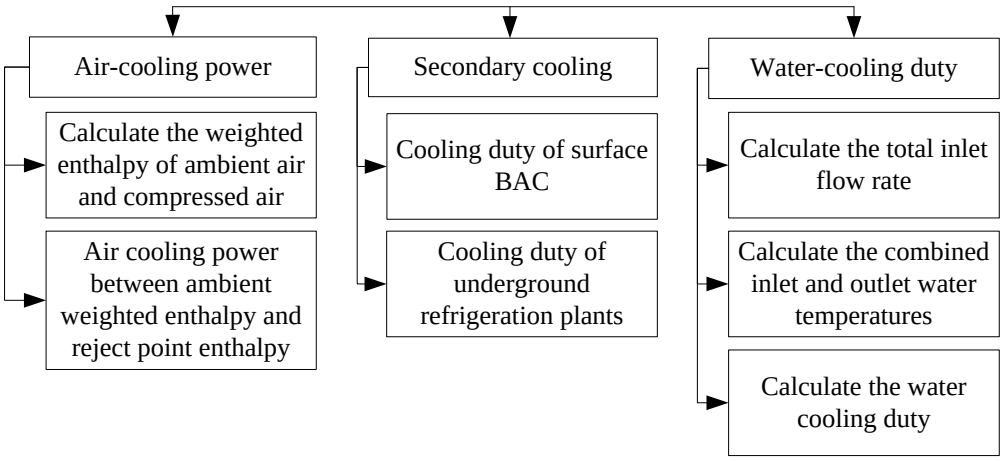

Figure 2-4: Summary of heat-sink calculation steps in deep-level mines

Air-cooling power

The air downcasted at a shaft has a specific energy content and hence specific psychometric properties. Most of this downcasted air is in the form of ventilation air; however, compressed air should also be accounted for. The weighted inlet ambient enthalpy can be calculated using the respective mass flows, as is shown in Equation 2-2.

Equation 2-2: Combined air mass flow-weighted enthalpy

$$h_{in} = \frac{\dot{m}_{vent} h_{vent} + \dot{m}_{comp} h_{comp}}{\dot{m}_{Total}}$$

Where

h_{in}	=	Combined enthalpy of inlet ventilation and compressed air	kW
$\dot{m}_{vent}$	=	Mass flow of ambient ventilation air	kg/s
h_{vent}	=	Enthalpy of ambient air	J/kg
$\dot{m}_{comp}$	=	Mass flow of compressed air	kg/s
h_{comp}	=	Enthalpy of compressed air	J/kg
$\dot{m}_{total}$	=	Total mass flow of downcasted air	kg/s

As the air moves through the mine, heat is transferred from the hot surroundings to the air, thus cooling the environment. This cooling potential is known as natural air-cooling power (ACP). Equation 2-3 can be used to calculate the natural ACP supplied.

Equation 2-3: Air-cooling power [34]

$$ACP = \dot{m}(h_{in} - h_{out})$$

Where

ACP	=	Air-cooling power	kW
$\dot{m}$	=	Mass flow	kg/s
h	=	Enthalpy	J/kg

When calculating the ACP, it is also important to account for leakages that might occur. The air mass flow reaching the intended workplace and contributing to the temperature of the reject point should be used for this calculation. Figure 2-5 illustrates the ACP sample point for a theoretical mine where no secondary (refrigeration) cooling or tertiary (air-cooling units) cooling is implemented underground.

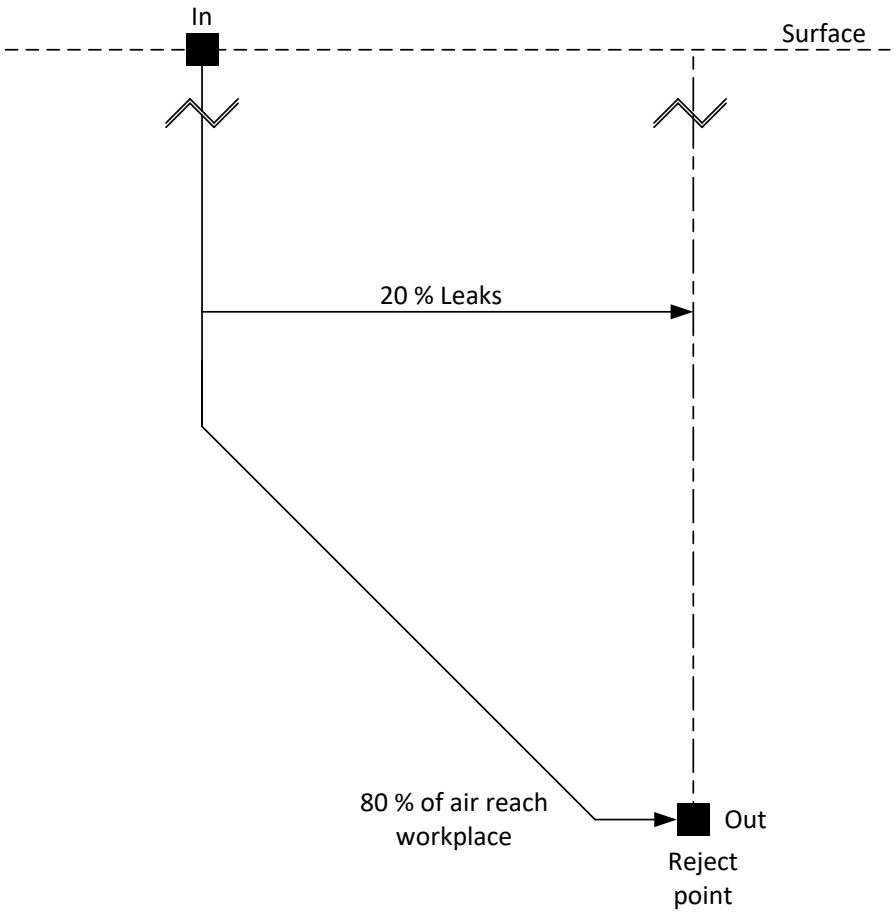

Figure 2-5: Air-cooling power (ACP) approach

Figure 2-5 shows that, to calculate the ACP for the theoretical mine, the difference in energy content of the air between point one and point two should be calculated, together with the air mass flow supplied to point 2. As a result of leaks prior to ventilation air reaching the working place, a portion of the ACP will be lost. For instances where these leaks cannot be accurately quantified, an estimated 20% leakage of the total air supply is normally assumed [23].

The ACP varies drastically during the summer and winter month. During winter the ACP of the ambient air increases, providing additional cooling, which results in scope to stop secondary/tertiary cooling. Theoretically, the same effect is observed daily when surface temperatures vary. However, due to the thermal flywheel effect (dampening effect), these daily surface fluctuations are negligible and the effect thereof undetectable in deep-level mines [14]

Secondary cooling (Refrigeration)

Refrigeration refers to the implementation of a mechanical cooling process where heat is moved from one place (where it is unwanted) to another place (where heat does not influence people) [23]. Mining at extreme depth leads to most of the natural ACP effect of ambient air to be diminished by the effect of auto-compression. This occurs at depth in the region of below two kilometres and therefore necessitates refrigeration [23].

These thermodynamic refrigeration cycles most commonly comprise of vapour-compression machines, which require mechanical work input energy to transfer the heat from one point to the other [44]. These machines consist of two opposing components called the condenser and evaporator, where heat is extracted from the evaporator and transferred to the condenser. Figure 2-6 shows the major component of the vapour compression cycle.

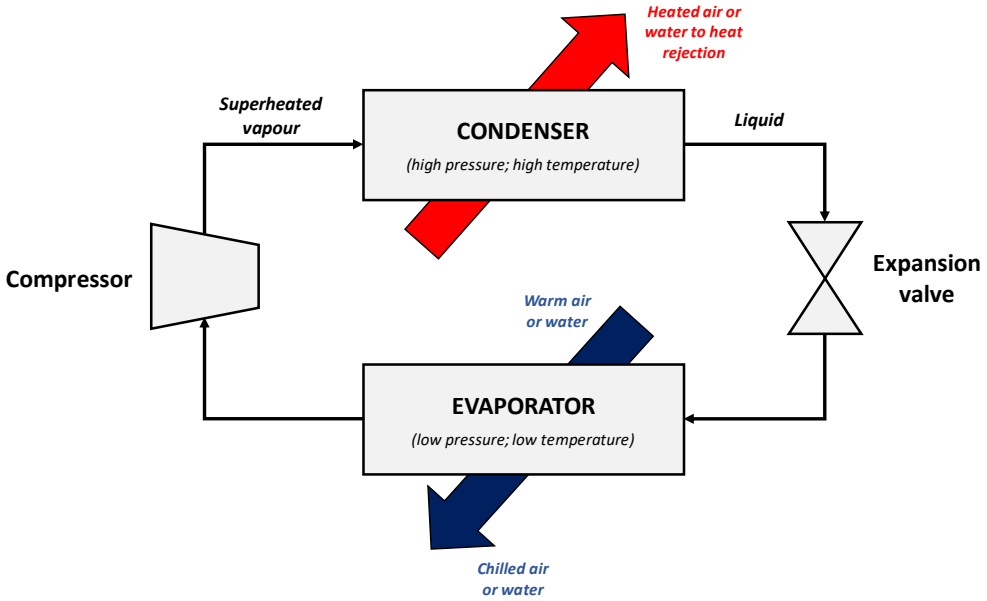

Figure 2-6: Major components of a vapour compression cycle [14]

The cold water supplied by the evaporator is used to supply bulk-air-cooling (BAC) units on surface and underground, which cools down the air flowing through the units. This directly removes sensible heat from the air, as well as lowers the humidity content in the air. It is important to differentiate regarding the location of the BAC with respect to the defined boundary. Figure 2-7 illustrates the different secondary cooling scenarios.

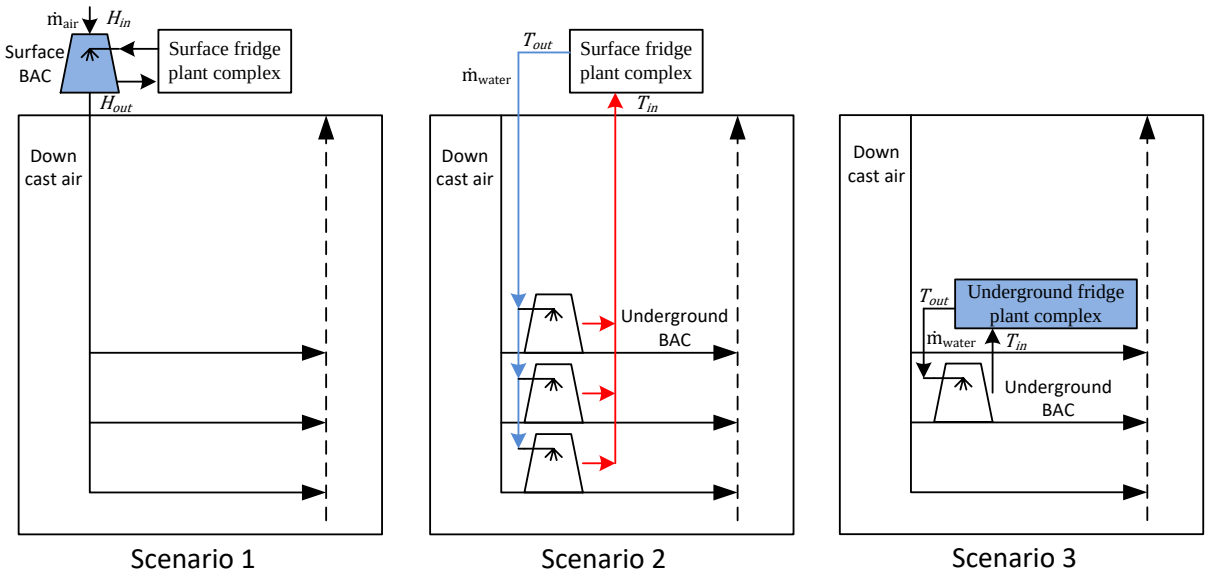

Figure 2-7: Secondary cooling evaluation scenarios

With reference to Figure 2-7: when the BAC is situated on the surface and supplied by surface refrigeration plants (Scenario 1), the duty of the BAC should be used as the secondary cooling duty. Equation 2-4 can be used to calculate the cooling duty of the air supplied by the surface BAC.

Equation 2-4: Induced cooling through surface BAC

$$Secondary\ cooling_{BAC\ duty} = \dot{m}_{air}(h_{out} - h_{in})$$

However, if the BAC is located underground and supplied with cold water from surface refrigeration plants (Scenario 2), the cooling does not need to be accounted for during the secondary cooling evaluation, since this cooling benefit will be evaluated during the water-cooling calculation step.

If the BAC is situated underground and supplied by an underground refrigeration plant (Scenario 3), the additional cooling can be calculated using the evaporator duty of the refrigeration plants, since any cooling losses (inefficiencies) also contribute to the overall cooling in the mine. Equation 2-5 can be used to calculate the evaporator cooling duty.

Equation 2-5: Induced cooling through underground refrigeration

$$Secondary\ cooling_{Evaporator\ duty} = \dot{m}_{water} C_{p,avg} (T_{out} - T_{in})$$

One benefit of the secondary cooling processes is that they usually feature some form of instrumentation. This means real-time data can be collected and used during the calculation of this heat sink. This benefit is also of great importance when wanting to implement a daily heat load report, as will be discussed in Chapter 4 of this study.

Water-cooling duty

Water entering a mine picks up heat and provides a form of cooling when leaving the mine. To account for this form of cooling, the representative temperature of all the water supplied underground should be evaluated. Figure 2-8 illustrates this concept more clearly.

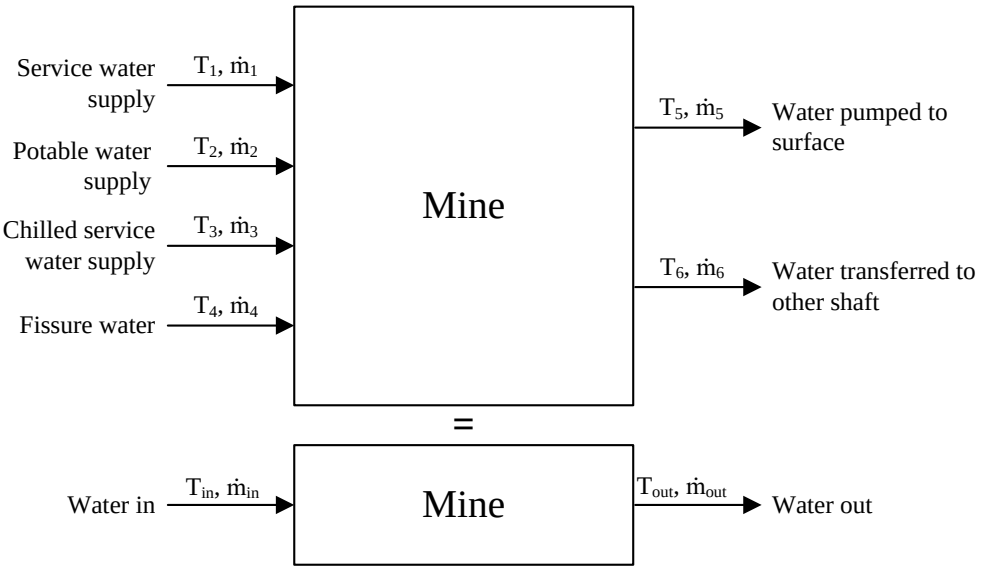

Figure 2-8: Combined water balance

In Figure 2-8 it is shown that the water sources entering and leaving the mine can be reduced to one inlet and outlet source respectively. Fissure water is deliberately excluded from this diagram since it will be accounted for separately as a heat source later in this study. This can be done since the exit temperature of fissure water leaving the mine will equal the exit temperature of the combined water sources leaving the mine.

To determine the combined inlet and outlet water temperature, a flow-weighted calculation should be performed. Equation 2-6 can be used to determine the inlet water temperature, and the same will apply for the outlet water temperature.

Equation 2-6: Flow-weighted water inlet temperature

$$T_{in} = \frac{T_1\dot{m}_1 + T_2\dot{m}_2 + T_3\dot{m}_3 + T_4\dot{m}_4}{\dot{m}_{in}}$$

With the combined inlet and outlet temperatures known (excluding fissure water), the cooling duty of the water can be calculated by using Equation 2-7.

Equation 2-7: Cooling duty of liquid water [14]

$$Water\ cooling\ (q) = \dot{m}_{in}C_p(T_{out} - T_{in})$$

Where

q	=	Cooling duty	kW
$\dot{m}_T$	=	Total water mass flow	kg/s
C_p	=	Specific heat of water	kJ/kg℃
T_{in}	=	Inlet water temperature	℃
T_{out}	=	Outlet water temperature	℃

Total heat sinks

With all the heat sinks known, the total supplied cooling can now be determined. Equation 2-8 illustrates the total supplied cooling which is a summation of all the calculated heat sinks.

Equation 2-8: Total heat sinks [14, 23]

$$Total\ heat\ sinks = Air\ cooling\ power + Secondary\ cooling + Water\ cooling$$

As discussed earlier, according to the first law of thermodynamics, this total supplied cooling can also be interpreted as the total heat-pickup of the mine for the specific boundary area. This enables an easy and quick method to verify the total heat-pickup for a given mine. The section to follow will focus on calculating the various heat sources contributing to the total heat-pickup of the mine.

2.3.3. Heat sources in mines

Heat sources can be defined as phenomena which add heat to the environment. There are various sources of heat in a deep-level gold mine, ranging in complexity when it comes to quantification of such sources. These sources can be divided between sensible and latent heat [14]. Figure 2-9 illustrates a detailed breakdown of the steps to be taken when calculating the heat sources of a mine.

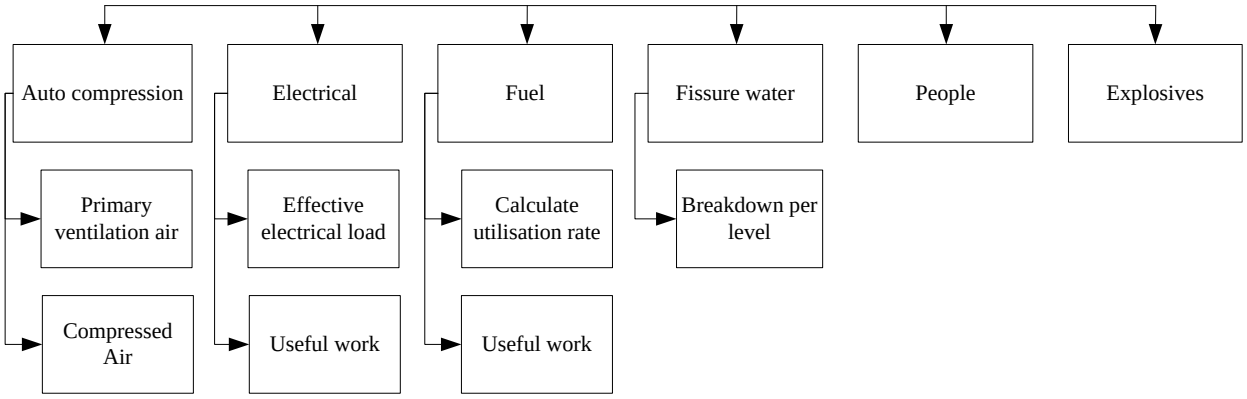

Figure 2-9: Heat sources summary

Figure 2-9 illustrates the various heat sources in deep-level gold mines, as well as some of the key steps to be taken to quantify each heat source. Each heat source will be discussed in more detail in the section to follow.

Auto-compression

Auto-compression refers to the phenomenon of a compressible fluid increasing in temperature as it flows from a higher elevation to a lower elevation [14]. This increase in temperature is caused by the conversion of potential energy into enthalpy [14]. The increase in enthalpy causes a rise in pressure and internal energy, resulting in a rise in temperature.

Auto-compression is strictly not a source of heat, rather a natural phenomenon, but should nonetheless be accounted for when working at extreme depths, as is the case in deep-level gold mines. Equation 2-9 can be used to calculate the effect of 'pure' auto-compression where there is no work being done, or heat transfer occurring.

Equation 2-9: Adiabatic 'pure' auto-compression [14, 34]

$$(h_2 - h_1) = \frac{u_1^2 - u_2^2}{2} + (Z_1 - Z_2)g$$

Where

u	=	Velocity	m/s
Z	=	Elevation	m
g	=	Gravitational constant	m/s^2
h	=	Enthalpy	J/kg
q	=	Heat transfer	J/kg

The kinetic energy component in Equation 2-9 represents the change in kinetic energy as a result of the change in density. However, this component is extremely small and is neglected in most calculations, hence reducing Equation 2-9 to Equation 2-10 [14].

Equation 2-10: Auto-compression [14, 34]

$$(h_2 - h_1) = (Z_1 - Z_2)g$$

The enthalpy difference shown in Equation 2-10 can be multiplied with the corresponding mass flow rate to determine the increase in heat at the specific depth. When calculating this heat gain for the downcast air in a shaft, it is essential to take the mass flow distribution into each level into consideration and not just use the total airflow value. Table 2-1 highlights the potential error when neglecting to evaluate the air mass flow distribution.

Table 2-1: Auto-compression air mass flow distribution impact

		Scenario 1			Scenario 2			Scenario 3		
Level	**Depth**	**Mean rock breaking depth [m]**	**Flow downcast [kg/s]**	**Auto-compression heat [kW]**	**Flow intake per level [kg/s]**	**Flow downcast [kg/s]**	**Auto-compression heat [kW]**	**Flow intake per level [kg/s]**	**Flow downcast [kg/s]**	**Auto-compression heat [kW]**
Surface		1 500	250	3 671		250	-		250	-
1	500				50	200	1 224	50	200	1 224
2	1 000				50	150	979	40	160	979
3	1 500				50	100	734	40	120	783
4	2 000				50	50	490	40	80	587
5	2 500				50	0	245	80	0	392
			Total	**3 671**		**Total**	**3 671**		**Total**	**3 965**

In Table 2-1 the total downcasted air mass flow is constant for all three scenarios, with the flow distribution the only changing parameter in scenario three. From this, we see that, when using the mean rock breaking depth (average mining depth), it is similar to assuming that the flow distribution through each level is equal. However, there is a difference in heat gain when an unequal flow distribution occurs, and it is important that the auto-compression of a mine be determined in accordance with the actual flow distribution for each level.

It should also be noted that the opposite effect occurs when compressible fluids flow from a lower elevation to a higher elevation, which is known as auto-decompression. However, in a typical gold mine setup, this occurs after the working areas as air is upcasted through the return airways. The decrease in temperatures causes condensation, which reduces the lifecycles of downstream equipment, such as surface fans [14].

Electrical heat load

To calculate the sensible heat added by electrical equipment, the useful work must first be accounted for. The useful work conducted by electrical equipment relates to the following activities:

- Hoisting of rock
- Incline conveyors
- Transporting of ore through electrically driven vehicles (elevation change)
- Pumping of water (dewatering to higher elevation)

Other than these activities, all electrical energy used within the mine will be transformed into sensible heat energy [14, 34]. Any electrically driven activity (resulting in a potential energy gain) will, therefore, be a form of useful work, which should be subtracted from the effective electrical heat load. The potential energy gain can be calculated using Equation 2-11.

Equation 2-11: Potential energy [14]

$$Potential\ Energy\ (P.E.) = \dot{m}gZ$$

Where

$\dot{m}$	=	Rock mass flow	kg/s
g	=	Gravitational constant	m/s^2
Z	=	Elevation	m

It is, however, important that the elevation of the potential gain be clearly defined. In the case of water, this point will be the area in the mine from which the accumulated water is initially pumped from for the first time. For instances where this happen at various depths, the separate pumping streams can be evaluated individually, as shown in Figure 2-10.

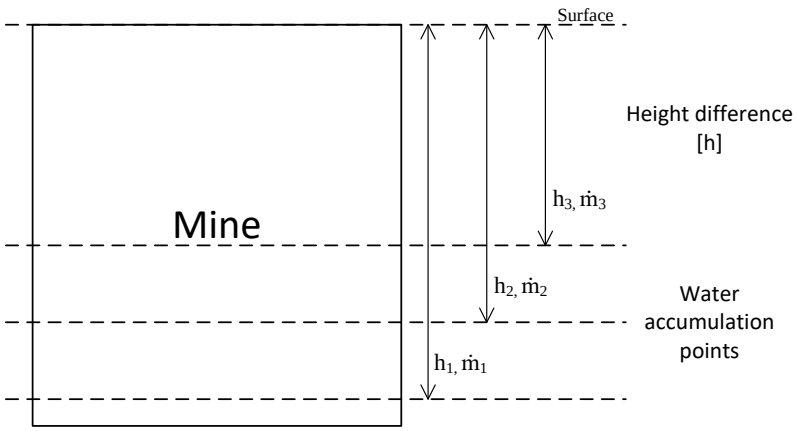

Figure 2-10: Potential gain of multiple water streams pumped to the surface

In the case of ore transportation, the point from which sub-shaft hoisting is done, as well as the point where ore is dropped onto an incline conveyor belt system, should be used. To calculate the effective electrical heat load, it is essential to only account for electrical energy consumed within the boundary of interest. Any electrical consumption after the reject point should not be added to the effective electrical heat load, such as condenser pond pumps, condenser fans etc.

In instances where sub-shaft hoisting occurs, the winder motors contribute to the electrical heat load. The useful work (potential gain induced) should, therefore, be subtracted from the electrical energy used by the motors. However, the surface winder motors will not dissipate their heat in the mine intake air and should not be counted as part of the electrical heat load. Neither should the useful work conducted by these surface winders be subtracted from the electrical heat load. This is more clearly illustrated in Figure 2-3.

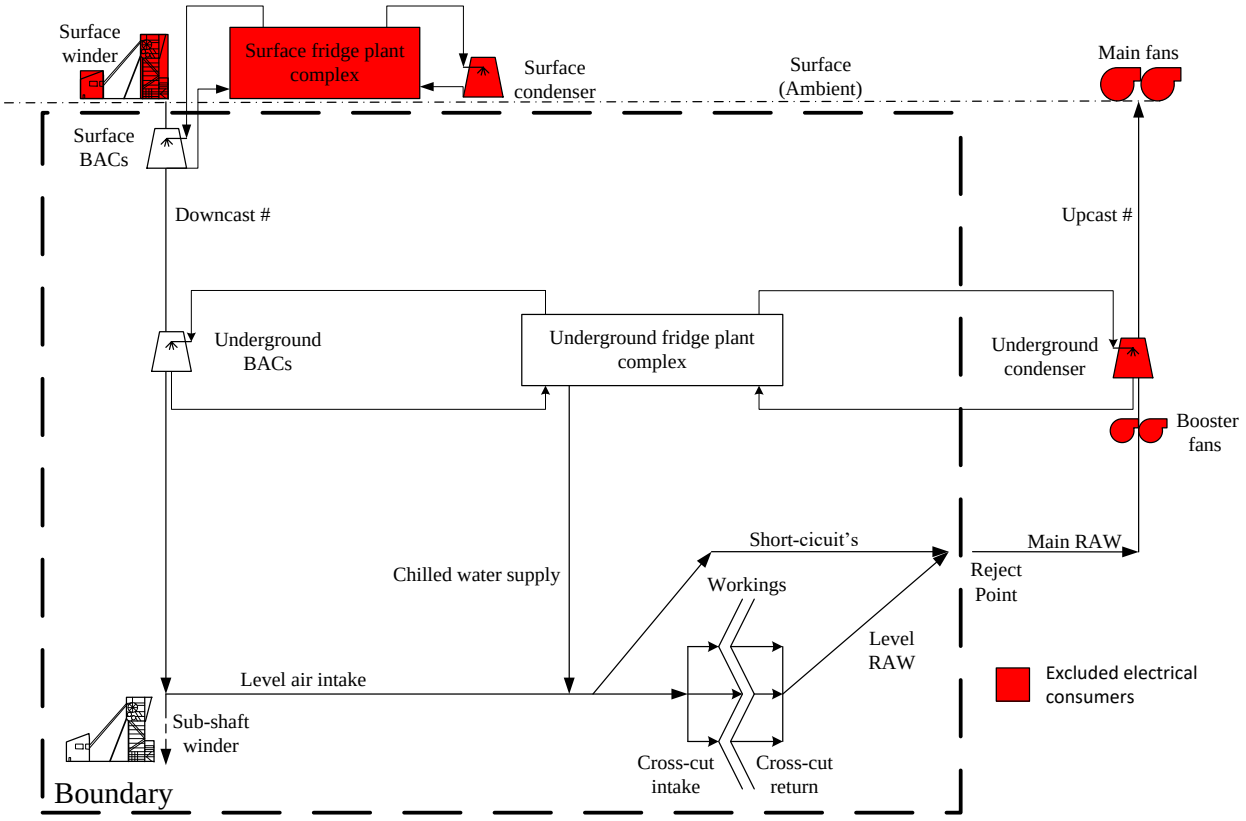

Figure 2-11: Excluded electrical consumers

Figure 2-11 illustrates which electrical activities should be excluded from the calculated effective electrical heat load, and is indicated in red. To calculate the effective electrical heat load:

Equation 2-12: Effective electrical heat load

$$Effective\ electrical\ heat\ load = Total\ supply - P.E. - Excluded\ equipment$$

Mechanised machinery

Today's mining climate is changing in many ways, one being that of mine mechanisation. The drive behind mine mechanisation is a call for increased production, and various mechanised processes have been introduced over the past number of years [45].

Previous heat studies concluded that geothermal heat was by far the dominant heat source for conventional mining, responsible for roughly 90% of the overall heat in a mine. However, this is not the case for mechanised mines, where mechanised equipment can contribute as much as one-third of the heat in a mine [25].

There are various methods to quantify the heat contributed by the mechanised equipment, depending on the data availability. It is not uncommon to find poor record-keeping of machine operating times, but with technological advances and tracking of mechanised machine operating patterns, these data discrepancies can be addressed.

A commonly used method is that of quantifying the heat released by the amount of diesel consumed. Since diesel supply is normally measured on the surface or can be tracked through financial invoicing, it is a convenient method to calculate the heat added by calculating the energy released by the diesel. This can be done using Equation 2-13.

Equation 2-13: Mechanised heat [14]

$$Mechanised\ heat = \dot{m}\ \times \eta_{Com} \times CV$$

Where

$\dot{m}$	=	Litres per second	$litre/s$
η_{Com}	=	Combustion efficiency	%
CV	=	Calorific value of diesel	$kJ/litre$

Using Equation 2-13 results in the total heat released by the mechanised equipment. However, this is for a given period and cannot just be averaged for a day. Such averaging will lead to instances where the actual heat released exceeds the estimated amount, resulting in surplus heat. It is important to calculate the actual duty cycle, which will then give the specific heat load profile.

To account for this duty cycle, the utilisation rate needs to be determined. This can be determined from the actual vehicle running hours, divided by a 24-hour period. For instances where such running hours are not available, a multiplication factor of between two to three can be used [46].

The heat released from mechanised equipment can also be divided into sensible heat and latent heat. Studies conducted have shown that approximately 3 - 10 litres of water are produced during the combustion of 1 litre of fuel [14]. This can be calculated using Equation 2-14.

Equation 2-14: Ratio of water produced per fuel consumed [14]

$$m_{Water} = m_{Fuel} \times \eta_{Com} \times VF$$

Where

m_{Water}	=	Litres of water	$litre$
m_{Fuel}	=	Litres of fuel	$litre$
η_{Com}	=	Combustion efficiency	%
VF	=	Vapour factor	–

From the amount of water produced, the latent heat can be calculated using Equation 2-15.

Equation 2-15: Mechanised heat (latent) [14]

$$Mechanised\ heat\ _{Latent} = m_{Water} \times L_V$$

Where

m_{Water}	=	Litres of water	$litre$
L_V	=	Latent heat of evaporation of water	kJ/kg

The final step is now to calculate the sensible heat. The sensible heat can be calculated using Equation 2-16.

Equation 2-16: Mechanised heat (sensible)

$$Mechanised\ heat\ _{Sensible} = Mechanised\ heat - Mechanised\ heat\ _{Latent}$$

As was the case for electrical machinery, it is important to account for any useful work conducted by the mechanised equipment. Such work will include the transportation of ore from a specific depth to a higher elevation, hence increasing the potential energy of the ore. To calculate such useful work for each working depth, Equation 2-11 can be used. To calculate the effective mechanised heat, Equation 2-17 can be used.

Equation 2-17: Effective mechanised heat load

$$Effective\ mechanised\ heat = Total\ mechanised\ heat - potential\ energy\ gain$$

Fissure water

Fissure water refers to water entering the mine uncontrollably through crevasses, faults, cracks or even old mined-out areas [14]. Two important assumptions are made when calculating the impact of fissure water on the heat load of a mine, namely:

1. The temperature of the water entering the mine can be taken at the virgin rock temperature (VRT) for the given depth since this water has been in direct contact with the rock for a prolonged period.
2. The fissure water's exit temperature from the mine can be assumed to be equal to that of the reject air's wet-bulb temperature. However, special care should be taken for instances where fissure water is present on the intake side of the mine since the exit temperature of the water will then equal the intake wet-bulb temperature.

To calculate this heat source, Equation 2-7 can be applied, where the outlet temperature will be equal to the reject wet-bulb temperature, and the inlet temperature equal to the respective VRT at the given depth. If various fissure water sources exist, as shown in Figure 2-12, each can be calculated separately for the various mass flows. The nett heat effect can then be determined from adding up all the individual fissure water heat sources or calculating a combined intake temperature using Equation 2-6.

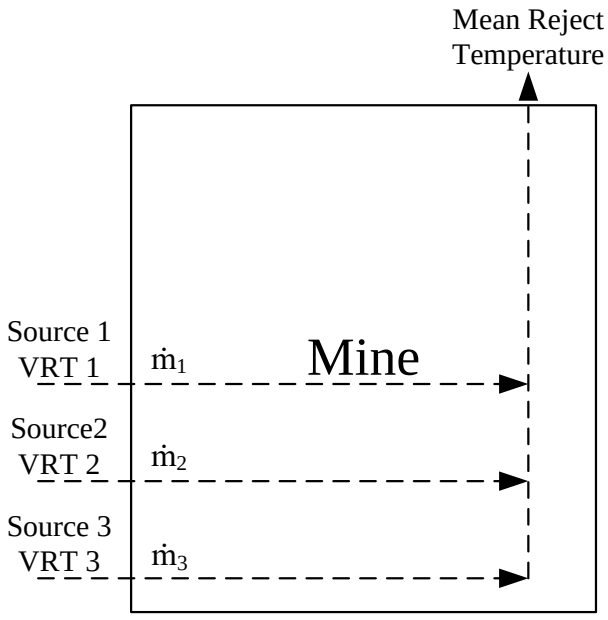

Figure 2-12: Fissure water source illustration

Compressed air

The heat added by compressors is addressed when calculating the overall effective electrical heat load. It is still important to consider the local impact of underground compressors and the cooling benefit derived from the exhaust air of the hand-held compressed air-driven drills.

For instances where the moisture content of the supplied compressed air is equal to that of the ambient ventilation air at the working area, there will be no nett heating or cooling effect [14]. This is due to the mechanical work, dissipated in frictional heat, equalling the cooling effect that the dry-exhaust air has on the ambient ventilation air. In cases where the supplied compressed air has a lower relative humidity than the ambient ventilation air, a small portion of cooling will be present and vice versa.

If we neglect the small difference in potential energy, as well as assume that no heat is transferred across the compressed air-driven drill body, the steady-state equation reduces to Equation 2-18.

Equation 2-18: Steady flow energy equation for compressed air nett heat/cooling [14]

$$C_p(\theta_2 - \theta_{amb}) + w_{in} = C_p(\theta_2 - \theta_1) - q$$

Where

q	=	Cooling/Heating	J/kg
w_{in}	=	Mechanical energy	J/kg
C_p	=	Specific heat of air	$J/kg.°C$
θ_1	=	Compressed air inlet temperature	kPa
θ_2	=	Compressed air outlet temperature	$°C$
θ_{amb}	=	Ambient ventilation air temperature	N

It is important to make use of the correct specific heat value for the air moisture in the compressed air supply and the ambient air, respectively.

Human effect (Metabolic)

The metabolic heat rate refers to the heat energy released through the workers in the mine. This heat source is relatively small when compared to other heat sources, although it might become significant if high worker concentration occurs at specific working areas [34].

There are widespread differences as to how much heat is generated for specific work conducted since it is based on a variety of factors. One such factor is individuality in workers, whose bodies respond differently in identical environments. Table 2-2 highlights typical metabolic heat rates for the standard person (70 kg, 1.73 m, 1.83m^2) [14, 47].

Table 2-2: Metabolic heat rate per activity [25, 34, 48, 49]

Activity	Metabolic heat production rate per area [W/m^2]	Metabolic heat production rate [W]
Resting	60	90 -115
Light manual work	115	200
Moderate manual work	180	275
Heavy manual work	240	470
Very heavy manual work	>240	>470

From a study conducted by Van Rensburg *et al.*, an important conclusion drawn, was that on average work rates in a mine range from moderate to heavy [48]. The difficulty comes in knowing what the frequency is and hence, for the purpose of this study, 250 W was used as the average metabolic heat rate per person [25]. This translates to an approximate metabolic heat rate of 370 W at a working tempo of 70%. Equation 2-19 can be used to estimate the metabolic heat load.

Equation 2-19: Metabolic heat load [14]

$$MHL = N.E. \times MHR$$

Where

MHL	$=$	Metabolic heat load	W
$N.E.$	$=$	Number of employees	$-$
MHR	$=$	Metabolic heat rate p.p.	W

Explosives

Explosives are used in deep-level gold mines to charge up drilled holes and blast ore bodies with the purpose of accessing the ore deposits. From previous studies, it was shown that the heat released after blasting was not noticeable in the return ventilation air [22, 33]. Since a large amount of heat energy is released during the blast, it suggests that a portion of the heat energy is released over a prolonged period. This portion of heat energy is transferred to the rock after the blast, rather than manifesting as an instantaneous spike in return air temperature [14].

The ratio between energy being transferred to the rock body and the instantaneous release will differ for various mining techniques. For instances where most of the heat is released rapidly into the ventilation air, it should be considered what portion of heat still needs to be removed after the re-entry period has elapsed. If, on the other hand, most of the heat is transferred to the surrounding rock body, the frequency of blasting needs to be used as the heat release period. Equation 2-20 can be used to calculate the heat produced by explosives.

Equation 2-20: Explosive heat load [14]

$$EHL = \frac{H.P. \times m}{R.P.}$$

Where

EHL	=	Explosive heat load	W
$H.P.$	=	Heat produced by the explosive type	kJ/kg
m	=	Total mass of explosives used	kg
$R.P.$	=	Release period	sec

Oxidation heat

This heat source refers to the process when heat is liberated as fragmented rock in coal or sulphur mines, and comes in contact with oxygen, resulting in oxidation. During oxidation, new bonds form and electrons are released as energy. The atomic weights for these materials are listed below:

$$C\ (Carbon) = 12\ u$$

$$O_2\ (Oxygen) = 32\ u$$

$$S\ (Sulphur) = 32\ u$$

This means that when carbon dioxide (CO_2) forms during oxidation, 0.375 kg of carbon is oxidised for every 1 kilogram of oxygen consumed. Carbon has a calorific value of 33 800 kJ/kg, which means that 12 765 kJ is liberated for every kilogram of pure oxygen consumed. Similar calculations can be performed for sulphur-rich mines [14]. Measuring the oxygen content at the mine entrance and the return will assist in quantifying this heat source. Fortunately such rock oxidation is not a problem in the South African rock formations for deep-level gold mines but may pose a serious concern elsewhere [34].

Rock movement

Although rock (strata) movement is a source of heat, such occurrences are highly unpredictable. Since these occurrences only lead to a short period of heat rise, these sources of heat can be neglected [34].

2.3.4. Geothermal balance (Heat balance)

The final step is to calculate the heat imbalance, also known as the geothermal heat. This source of heat refers to the heat flux from the surrounding rock body and is one of the largest heat sources

in deep-level gold mines. As mentioned previously, this is also the most difficult heat source to calculate, due to the vast number of influencing parameters and information required.

Calculating this heat source as the remainder of the heat (energy) balance from all the previous calculated heat sinks and heat sources enables a quick and accurate heat load determination. Equation 2-21 illustrates this balance.

Equation 2-21: Geothermal heat load balance

$$Geothermal\ heat = Total\ cooling - Autocompression - Electrical\ heat - Mechanised\ heat - Fissure\ water - Compressed\ air - Metbolic\ heat - Explosives - Oxidation - Rock\ movement$$

With the geothermal heat load now known, the heat load study can be concluded, and the next step will focus on verifying the results obtained.

2.3.5. Study verification

To verify the geothermal heat, computer modelling packages will be used. These ventilation modelling tools have the advantage of solving complex networks iteratively, whilst taking a vast number of parameters into account. Detailed simulation models give invaluable information regarding network constraints and allow both a holistic and localised oversight of the network.

Various studies (case studies) support the use of such simulation software for mine ventilation design and ventilation evaluation. A wide variety of computer software packages with such functionality currently exist, with only a few shown in Table 2-3.

Table 2-3: Computer model ventilation software evaluation

Simulation software	Advantages	Disadvantages	Previous case studies
Vuma	- User-friendly - Well known in the industry	- Does not allow for mine ventilation cooling systems to be fully integrated into one model - Steady-state solver	[26, 49, 50]
Ventsim	- User-friendly - Well known in the industry	- Expensive - Steady-state solver	[51, 52]
Process Toolbox (PTB)	- Accurate for mining applications - Can solve for transient application - Applicable for integrated mine ventilation cooling systems	- Fairly new to the market	[53, 54]

To verify the calculated geothermal heat, the complete ventilation system will be simulated using Process Toolbox. Process Toolbox is a transient thermal flow solver. It enables solving complex

systems dependent on a wide variety of parameters, whilst having the functionality of solving various mine cooling- and ventilation systems as an integrated model. The model will be used to serve as a theoretical evaluation, and the fundamental calculations can be viewed in APPENDIX D and APPENDIX G as supplied by the developers of the software.

It takes time (usually numerous required manual measurements) and money to develop detailed simulation models. The method discussed in this study provides an alternative for mines not having the required capital to develop such simulation models. Additionally, this method can also be applied to mines consisting of strict timeframes to meet budgeting cycles (sometimes less than a month), or mines with a short life-of-mine (less than a year).

2.3.6. Cooling shortage/surplus

The cooling shortage or surplus can be quantified through defining the planned reject point and evaluate the difference between the planned- and actual reject point. For such quantification, Equation 2-22 can be used.

Equation 2-22: Cooling shortage

$$Cooling\ \frac{shortage}{surplus} = \dot{m}(h_2 - h_1)$$

Where

$\dot{m}$	=	Current mass flow	kg/s
h_1	=	Current reject enthalpy	kJ/kg
h_2	=	Planned reject enthalpy	kJ/kg

2.3.7. Seasonal impact

Any seasonal changes will impact the heat sinks discussed earlier, and during these final steps, various ambient conditions can be explored to investigate this impact. These variations will assist in maintenance planning schedules to ensure optimal performance is achieved when required.

2.4. Conclusion

This chapter elaborated on the development of a methodology and discussed in detail each step to be taken to determine a heat load study by using an energy balance approach. Figure 2-13 illustrates the summary of all the steps taken during the heat load calculation methodology. The required inputs for determining the heat load of a mine using an energy balance approach can be viewed in Table C-1 under Appendix C. This method will be applied to several case studies and the results evaluated accordingly in the following chapter.

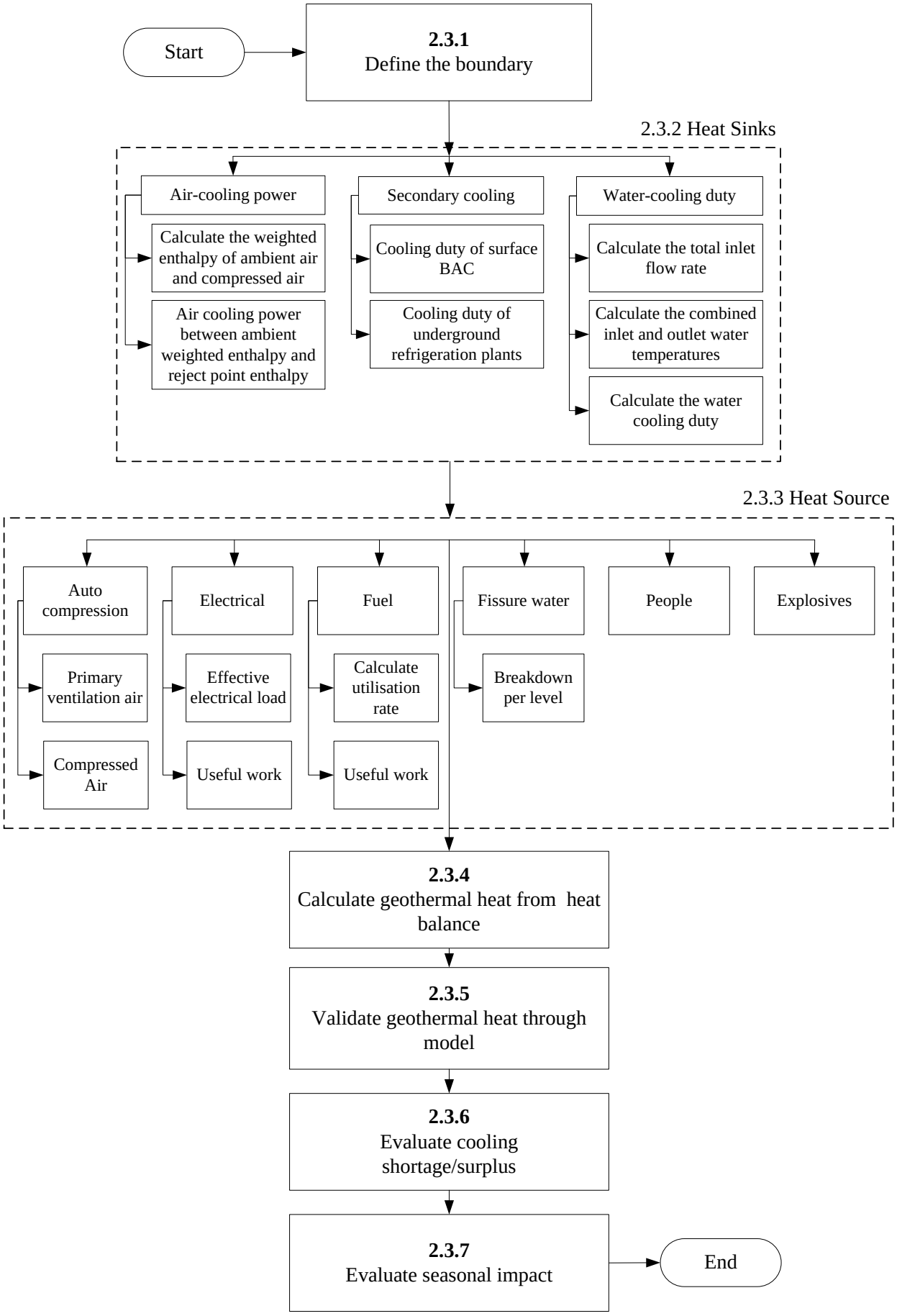

Figure 2-13: Detailed heat load calculation methodology

3

CHAPTER 3

Results and discussions

"However beautiful the strategy, you should occasionally look at the results."

Sir Winston Churchill[3]

[3] The quotation page, http://www.quotationspage.com/quote/40178.html, [2019/11/10]

3. RESULTS AND DISCUSSIONS

3.1. Preamble

In this chapter, the methodology steps (developed in Chapter 2 and shown in Figure 2-13) will be applied to two case studies. The results of each case study will be evaluated in detail and validated accordingly.

3.2. Case study 1: Mine A

3.2.1. Background

Mine A is a deep-level gold mine, situated in the Free State. Figure 3-1 illustrates the orebody layout of Mine A. The orebody consists of between 67 - 69 different reef bands stacked in a fan-shaped sequence. The most cost-effective mining comes from the EA3, EA7 and EA13 (Elsburg) reef bands, as well as the DK4 (Dreyerskuil) reef.

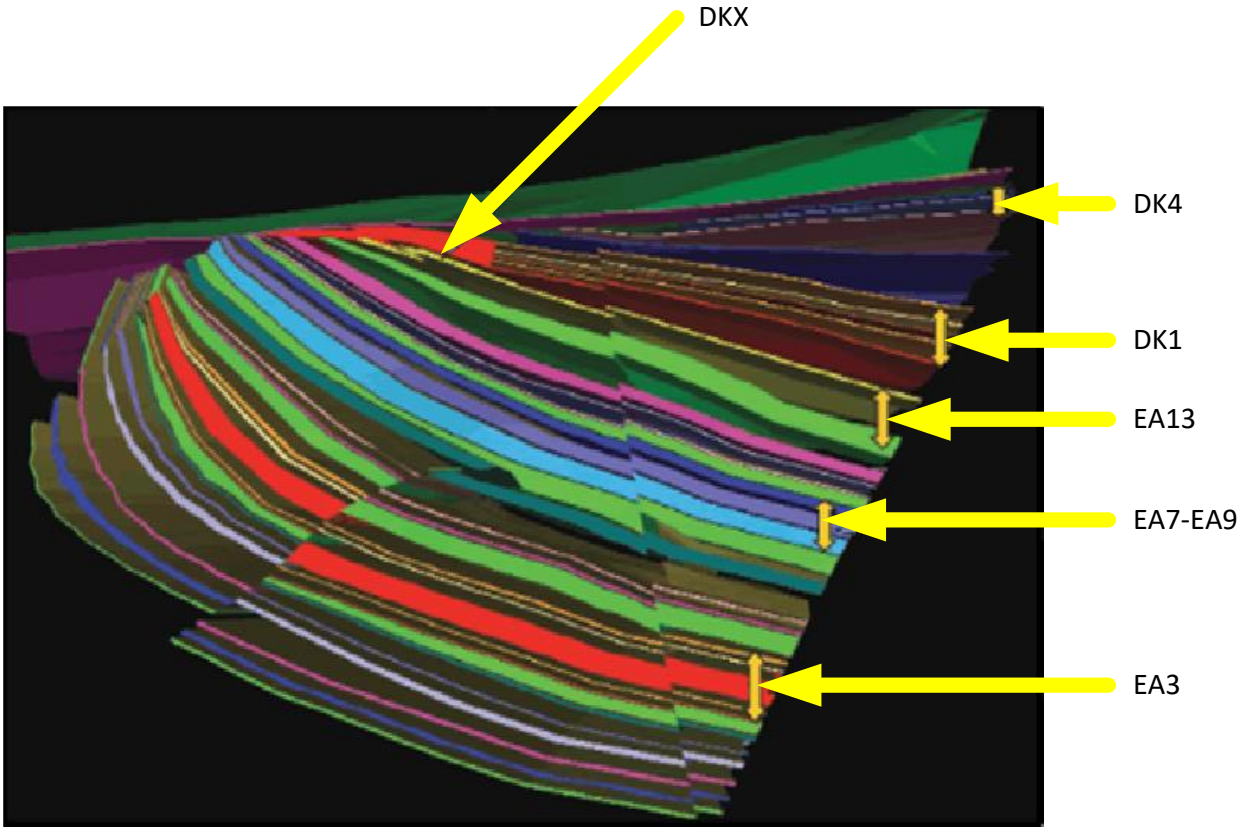

Figure 3-1: Mine A orebody layout

The initial mine strategy in the 1960s was that of conventional narrow reef mining. However, from the 1990s a new deepening project commenced, converting the mine into a mechanised mine,

adapted for ‘massive’ mining techniques [55]. These mining techniques have led to a complex array of ventilation strategies in an attempt to exploit the orebody.

The mining activities are situated approximately 7 360 m from the intake, and fresh air is supplied through two downcast shafts. Air is returned using one axial surface fan, four underground booster fans and numerous fans in tight circuit via a single upcast shaft situated approximately 13 100 m from the nearest reject point.

The mine features underground refrigeration and BACs exclusively through a refrigeration complex situated approximately 2 500 m from the furthest working face. All activities in need of water supply make use of chilled water supplied by the refrigeration plants. The planned reject air temperature for this mine is 29.5℃ $T_{wet-bulb}$ and 31℃ $T_{Dry-bulb}$.

Mining depths extend to close to 3 000 m below surface, with new projects underway to extend these depths beyond 3 000 m. Mined ore is transported mainly through dump trucks to a conveyor system, which in turn transports it to the main shaft where it is hoisted to the surface. Figure 3-2 shows the mine layout and location of key infrastructure.

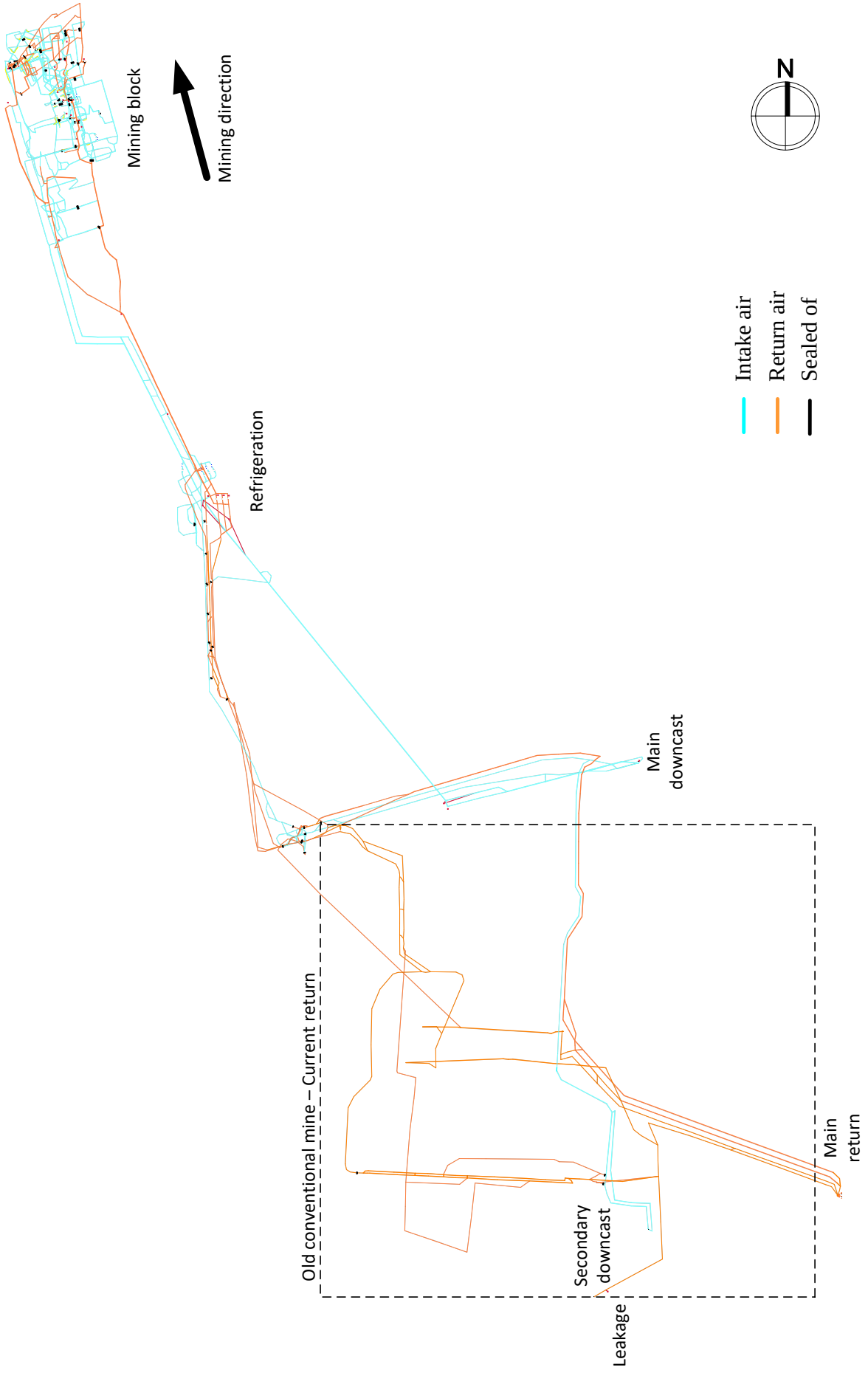

Figure 3-2: Mine A layout (Process toolbox)

From Figure 3-2 it can be seen that the mining direction is continuously moving away from the established return point (upcast shaft), resulting in an ever-increasing ventilation constraint as mining progresses. This is one of the many problems causing excessive heat at Mine A.

Mine A also relies on several old, inaccessible areas as part of its return airways, making inspections of such airways difficult. Some of these airways do not feature proper support and this might lead to potential restrictions in the near future.

3.2.2. Define the boundary

The boundary for the heat load study at Mine A encapsulates all primary mining activities. In Figure 3-3 the boundary entry points were selected to be at the respective downcast shaft intakes and the exit point was taken prior to the condenser circuit. The diagram was also divided into segments for reference purposes.

Although there are people working at the condenser circuits (after the boundary exit point), the worker-to-environment exposure time is kept to a minimum. There are also special cooling chambers supplied for these working conditions where workers can rest and closely monitor the work cycles when conducting crucial maintenance tasks. Larger maintenance tasks are conducted during mine stoppage periods, such as December. The data used for this case study comprises average values for March 2019.

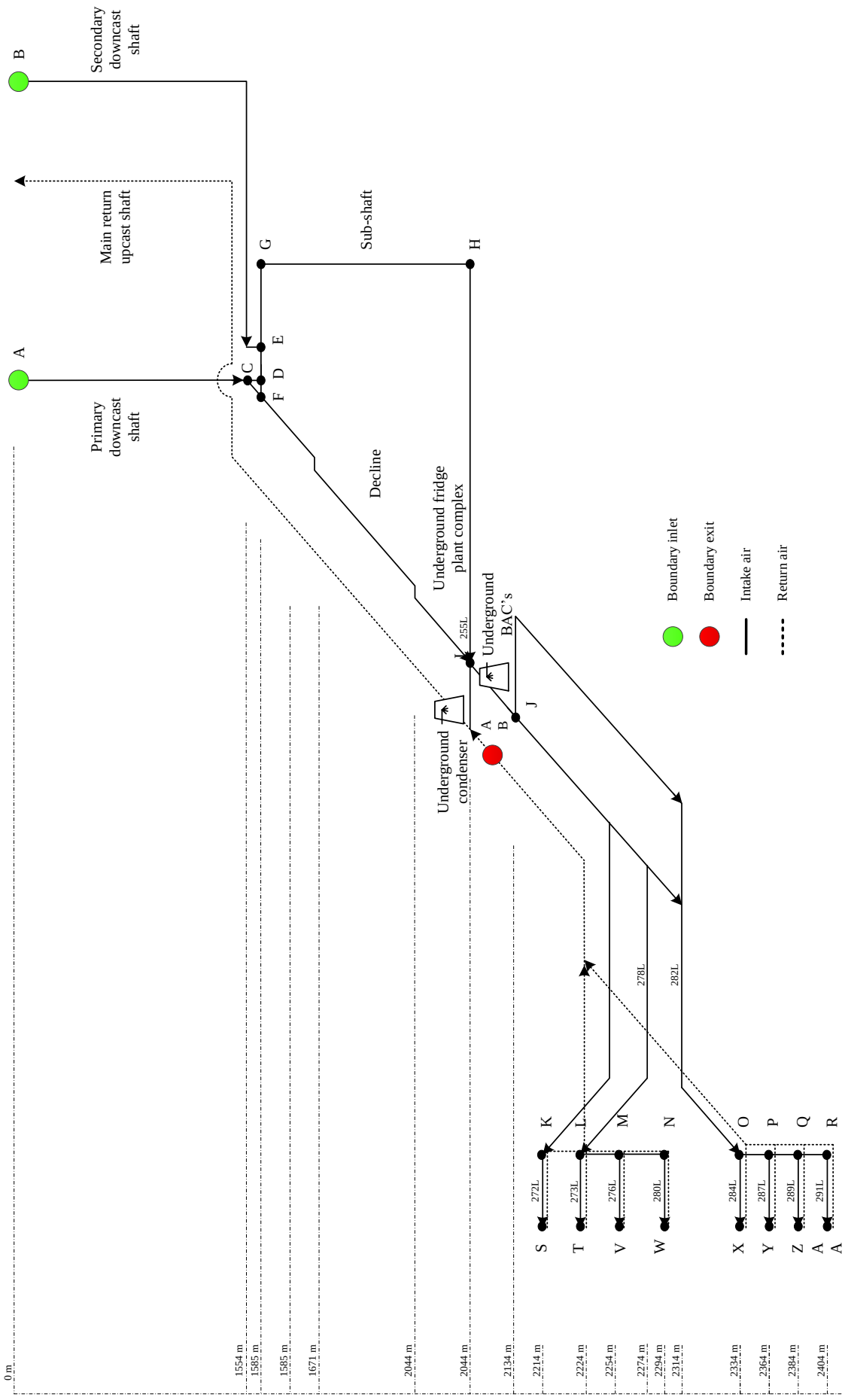

Figure 3-3: Mine A simplified boundary side view layout

3.2.3. Heat sinks in mines

Air-cooling power (ACP)

The first essential cooling component at Mine A is that of natural air cooling. To calculate the ACP of Mine A, Equation 2-2 and Equation 2-3 was used. The typical average summer conditions during March (2019) was used for ambient conditions, as measured by a weather station. Table 3-1 summarises the input values used, as well as the calculated results.

Table 3-1: Air-cooling power (Case study 1)

	Parameter	Unit	Boundary inlet		Boundary exit
			Compressed air	Ventilation air	Reject air
Measured	*Air dry-bulb temperature*	℃	48	22.7	34
	Air wet-bulb temperature	℃	36	17.2	32.5
	Barometric pressure	kPa	666.5	86.5	108
	Air mass flow	kg/s	0.88	231	231
Calculated	*Relative humidity*	%	≈ 0	60	90
	Enthalpy	kJ/kg	48.82	56.32	108.19
	Combined enthalpy	kJ/kg	56.29		108.19
	Combined air-cooling power	kW	**12 591**		

From Table 3-1 it can be seen that the effect of the compressed air at Mine A is negligible. Since surface compressed air units are only used to pressurise the refuge chambers, all other activities requiring compressed air is supplied through underground compressed air units.

Since these underground compressed air units have no air dryers fitted and are situated a distance from the working face, it is assumed that the moisture content would be relatively similar to that of the surrounding air. There will, therefore, be no nett cooling benefit from these units, as was discussed in Chapter 2 of this study.

Secondary cooling

As mentioned, Mine A has underground refrigeration plants and rejects heat in the return airway. This corresponds with scenario 3, as shown in Figure 2-7. The cooling duty of the evaporator plants will, therefore, be used to account for secondary cooling. To calculate the cooling duty achieved by each plant, Equation 2-5 was used for March. The plant utilisation rates were also included to account for any possible downtime which might have occurred.

Table 3-2: Secondary cooling (Case study 1)

Plant	$\dot{m}_{Evaporator}$ $[l/s]$	T_{in} [°C]	T_{out} [°C]	Duty [kW]	Utilisation [%]	Effective duty [%]
Refrigeration Plant 1	56.8	20	12.4	1 811	97.1	1 758
Refrigeration Plant 2	126.8	19.6	12.5	3 642	80.2	2 921
Refrigeration Plant 3	59.2	20.2	12.5	1 863	74.6	1 390
Refrigeration Plant 4	64.6	20.2	12.3	2 144	78.7	1 687
Refrigeration Plant 5	139.8	23.2	15.5	4 479	52.5	2 351
Total						**10 108**

The combined secondary cooling supplied is distributed to various end-users. These users include BACs, cooling cars, narrow-reef hand-held drilling units, as well as the drill rigs used for massive mining.

Water-cooling duty

Mine A does not supply any service water from the surface, although potable water is supplied to underground. The potable water is mainly used by employees for drinking, as well as to ensure that adequate conductivity levels of the condenser water are maintained.

Since none of this water is pumped to the surface to provide a direct cooling benefit, this cooling source has been neglected. The water introduced in the condenser dams also falls outside the boundary perimeter and is evaporated into the return air.

Total heat sinks

The total supplied cooling can, therefore, be calculated using Equation 2-8.

Table 3-3: Summary of heat sinks (Case study 1)

Heat sink	Value [kW]
Air-cooling power	12 591
Secondary cooling	10 108
Water-cooling duty	-
Total heat sinks	**22 699**

The total cooling duty for Case study 1, as shown in Table 3-3, reflects the total average heat load during March 2019. The various heat sources contributing to this total heat will be calculated in the following section.

3.2.4. Heat sources in mines

Auto-compression

The auto-compression for Mine A was calculated using the segments shown in Figure 3-3 in conjunction with Equation 2-10. Table 3-4 shows the calculated values for each segment, accounting for any air leakages as well.

Table 3-4: Auto-compression (Case study 1)

Ref	Elevation entry [m]	Elevation exit [m]	Air mass flow [kg/s]	Enthalpy change [kJ/kg]	Auto-compression [kW]
A-C	0.0	1524.0	234.0	14.9	3491.3
B-E	0.0	1584.0	48.1	15.5	745.9
C-D	1524.0	1584.0	74.3	0.6	43.6
G-H	1584.0	2042.0	71.6	4.5	321.0
C-F	1524.0	1584.0	159.7	0.6	93.8
F-I	1584.0	2044.0	213.3	4.5	960.6
H-J	2042.0	2132.0	60.0	0.9	52.9
I-J	2044.0	2132.0	190.0	0.9	163.7
J-K	2132.0	2242.0	39.8	1.1	42.9
J-L	2132.0	2231.0	66.3	1.0	64.3
J-M	2132.0	2252.0	-31.1	1.2	-36.5
J-N	2132.0	2271.0	21.7	1.4	29.6
J-O	2132.0	2334.0	17.7	2.0	35.0
J-P	2132.0	2312.0	45.4	1.8	80.0
J-P	2132.0	2372.0	21.5	2.3	50.6
J-Q	2132.0	2392.0	40.9	2.5	104.1
J-R	2132.0	2404.0	31.4	2.7	83.6
K-S	2242.0	2192.0	39.8	-0.5	-19.5
L-T	2231.0	2206.0	66.3	-0.2	-16.2
M-V	2252.0	2255.0	-31.1	0.0	-0.9
N-W	2271.0	2321.0	21.7	0.5	10.6
O-X	2334.0	2337.0	17.7	0.0	0.5
P-Y	2312.0	2359.0	45.4	0.5	20.9
Q-Y	2372.0	2379.0	21.5	0.1	1.5
Q-Z	2392.0	2383.0	40.9	-0.1	-3.6
R-AA	2404.0	2408.0	31.4	0.0	1.2
Total					**6321**

In Table 3-4, special attention should be given to the areas where negative auto-compression (decompression) was calculated. This can either be due to a negative flow, as was the case for

segment J-M and M-V, where hot air re-circulated from the return airway (RAW) or caused by change in elevation from a lower point to a higher point. In such instances, care should be taken that the total calculated auto-compression reflects the maximum auto-compression that can be experienced. For this case study it does not pose a problem since the values are small.

Electrical heat

To calculate the electric heat load, the potential energy gained from the electrical equipment was first determined using Equation 2-11. Table 3-5 illustrates the potential energy gained by the ore and water as a result of the electrical equipment.

Table 3-5: Potential gain from electrical equipment (Case study 1)

Parameter	Amount [kg/s]	Elevation gain [m]	Potential energy gain [kW]
Water pumped to the surface	30	2310	678
Rock transported on conveyor	21	790	162
Total			**840**

In Table 3-5, the elevation gained by the water pumped to the surface was calculated from the elevation of the deepest pump station in Mine A. In the case of the ore transportation, the elevation gain was calculated using the start and end elevation of the conveyor belt system. The total potential energy gained needs to be subtracted from the total underground electrical supply.

Additionally, the underground electrical equipment supplied through the surface feeders, but falling outside the boundary of the study, should also be subtracted. Table 3-6 highlights equipment to be excluded from the electrical heat load during Case study 1.

Table 3-6: Equipment to be excluded from effective electrical heat load (Case study 1)

Electric equipment	Design duty [kW]	Quantity	Utilisation [h]	Total design duty [kW]	Duty @ utilisation [kW]
Condenser return pumps	350	4	24	1 400	1 400
Condenser spray pumps	350	4	24	1 400	1 400
Condenser fans	450	4	24	1 800	1 800
FP Motors	1 001	5	24	5 006	4 606
Mining block booster fans	75	12	24	900	900
Total					**10 106**

In Table 3-6 the total design duty was used to calculate the electrical load falling outside the boundary since the inefficiencies resulting in heat also fall outside the boundary. However, in the case of the refrigeration plants, 10% inefficiencies were deducted, since the plants are in the intake

air and the heat from the inefficiencies contribute to the overall heat load. The total electrical heat can be calculated using Equation 2-12 and is summarised in Table 3-7.

Table 3-7: Effective electrical heat load (Case study 1)

Parameter	Value [kW]
Total electric load supplied	15 303
Potential gain	840
Excluded equipment	10 106
Effective electrical heat load	**4 357**

Mechanised machinery

Mine A is a mechanised mine and consists of a wide variety of diesel-powered machinery. As was the case for the electrical heat load, the useful work (potential gain) first needs to be calculated. Equation 2-13 was used and the results are summarised in Table 3-8.

Table 3-8: Potential gain from mechanised equipment (Case study 1)

Parameter	Amount [kg/s]	Elevation gain [m]	Potential energy gain [kW]
Level 1	2.5	-81	-2
Level 2	2.8	-67	-1.8
Level 3	2.7	-18	-0.4
Level 4	1.3	48	1
Level 5	2.6	64	2
Level 6	0.6	86	1
Level 7	0.6	106	5
Level 8	4.6	110	4
Total	**20.9**	**40**	**8**

From Table 3-8 it is seen that the total potential energy gain as a result of the mechanised equipment is relatively small and can be neglected for this case study. Table 3-9 shows the results for the total mechanised heat load using Equation 2-13, as well as the latent heat from using Equation 2-5.

Table 3-9: Mechanised heat load (Case study 1)

Parameter	Unit	Value
Total diesel consumption	$\ell/month$	138 694
Calorific value of diesel	MJ/kg	45.6
Diesel density	kg/m^3	0.85
Daily average	kW	2 036
Vapour ratio	-	5
Heat evaporation of water	kJ/kg	*2450*
Combustion efficiency	*%*	0.95
Multiplication factor	-	2
Latent heat of diesel	kW	1 228
Mechanised heat load	***kW***	**4 072**

In Table 3-9 a utilisation multiplication factor of two has been selected, as recommended by Nixon [46]. This value was verified from collected pre-start-up data of each vehicle, which was translated into an effective utilisation rate, as is shown in Table 3-10.

Table 3-10: Diesel machinery utilisation breakdown (Case study 1)

Machinery	Design duty [kW]	Quantity	Average running hours [h]	Total duty [kW]	Utilisation [%]	Heat @ utilisation [kW]
Sanvik 514	256	5	10.2	1 280	0.42	544
Atlas Copco ST	136	1	10.2	136	0.42	58
Torrow 1400	160	1	10.2	160	0.42	68
Trucks	300	10	12.0	3 000	0.50	1 502
Drill rigs	110	8	2.1	880	0.09	77
Charging-up machines	120	3	1.1	360	0.05	17
Graders	94	2	5.3	188	0.22	41
Forklifts	55	3	5.4	165	0.23	37
AGI cars	264	1	2.4	264	0.10	27
Deutz 1013	200	21	5.4	4 200	0.22	937
Deutz 1914	130	1	5.4	130	0.22	29
4.2 ℓ Toyota (Normal Aspirated)	158	15	5.2	2 370	0.22	513
3.0 ℓ Toyota	150	10	5.2	1 500	0.22	325
Workshops	0	1	0.0	0	0.00	0
Locomotives	51	7	19.0	357	0.79	283
Total						**4 457**

It can be seen from Table 3-10 that the released heat closely relates to the calculated released heat from the diesel consumed, shown in Table 3-9, with an error of approximately 8%. The

multiplication factor of 2 was therefore deemed satisfactory to use. The effective mechanised heat load was calculated using Equation 2-17, and the results are shown in Table 3-11.

Table 3-11: Effective mechanised heat load (Case study 1)

Parameter	Unit	Value
Total mechanised heat	$[kW]$	4 072
Potential gain	$[kW]$	8
Effective mechanised heat load	$[\boldsymbol{kW}]$	**4 064**

Human effect (Metabolic)

To calculate the metabolic heat rate, Equation 2-19 and Equation 2-19 were used, along with an average metabolic heat rate of 250 W, as was discussed during Chapter 2 of this study. Table 3-12 illustrates the calculated results.

Table 3-12: Metabolic heat rate (Case study 1)

Parameter	Unit	Value
Employees	$[-]$	1100
Average metabolic rate	$[W]$	0.25
Metabolic heat load	$[\boldsymbol{kW}]$	**275**

Explosives

Mine A blasts twice a day. The instantaneous heat spike can be neglected since there is an adequate re-entry period. The heat load was therefore calculated from the principle that the heat is transferred to the rock and released over a 12-hour period before the next blast commences. Equation 2-20 was used to calculate the explosive heat load. Table 3-13 illustrates the results.

Table 3-13: Explosives heat load (Case study 1)

Parameter	Unit	Value
Explosives used (monthly)	$[kg]$	68 880
Heat produced per kilogram	$[MJ/kg]$	4030
Blast frequency	$[hours]$	12
Explosives heat load	$[\boldsymbol{kW}]$	**106**

3.2.5. Geothermal balance

The geothermal heat can be calculated as the balance of the heat sinks and heat sources, using Equation 2-21. Table 3-14 illustrates the calculated values for the geothermal heat.

Table 3-14: Geothermal heat load balance

Parameter	Unit	Value
Total heat sinks	[kW]	22 699
Total heat sources (Excluding geothermal heat)	[kW]	15 115
Geothermal heat (heat balance)	**[kW]**	**7584**

The geothermal heat calculated in Table 3-14 represents total heat flux from all the exposed surface rock areas within the boundary perimeter. It is, therefore, this value that will be validated in the next section. Figure 3-4 illustrates the various calculated heat sources.

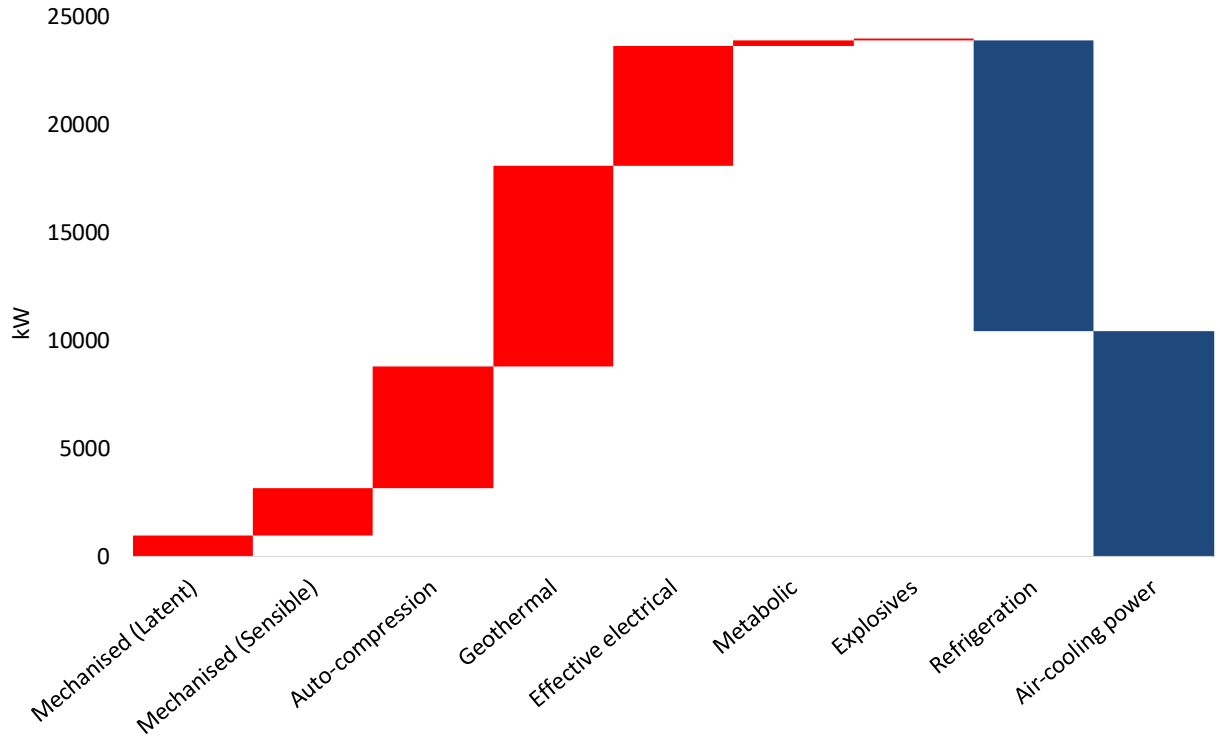

Figure 3-4: Heat load graph of Mine A

Figure 3-4 shows that the heat load is balanced (steady-state) for the evaluated conditions. This balance will be discussed in more detail at a later stage.

3.2.6. Results validation

To validate the results, two approaches will be followed, namely:

1. The current industry approach will be applied to evaluate the geothermal heat
2. Simulation (digital twin) will be used to calculate the geothermal heat

Industry approach

Validating the obtained results for Mine A by using the current industry approach of heat production graphs, proved to be a challenge. With mining commencing nearly 7 360 m from the main shaft, the heat production chart cannot be readily used. The current heat production chart is only suited for a maximum distance of 4 500 m from the shaft.

The heat production lines shown in Figure B-1 was therefore extended through extrapolation, as can be viewed under Appendix B. Using this updated graph shown in Figure B-2, the results obtained are shown in Table 3-15.

Table 3-15: Industry approach results (Case study 1)

Parameter	Unit	Value
Heat production	[kW]	15 273
Auto-compression	[kW]	6 321
Effective electrical heat	[kW]	4 357
Total heat	**[kW]**	**21 594**
Geothermal heat*	**[kW]**	**10 916**

** Using the same calculated heat source breakdown values*

From Table 3-15 it is evident that the heat production approach yields a much higher geothermal value, although this value does not account for the portion of heat contributed by the mechanised machinery. The high tonnage of Mine A leads to the industry approach yielding a much higher geothermal value, although the rock per ratio is, in fact, much greater in a mechanised mine.

Simulation model

A simulation model for the shaft was constructed over a period of three years, as can be seen in Figure 3-2 (Section 3.2.1). To develop the model, mine layouts was used to discretise the model into 2515 nodes and connections as well as including an additional 120 components ranging between fans, ventilation doors, bulk air coolers and seals at the relevant locations.

For more information regarding the PTB solver please refer to APPENDIX D and APPENDIX G respectively. Figure 3-5 illustrates a portion of the un-rendered model and indicates the discretised regions.

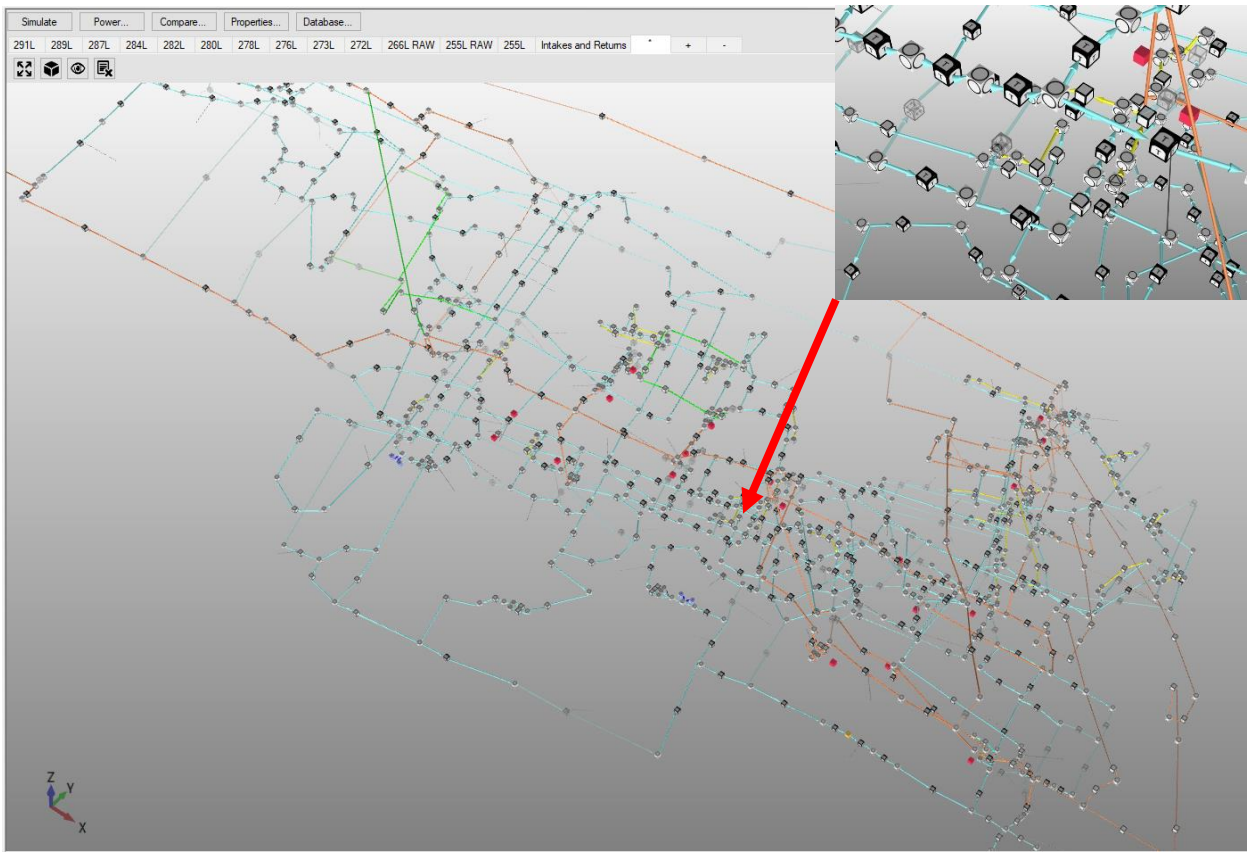

Figure 3-5: Screenshot of a portion of the discretised model (Case study 1)

All airway dimensions were accurately specified and the respective virgin rock temperatures (VRT) supplied as a boundary condition at the various depths for each airway. The haulage exposure time (age) was also accounted for from Mine A's history logs, showing when each haulage was mined. Table 3-16 summarises the rock properties used in the simulation, measured from previous studies to account for the heat transfer between the air and the rock surface.

Table 3-16: Rock properties used for simulation [14, 34, 56, 57]

Parameter	Unit	Value
Predominant rock type	-	Quartzite
Rock density	kg/m^3	2756
Thermal conductivity	$W/m/℃$	6.2
Specific heat capacity	$J/kg/℃$	850
VRT gradient	℃	*20 + 14.6 * depth / 1000*

The PTB simulation model assigns a specific boundary condition (VRT - virgin rock temperature) to an air tunnel as specified by the user for a given depth. The correlation between the depth and respective VRT is based on the virgin rock gradient derived for the Free State area [34]. Additionally, the age of the haulage is also specified in PTB to ensure that the conduction heat transfer coefficient is adjusted accordingly for older haulages [34].

The calculated conduction heat transfer coefficient (based on the number of days the haulage has been exposed to ventilation air, rock thermal conductivity, rock density and rock specific heat) is used to calculate the heat transfer from the virgin rock boundary to the passing air [58].

All external heat sources such as electrical heat or mechanised heat was added by introducing local heat sources across the model connections/nodes where such sources occurred to ensure accuracy. The localised heat sources where determine through underground visits added as a sensible heat component on a node for the respective areas.

To account for the required pressure drops throughout the model, a typical Atkinson's rock wall friction factor of 0.011 $[N/m^4]$ was used on all air haulages [23]. Additional pressure drops caused by obstructions, equipment etc. was accounted for by using door fraction control. This induced a pressure drop by throttling the specified air haulage area. These fractions were calibrated by using manual measurements.

The underground refrigeration complex was also simulated and incorporated into the ventilation simulation model to accurately account for the dynamic underground cooling effect. This allowed for an integrated model where both the ventilation network and refrigeration circuit are interdependent and account for any changes. It was important to specifically consider the dynamic changes in the RAW, since this directly impacts the performance of the condenser circuit and consequently the cooling supplied.

With regards to moisture, the humidity ratio was kept the same as was measured in the RAW of Mine A. This moisture increase was introduced into the working areas through specifying the wet area fraction observed in the workings and is specified accordingly in the solver for each air haulage. This led to an increase in latent heat, reducing the sensible heat. This resulted in a higher temperature difference between the air and the rock, inducing an increase in geothermal heat flow. The main results are shown in Table 3-17.

Table 3-17: Simulation results (Case study 1)

Parameter	Unit	Value
Total heat	[kW]	22 997
Electrical heat to be excluded	[kW]	4 357
Mechanised	[kW]	4 072
Metabolic	[kW]	275
Explosives	[kW]	106
Auto-compression	[kW]	6321
Geothermal heat (heat balance)	**[kW]**	**7874**

Table 3-17 shows that there is a relatively small error when compared to the initial calculated geothermal heat by using the energy balance approach. These results show that the geothermal heat can be accurately and easily calculated using the energy balance method, especially in mines where such digital twins have not yet been successfully established. The auto-compression used was selected at the specified depth in the model.

3.2.7. Cooling shortage/surplus

To account for the current cooling shortage with respect to the planned reject temperature, Equation 2-22 can be used. The results for an air mass flow of 231 kg/s are shown in Table 3-18.

Table 3-18: Cooling shortage/surplus (Case study 1)

Parameter	Unit	Currently	Planned
Dry-bulb reject temperature	[℃]	34	31
Wet-bulb reject temperature	[℃]	32.5	29.5
Cooling shortage	**[kW]**	**3 578**	

The cooling shortfall is the theoretical additional cooling required to obtain the planned reject conditions. This, however, does not account for any system inefficiencies and should be adjusted. This can be done under the assumption that only 80% of the air will reach the intended workplace, as discussed in Chapter 2.

It is also important to note that the point where such cooling is introduced is critical. The closer this cooling can be introduced to the working area, the greater the impact it will have, since extended distances between the working area and the point of cooling will lead to an increase in heat flow from the rock.

3.2.8. Seasonal impact

Evaluating the seasonal impact enables adequate planning with regards to the maintenance of critical components. Table 3-19 illustrates the local weather conditions of Mine A, as was obtained by a local weather station measuring point.

Table 3-19: Monthly ambient seasonal weather conditions (@ 86.5 kPa)

Parameter	Jan	Feb	Mar	Apr	May	Jun	Jul	Aug	Sep	Oct	Nov	Dec
Dry-bulb temperature [℃]	24.3	22.5	22.7	17.3	15.2	12.3	11.8	13.2	16.4	20.4	22.3	25.7
Relative humidity [%]	52.6	63.9	59.8	72.1	51.5	44.2	44.0	38.8	30.2	36.9	38.7	36.2

Using the ambient weather conditions shown in Table 3-19, the variable surface air-cooling power for Mine A can be calculated. However, Mine A only consists of underground refrigeration at approximately 2 000 m below surface. As a result of the thermal flywheel effect, the variable seasonal conditions should be determined prior to the underground refrigeration.

This underground seasonal impact can be measured (prior to underground refrigeration) and used to determine a new air-cooling profile. Since these measurements were not taken for a complete year cycle, the simulation software was used to determine the underground conditions accordingly, although this can easily be measured. Figure 3-6 illustrates the underground seasonal impact prior to the refrigeration complex situated approximately 2 000 m below surface.

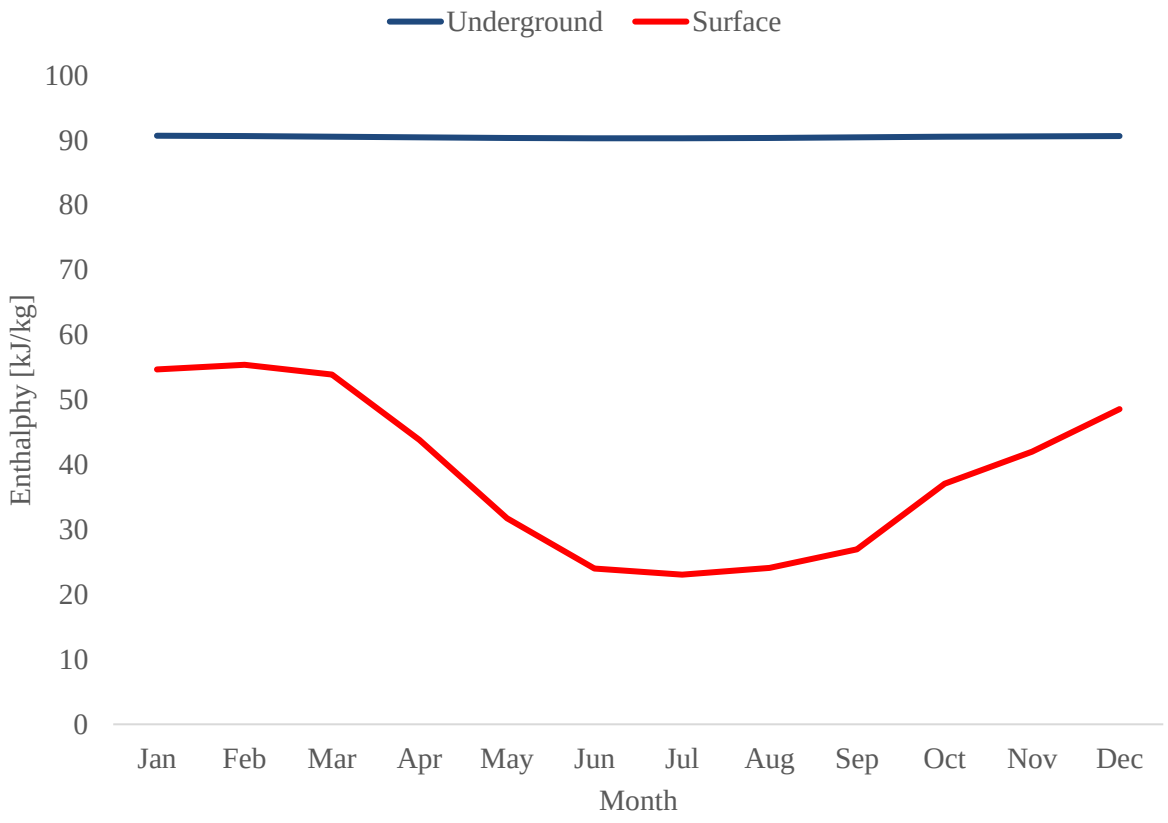

Figure 3-6: Underground seasonal effect at refrigeration complex (Case study 1)

From Figure 3-6, it is evident that the seasonal impact is negligible at the refrigeration complex inlet as a result of the thermal dampening (thermal flywheel). The refrigeration load can, therefore, be calculated using the current secondary cooling, along with the calculated cooling shortage. This can only be done under the assumption that the cooling shortfall is introduced as close as possible to the working areas and, therefore, directly affecting the reject temperature. Figure 3-7 illustrates the required cooling (broken up between the refrigeration complex's load and the cooling required to be introduced in the working areas) and the actual cooling.

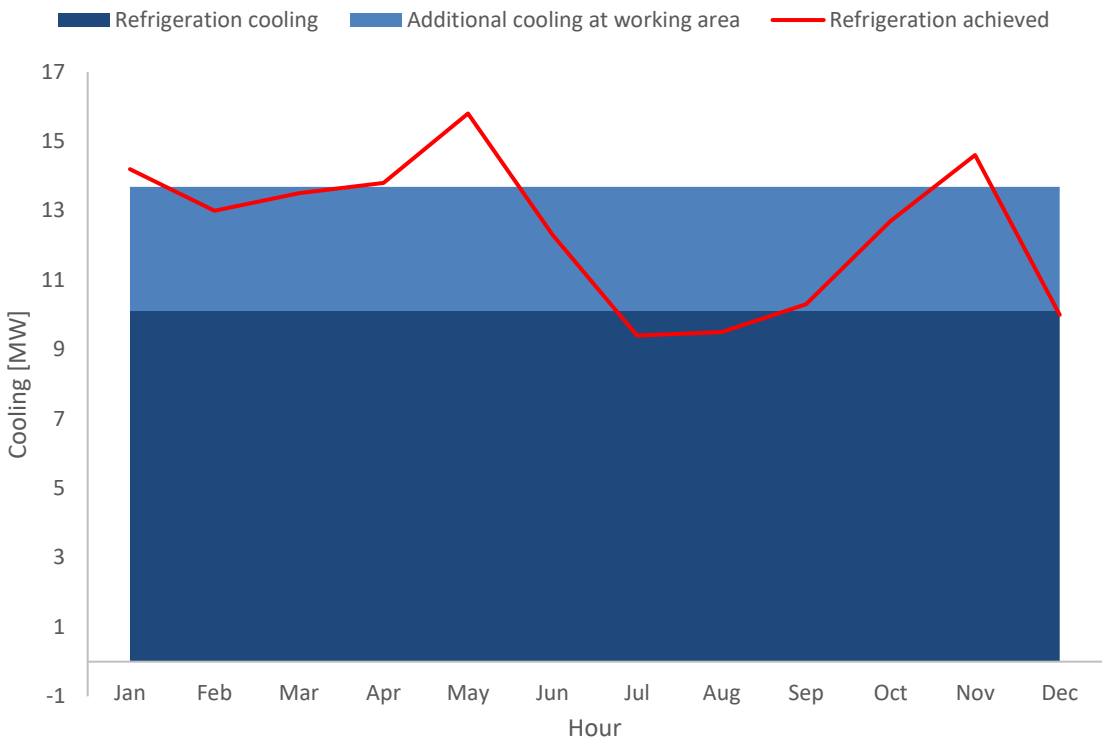

Figure 3-7: Required versus actual refrigeration demand (Case study 1)

From Figure 3-7 it can be seen that the cooling supplied for certain months exceeds that of the demand, although this is all introduced through the refrigeration complex. There are also months where the supplied cooling does not reach the cooling demand. This will necessitate more accurate planning to ensure this is achievable.

Evaluating the energy cost for an average refrigeration coefficient of power (COP) of 3 the importance of effective cooling becomes apparent. The results are shown in Table 3-20.

Table 3-20: Energy cost comparison – Required vs achieved cooling (Case study 1)

Parameter	Summer	Winter
Achieved cooling	R16 286 988	R7 407 531
Required cooling	R 17 014 435	R 9 747 193
Energy cost difference p.a.	**R 3 067 109**	

In Table 3-20, the increase in cooling cost is shown to reach the respective planned reject temperature. However, there will be a margin of inefficiency and the cost shown is therefore for a best-case scenario and will increase proportionally to the system's cooling inefficiency.

3.2.9. Results discussion

The main results obtained from Case study 1 for each approach are shown in Table 3-21.

Table 3-21: Case study 1 results summary

Parameter	Unit	Energy balance	Industry approach	Simulation Model
Total heat	[kW]	22 699	21 594	-
Geothermal heat	[kW]	7584	10 916	7874
Total error *(Compared to energy balance approach)*	%	-	**5.3 %**	-
Geothermal error *(Compared to energy balance approach)*	%	-	**19.6**	**3.8 %**

From Table 3-21, when comparing the results of the energy balance approach to that of the simulation model, the results deliver a very small error. For more details regarding the sensitivity of the parameters used, please refer to APPENDIX H.

The industry approach could initially not be used since the heat production graph did not allow for mining distances from the shaft in excess of 4500 m. Through extrapolating the graph, as shown in Appendix B, the industry approach could be executed. However, from Table 3-21 it is evident that the industry approach, through using heat-prediction graphs, yields a substantially higher geothermal value, even though the total heat calculated does not differ much.

These results, therefore, show that the heat-prediction graph over-allocates heat towards the geothermal heat source component, whilst under-allocating the equivalent heat to that of mine mechanisation. This can be attributed to the fact that the empirical data set of the heat-prediction graph translates tonnage to a certain rock surface exposure (tunnel length) since, in conventional mining, a stoping panel can only yield a certain number of tonnes. In a mechanised mine, such as Mine A, much greater volumes of ore can be removed from massive stopes with a smaller rock surface exposure area.

These results show that the energy balance can successfully be used for evaluating the heat load of a mechanised mine, and verified that, when extrapolating the heat production graph, the various heat sources are misrepresented. The results obtained from the cooling seasonal impact show that at the given depth the refrigeration complex is situated, there is little to no effect from seasonal changes. The required cooling demand was therefore calculated, and by using the cooling shortfall, showed that an annual expenditure of approximately R3 million will be required in energy cost to address this shortfall.

3.3. Case study 2: Mine B

3.3.1. Background

Mine B is situated in the Free State where shaft-sinking operations commenced as early as 1969. Conventional narrow reef mining techniques are practised (accessed through compressed air hand-held drilling), with the shaft nearing the end of its life span. Currently mine B is mining the high-grade shaft pillar, which results in concentrated mining activity close to the main shaft.

Key challenges entails ventilating extended face lengths, as old stoped are interconnected when the pillar is removed, highlighting the importance of in-stope control measures. The sub-vertical shaft, extending to 107L, has already been flooded to below 75L and required constant dewatering as a result of high fissure water influx. Figure 3-8 illustrates the model layout of Mine B.

Figure 3-8: Mine B model layout (Process toolbox)

Fresh air is supplied through two downcast shafts, which is interconnected with various surrounding shafts. Air is return at Mine B through a single up cast shaft equipped with two large centrifugal surface fans. A small number of underground fans, in a tight circuit, assists in ventilating the shaft, with the planned reject wet-bulb temperature being 29.5℃.

Refrigeration on surface serves as a dedicated supply to the surface BAC, whereas the cold water supplied by the underground plants are used to supply an underground BAC unit and supply mining activities.

3.3.2. Define the boundary

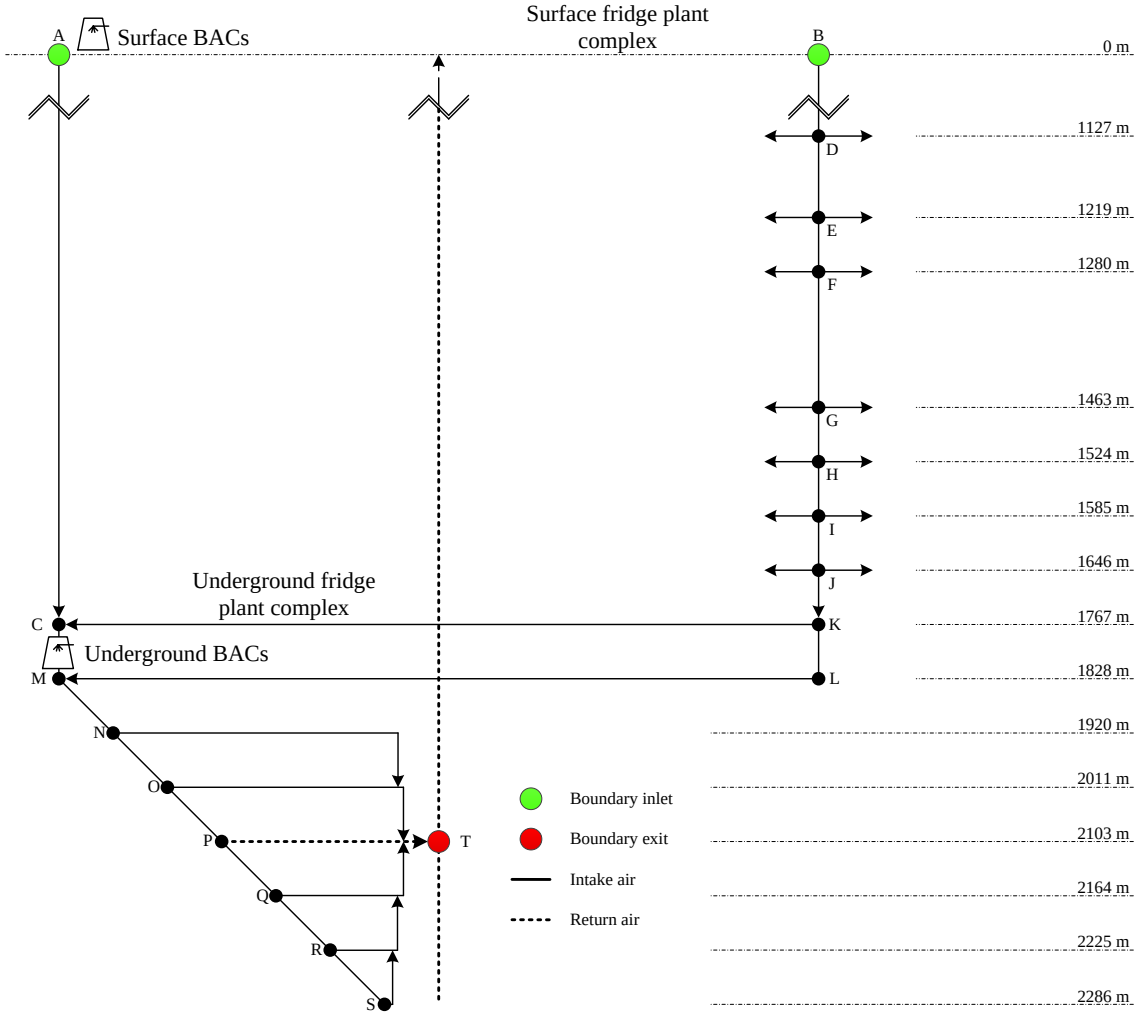

Figure 3-9: Mine B simplified boundary side view layout

As can be seen in Figure 3-9, mining commences to a depth of 2 286 m. All air is returned through one level towards the upcast shaft. To prevent unnecessary duplication, only the methodology steps unique to Mine B will be shown in this section, with the remainder of the steps available under Appendix E.

3.3.3. Heat sinks in mines

Air-cooling power (ACP)

Mine B consists of two large operating compressors on the surface, supplying all compressed air activities underground. The combined surface enthalpy is calculated, with the ACP, in Table 3-22.

Table 3-22: Air-cooling power (Case study 2)

	Parameter	Unit	Boundary inlet		Boundary exit
			Compressed air	Ventilation air	Reject air
Measured	*Air dry-bulb temperature*	℃	40	22.7	33
	Air wet-bulb temperature	℃	39	17.2	29.6
	Barometric pressure	kPa	561.5	86.5	107.4
	Air mass flow	kg/s	14.5	243	243
Calculated	*Relative humidity*	%	≈ 1	59.8	78
	Enthalpy	kJ/kg	59.35	53.7	93.45
	Combined enthalpy	kJ/kg	54.2		93.45
	Combined air-cooling power	kW	**9 658**		

The ACP, illustrated in Table 3-22, excludes the effect of the surface BAC, which will be evaluated during the secondary cooling section. The total mass flow for the ACP was used and calculated per section, shown in Figure 3-9. The detailed breakdown can be viewed under Appendix E.

Secondary cooling

Mine A reflects both scenario 1 and scenario 3, as discussed in Chapter 2. The results of the combined secondary cooling effect can be seen in Table 3-23.

Table 3-23: Secondary cooling (Case study 2)

Plant	$\dot{m}_{Evaporator}$ $[l/s]$	T_{in} [℃]	T_{out} [℃]	**Duty** [kW]	**Utilisation** [%]	**Effective duty** [%]
Refrigeration plant 1	50.7	15	7.2	3 583	60	2 149
Refrigeration plant 2	146.7	23	14.9	3 682	59.9	2 206
Sub-total						**4 355**
BAC	$\dot{m}_{airflow}$ $[kg/s]$	H_{in} $[kJ/kg]$	H_{out} $[kJ/kg]$	**Duty** [kW]	**Utilisation** [%]	**Effective duty** [%]
Surface BAC	195	56.32	37.56	3 658	23	839
Sub-Total						**839**
Total						**5 194**

Total heat sinks

The total cooling supplied can, therefore, be calculated using Equation 2-8, as shown in Table 3-24.

Table 3-24: Summary of heat sinks (Case study 2)

Heat sink	Value [kW]
Air-cooling power	9 658
Secondary cooling	5 194
Water-cooling duty	-
Total heat sinks	**14 876**

The next sections will calculate all the relevant heat sources at Mine B.

3.3.4. Heat sources in mines

Fissure water

Mine B struggles with large quantities of fissure water at the lower levels. The heat effect thereof was evaluated using Equation 2-7 and the results are shown in Table 3-25.

Table 3-25: Fissure water (Case study 2)

Plant	$\dot{m}_{Evaporator}$ $[l/s]$	T_{in} [°C]	T_{out} [°C]	**Duty** [kW]
Source 1	18	65	29.6	2 672
Source 2	10	35	29.6	230
Sub-total				**2 901**

As mentioned earlier, the remainder of the heat sources were calculated using the same approach as illustrated during Case study 1. All the relevant inputs and calculation results for these steps can be viewed under Appendix E. Table 3-26 shows a summary for each of the various calculated heat sources.

Total heat sources

Table 3-26: Summary of heat sources (Case study 2)

Parameter	Unit	Value
Auto-compression	[kW]	6 782
Effective electrical heat	[kW]	2 353
Effective mechanised heat	[kW]	29.4
Fissure water	[kW]	2901
Metabolic heat	[kW]	185
Explosive heat	[kW]	23
Total heat sources (excluding geothermal heat)	**[kW]**	**12 274**

Using the heat sources (Table 3-26), the energy balance (geothermal heat) can now be determined.

3.3.5. Geothermal balance

Table 3-27 illustrates the geothermal heat from the known heat sinks and heat sources calculated as the nett energy balance.

Table 3-27: Geothermal heat load balance (Case study 2)

Parameter	Unit	Value
Total heat sinks	[kW]	14 876
Total heat sources (excluding geothermal heat)	[kW]	12 274
Geothermal heat (heat balance)	**[kW]**	**2 602**

Figure 3-10 illustrates the various heat sinks and heat sources, shown in Table 3-27 through the waterfall graph.

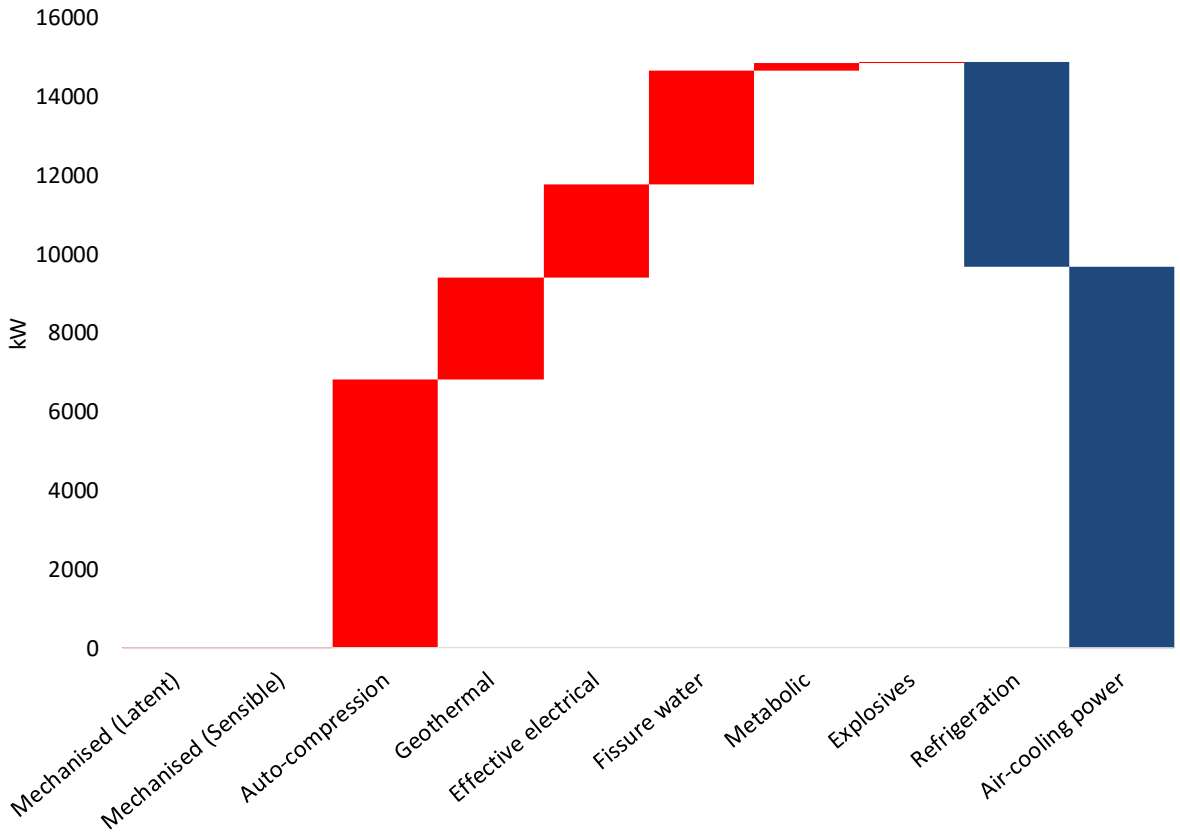

Figure 3-10: Heat load graph of Mine B

3.3.6. Result validation

The result validation will be performed in the same fashion as during Case study 1.

Industry approach

Mining at Mine B commences relatively close to the shaft, although air has to travel extended distances in a circular pattern to reach the working face. These distances were calculated to be 3 240 m, with a mean VRT set at 50.6℃ and a tonnage yield of 17 282. Using the heat-production graph shown in Figure B-1, the obtained values can be seen in Table 3-28.

Table 3-28: Industry approach results (Case study 2)

Parameter	Unit	Value
Heat production	[kW]	3 836
Auto-compression	[kW]	6 782
Fissure water	[kW]	2 901
Total heat	**[kW]**	**13 519**
Geothermal heat	**[kW]**	**1 482**

From Table 3-28, the industry approach yields a much lower geothermal value due to the low quantity of ore mined. This low value will be discussed in the result-discussion section for Case study 2.

Simulation model

The digital twin of Mine B was developed in a similar fashion to that of Mine A, using the rock properties discussed in Table E-8. The mine haulages, as received from the planning department and verified through extensive underground visits, was discretised into 1981 sections, and adjusted for the specific VRT and haulage age factor. Three airflow boundaries were specified namely the inlet conditions of the two downcast shafts as well as the exit boundary for the upcast shaft. Figure 3-11 illustrates a portion of the discretised model for case study 2.

For more information regarding the PTB solver please refer to APPENDIX D and APPENDIX G respectively. Also, refer to the simulation section in case study 1 for more clarity on how the model was constructed.

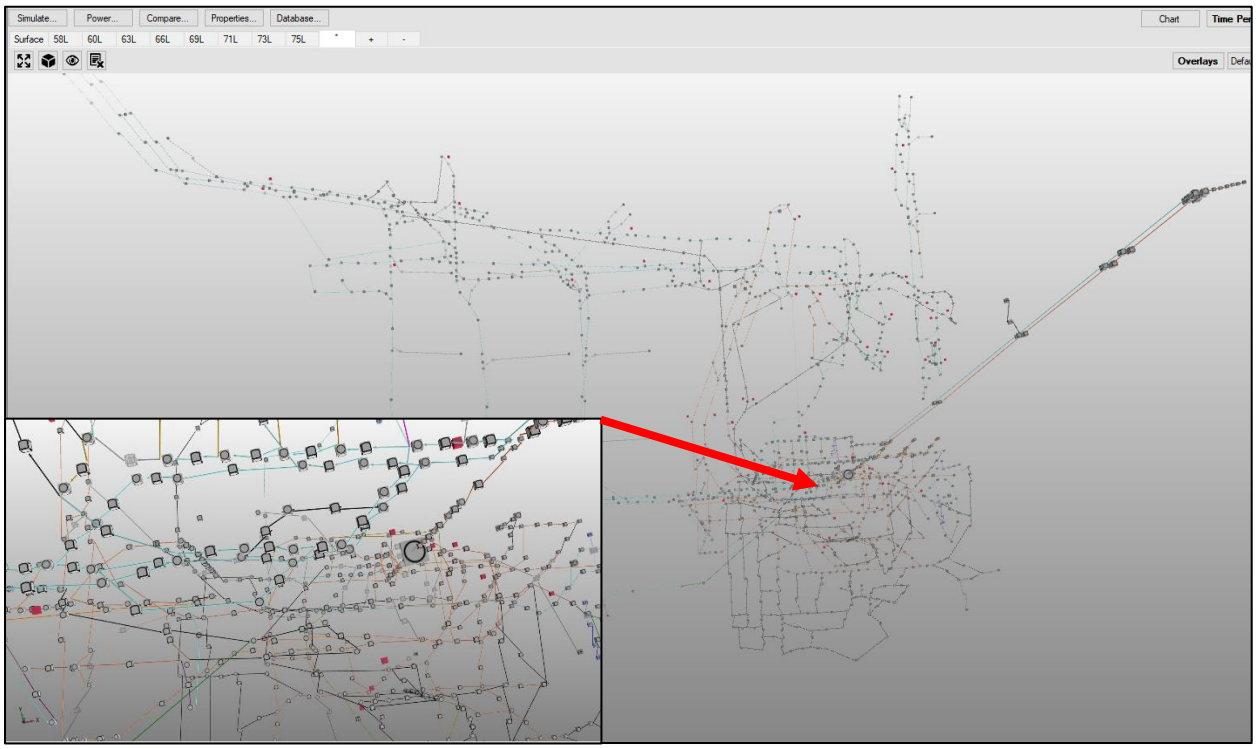

Figure 3-11: Screenshot of a portion of the discretised model (Case study 2)

The various heat sources, as was shown in Table 3-26, were incorporated into the model through allocating the respective sources to the regions in the model where they were identified. The main results are shown in Table 3-29.

Table 3-29: Simulation results (Case study 2)

Parameter	Unit	Value
Total heat	[kW]	15 075
Auto-compression	[kW]	6 782
Excluded electrical heat	[kW]	5 487
Geothermal heat (heat balance)	**[kW]**	**2 806**

The results shown in Table 3-29 account for all the forms of heat introduced at the respective locations, as well as reflect a corresponding humidity increase through introducing moisture (at 20%) at the working areas, as well as small amounts of moisture throughout all haulages.

3.3.7. Cooling shortage/surplus

Since the measured reject temperature is 0.1℃ from the planned reject temperature, there is no need to calculate the air-cooling shortage/surplus for Mine B.

3.3.8. Seasonal impact

The ambient surface conditions for Mine B is similar to that of Mine A and can be viewed under Table 3-19. Using this variable ambient air-cooling profile, the refrigeration requirements can be deduced. Figure 3-12 illustrates the required refrigeration demand for a period of one year versus the actual achieved cooling.

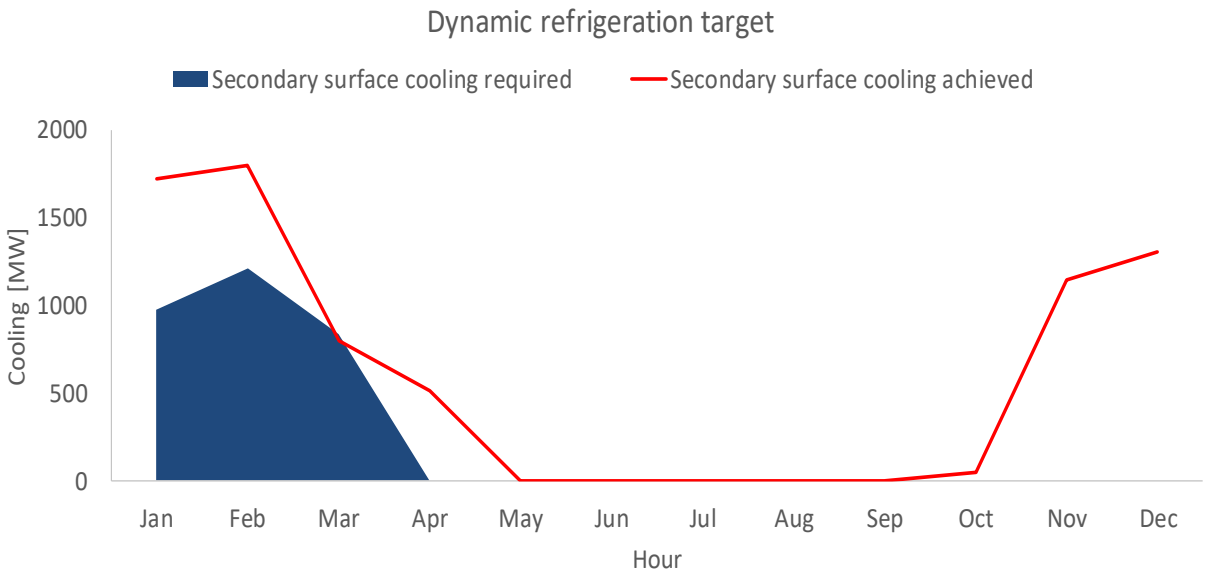

Figure 3-12: Secondary cooling required at Mine B

From Figure 3-12 it is evident that no secondary cooling is theoretically required in the colder winter months, as has also been proven by the actual achieved cooling. However, it should not be necessary to introduce any surface cooling for the measured ambient conditions during November and December. Table 3-30 summarises the energy cost implication of the difference between the required cooling and the actual cooling achieved for a COP of 5.5 for both a pure theoretical case and a safety factor of 10%.

Table 3-30: Energy cost comparison - Required vs achieved cooling (Case study 2)

Parameter	No safety margin		10% safety margin	
	Summer	**Winter**	**Summer**	**Winter**
Required cooling [kW]	61	0	314	0
Achieved cooling [kW]	148	0	148	0
Energy cost difference p.a.	**R324 518 (Saving)**		**R617 540 (Expense)**	

From Table 3-30 it is clear that large potential savings exist should the ventilation inefficiencies be addressed, and secondary cooling reduced accordingly.

3.3.9. Result discussion

The main results obtained for each approach from Case study 2, are shown in Table 3-31.

Table 3-31: Case study 2 results summary

Parameter	Unit	Energy balance	Industry approach	Simulation Model
Total heat	[kW]	14 876	13 519	15 075
Geothermal heat	[kW]	2 602	1 482	2 806
Overall error *(Compared to energy balance approach)*	%	-	**9.1%**	**1.3%**
Geothermal error *(Compared to energy balance approach)*	%	-	**43 %**	**7.3%**

Table 3-31 highlights the fact that there is a good correlation between the simulation model and that of the energy balance approach. However, when using the heat-prediction graphs, the heat load of Mine B greatly differs from the obtained results of the energy balance approach and simulation model. For more details regarding the sensitivity of the parameters used, please refer to APPENDIX H.

Mine B is currently conducting shaft pillar mining, and the low tonnage produced serves as the main driver for the misrepresented size of the mine. The chosen route to access the ore body is still in the vicinity of 3.2 kilometres from the station to the mean intake of the active levels, which would normally not be the case, since this adds geothermal heat to the ventilating air. This increase in distance and the additional air downcasted from an adjacent shaft are the main contributors to the higher than anticipated geothermal heat value.

As was the case during Case study 1, there is a distinct disconnect between the cooling demand and the supplied cooling. Table 3-30 highlighted the potential in energy cost saving should the ventilation strategies be optimised for optimal cooling. It is therefore not advised to use heat-prediction graphs for mines which greatly differ in nature to the typical conventional grid mine. Also, it should be remembered that the heat-prediction graphs where developed on full production mines and not mines nearing the end of their life cycle.

3.4. Conclusion

A heat load was determined for two case studies using an energy balance approach. The results were evaluated and shown that a heat load for a mine can be successfully determined by using the energy balance approach.

The industry approach of using heat-prediction graphs was also performed to enable a comparison between the obtained heat load values. However, for instances where the case studies consisted of parameters outside the range of the heat-prediction graphs, it was shown that significant errors will be made through applying the industry approach.

The causes of the error size were discussed in depth during the result discussion of each case study, with the most common reason being that the mining operations fall outside the boundary parameters of heat-prediction graphs.

A simulation model was developed for each case study to validate the values obtained from the energy balance approach. It was shown that a good correlation was obtained between the energy balance approach and that of the simulation models, which catered for all forms of heat added to the respective locations in the model.

4

CHAPTER 4

Industry application

"Knowledge without application is like a book that is never read"

Christopher Crawford[4]

[4] Good reads, https://www.goodreads.com/quotes/tag/application, [2019/11/10]

4. INDUSTRY APPLICATION

4.1. Preamble

The heat sinks and heat sources in a mine form part of a complex thermodynamic system and as the name implies is dynamic by nature. Understanding and evaluating such a system only statically will either lead to a large cooling shortfall or major oversupply. Since the system is constantly changing, the underground environment should be evaluated in a similar dynamic approach [37].

Currently, as mentioned previously during the introduction to this study, heat loads are estimated for a mine on an annual basis. The aim of this exercise is to establish the required cooling that needs to be supplied to mitigate the heat load for current reject conditions, as well as the planned reject conditions. However, this static approach contradicts the nature of mining. To merely increase the frequency of such a study directly results in an increase in repetition which might lead to strain on the daily tasks of the ventilation engineer.

In an article issued by Deloitte [59] and a case study performed on a uranium mine [60] it is clear that with Industry 4.0 on the horizon, the South African mining industry is yet to discover how this new technological front will form part of its day-to-day operations. Facing many social challenges, the adoption of this new technology needs to be a guided process whereby the value is realised up to the level of the miner. This will ensure these technological advances serve as a real alternative to previous outdated approaches.

To guide this integration process of new technological advances, a model tailored for the mining industry needs to be implemented [61]. One such approach is that of a data-information-knowledge-wisdom (DIKW) model, as seen in Figure 4-1.

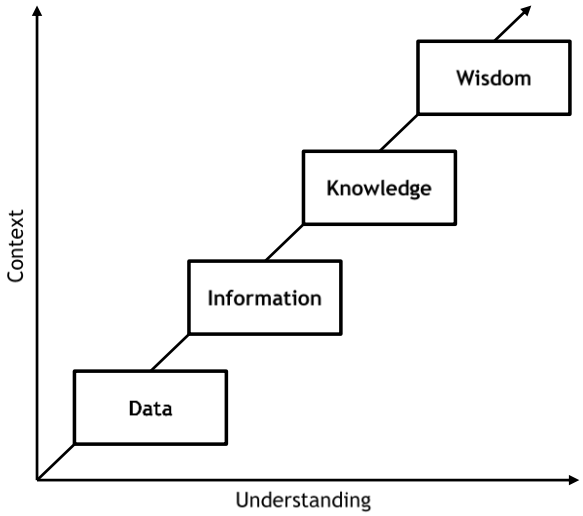

Figure 4-1: DIKW Model [62, 63]

Figure 4-1 highlights that to fully understand and have complete context of a problem, data needs to be translated into wisdom which will deliver actionable steps to address the problem.

In a study conducted by Pretorius JG *et al*. [61], it was proven that significant improvements were realised by implementing an effective reporting platform on the cooling circuit of a mine. In much the same fashion, substantial benefits can be realised in understanding and reporting on daily heat sources to allow the ventilation engineer and management to have an improved understanding of the nature of the heat sources and how to mitigate it.

The methodology in the next section will elaborate on how this model can be used as a roll-out strategy for the mining industry.

4.2. Methodology

The methodology is focused on implementing the DIKW model with the aim of obtaining wisdom of the system which can lead to clear actionable tasks daily. The method is therefore divided into the four pillars of the DIKW model highlighted in Figure 4-1[63].

4.2.1. Data

Today a wide variety of technology is available on the market, specifically designed to monitor/analyse the ventilation network of a complex system such as a mine. These indicators assist in continuously monitoring the system and lead to an improved understanding of how various sub-systems interact with one another and which systems are parameters are sensitive to change. To understand where these technologies need to be implemented it is important to first understand the basic ventilation network layout of a mine. Figure 4-2 illustrates such a simplified layout, indicating the location of bulk air coolers (BACs) and return airways (RAWs).

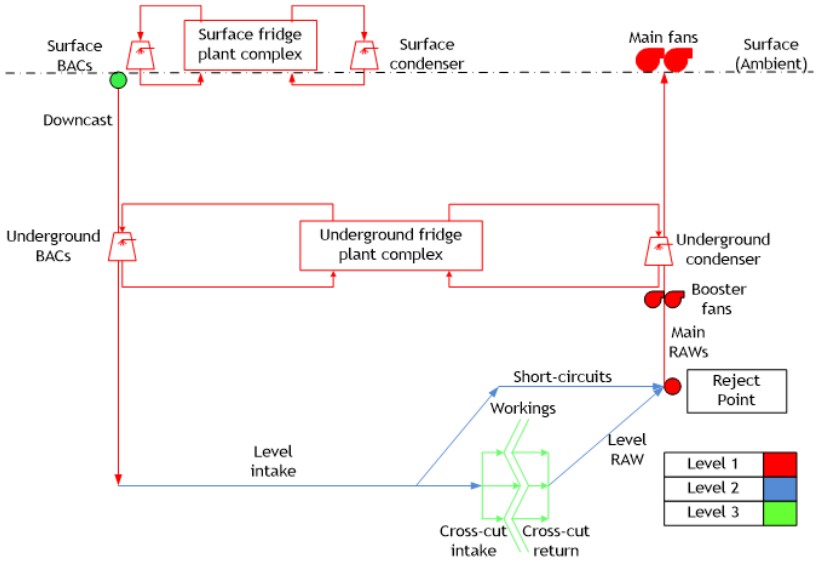

Figure 4-2: Basic mine ventilation flow diagram [14]

From Figure 4-2 it is evident that numerous components play a role in the ventilation network of a mine. The figure shows the boundary inlet (green dot) and boundary exit (red dot) and highlights the various levels of data collection. Table 4-1 summarises these various data levels.

Table 4-1: Data acquisition detail level

Level	Description	Data Points
Level 1	Aimed at holistically evaluating the mine. It gives valuable insight into global problems and highlight system constraints such as inadequate cooling infrastructure. This data-level approach can, therefore, be implemented to verify if the current infrastructure is adequate. This will also give valuable insight into thermodynamic damping effect "thermal flywheel" and the expected response rate of such damping.	Ambient air conditions, fridge plants, BACs, main return airway, intakes airways and main fans
Level 2	Focuses on specific mining levels. This approach is specifically useful to determine how the intensity of mining processes are distributed and where additional infrastructure needs to be introduced. Applying this level of data collection will highlight sub-standard supply conditions places.	Level returns, Level intakes, Level specific cooling.
Level 3	Focus on specific workplaces and gives valuable insight into daily activities and task concentration. This also assists in the monitoring of the efficiency of ventilation appliances	Cross-cut intakes/return airways (RAW), fridge plants, mobile coolers.

At each of the mentioned data levels, energy flows in various forms that need to be measured. In most instances, the main form of energy will be heat transported to the air and it is crucial that the psychometric properties of the air are measured [34]. In instances where heat is transferred from the boundary other than through air (e.g. return water from the BAC) the energy transferred can be monitored through instrumenting the specific energy stream.

In most instances, mines implement supervisory control and data acquisition (SCADA) systems without utilising such systems to their full potential [61]. Ideally having a mine comply with all three these levels will enable precise heat load source breakdown and cater for the specific needs at each work station. However, implementing such a system can be a costly and timeous undertaking and should rather be phased in gradually.

In cases where capital is not available for such instrumentation roll-out phase, key points can be instrumented in conjunction with implementing a dynamic thermal model to account for unmeasured points [14]. These models bridge the gap between the unknown and the immeasurable and give valuable insight into daily operational constraints.

As part of this phase-in-plan, it should also be accounted for that as the level of detail increases, the demand in maintaining and roll-out of such a system will also increase. The required manpower should therefore also be taken into consideration.

4.2.2. Information

The acquired data needs to be translated into useful information. This is done using an energy balance for the specific levels by accounting for all the forms of energy. This balance will ensure the mining levels are accurately characterised and assist in determining an accurate heat load of the mine or specific workplace.

In most instances mines in South Africa are fairly established and, together with the availability of Industry 4.0 technology, these heat sources can be actively measured rather than predicted. Figure 4-3 elaborates on the methodology of deterring the various heat sources/sinks as was discussed in detail during Chapter 2 of this study.

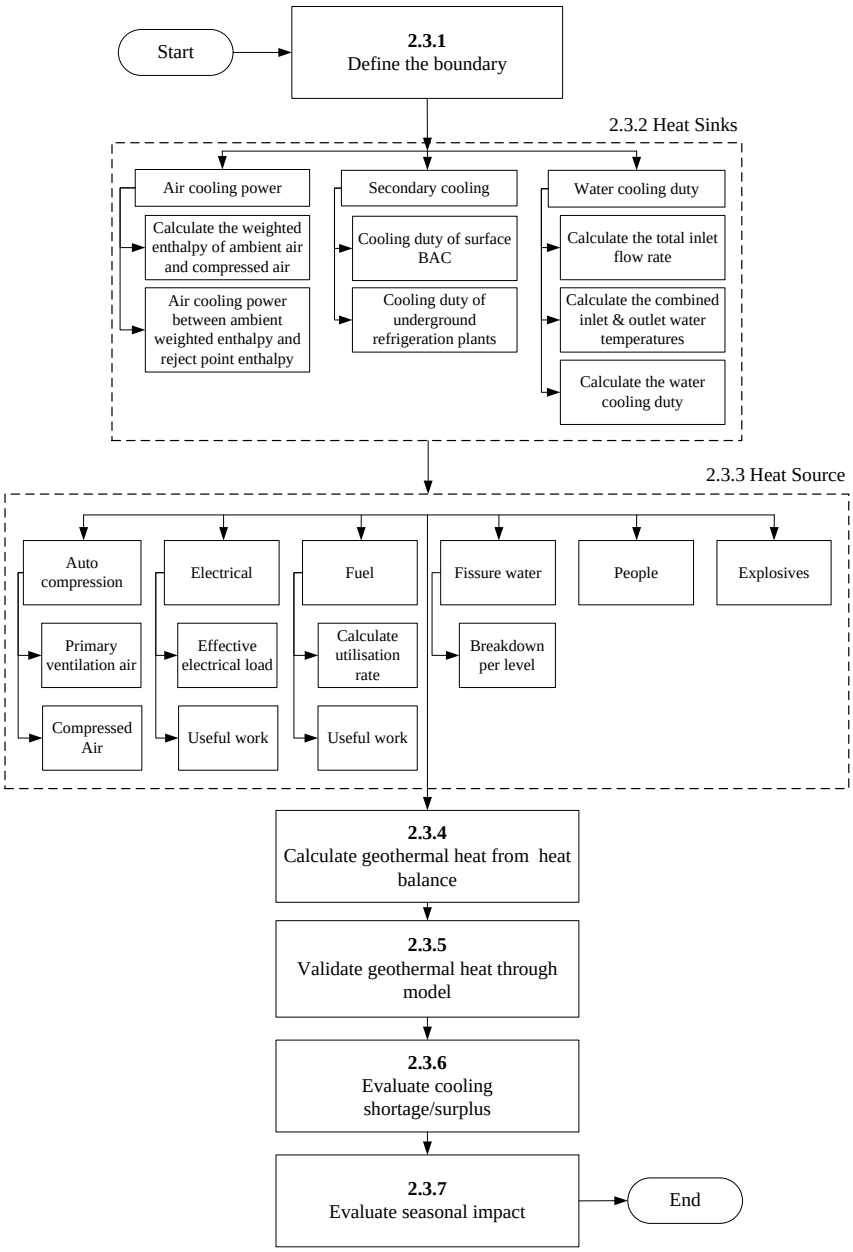

Figure 4-3: Detailed heat load calculation methodology

4.2.1. Knowledge

The daily heat load profile can be determined through real-time information which will better reflect the dynamic nature of the system. This profile will capture the spike in mining intensity as well as the effect of the ambient conditions and thermal dampening thereof.

This is achieved by identifying key performance parameters (KPIs) and translating these parameters into a daily automated reporting/monitoring system. All relevant role-players receive these reports and can action tasks based on dynamic system changes occurring. These KPIs will include:

- System resistance curves of the key fans to assist in monitoring system changes,
- Fan utilisation and condition monitoring,
- Air properties of level intakes/returns (quantity and quality),
- Heat load component breakdown to monitor changes such as mechanisation, geothermal heat exposure etc., and
- Dynamic heat load balance to track supplied cooling compared to the heat load.

4.2.2. Wisdom

The final step is to translate knowledge into actionable wisdom. The derived knowledge will enable applying wisdom to the system and understanding the interdependencies of the system. This will entail some of the following:

- The dynamic heat load profile can be used to structure the planned maintenance of the secondary cooling circuits to ensure the required cooling is always supplied whilst maintaining infrastructure.
- Planning can be optimised by adding the required infrastructure to address a cooling shortfall to achieve the planned reject temperature (return temperature from the workings). The capital costs involved for such infrastructure as well as the operating costs can be accurately determined from the cooling shortfall to optimise costs.
- From the dynamic heat load profile, the current cooling infrastructure can also be planned to advance alongside mining activity to prevent a situation where mining exceeds the supply scope of secondary cooling infrastructure system.
- The profiles will give insight into over-concentrated mining activity and assist the manager to distribute these activities more effectively leading to reduced concentration-induced heat spikes throughout the mine.
- Problem identification will be greatly accelerated through active monitoring. In cases where fall of ground, ventilation appliance damage or any other form of ventilation alteration occurs, the daily monitoring will enable quick response to these occurrences.

The system architecture described will form the backbone of implementing a ventilation-on-demand system. This will be a final optimisation step in the mine of the future to ensure localised mining commences at optimal efficiency levels.

4.3. Results and discussion

The mine under investigation has partially adopted Industry 4.0 technologies with the aim of monitoring at a level similar to that of level 1 as discussed in Table 4-1. The results were therefore constructed through recorded data as well as audited data which was translated into an automatic daily report being generated. The report could then be sent to all involved parties to inform them of any key system changes. The main findings are shared below based on the holistic energy balance approach.

Figure 4-4 illustrates the daily heat load profile as well as the supplied cooling. This was done at the current reject temperature of 32.5℃ wet-bulb.

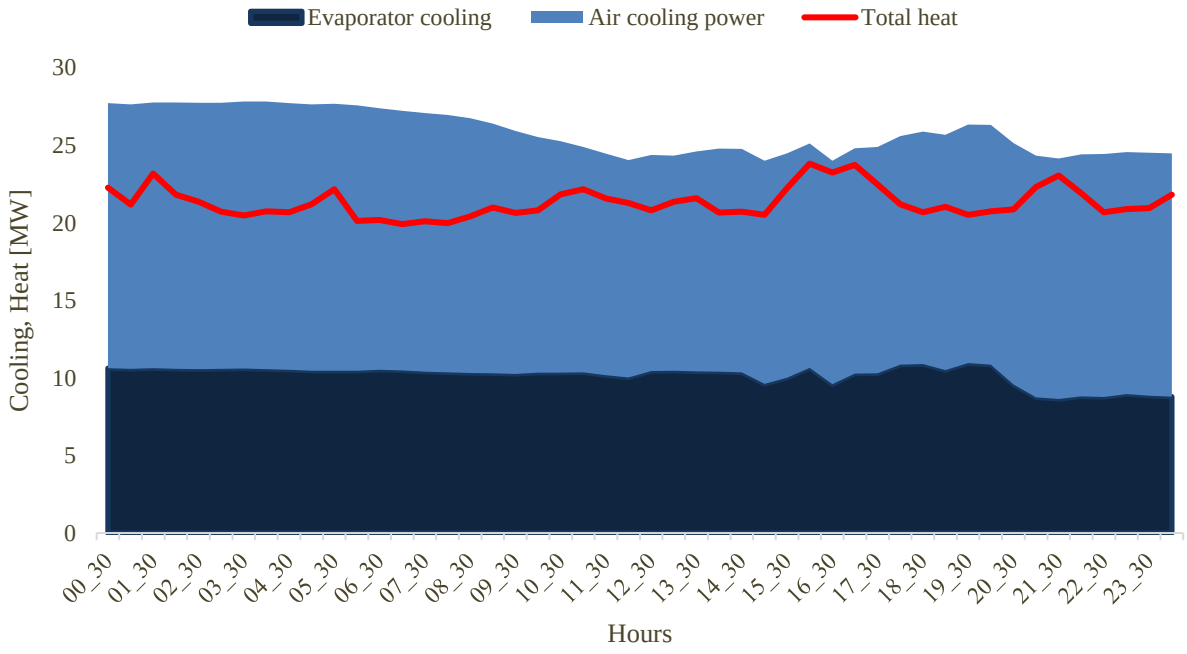

Figure 4-4: Dynamic heat load – Current conditions

From Figure 4-4 it is evident that enough cooling is supplied for the calculated heat load. However, it is a well-known fact that the mine used for this case study is extremely hot. This serves as a first level indication that although the secondary cooling infrastructure might be sufficient there exists large ventilation system inefficiencies.

A next step was plotting the heat load breakdown for the day. This breakdown of all the heat sources as well as supplied cooling is daily monitored and automatically generated. Figure 4-5 illustrates this breakdown.

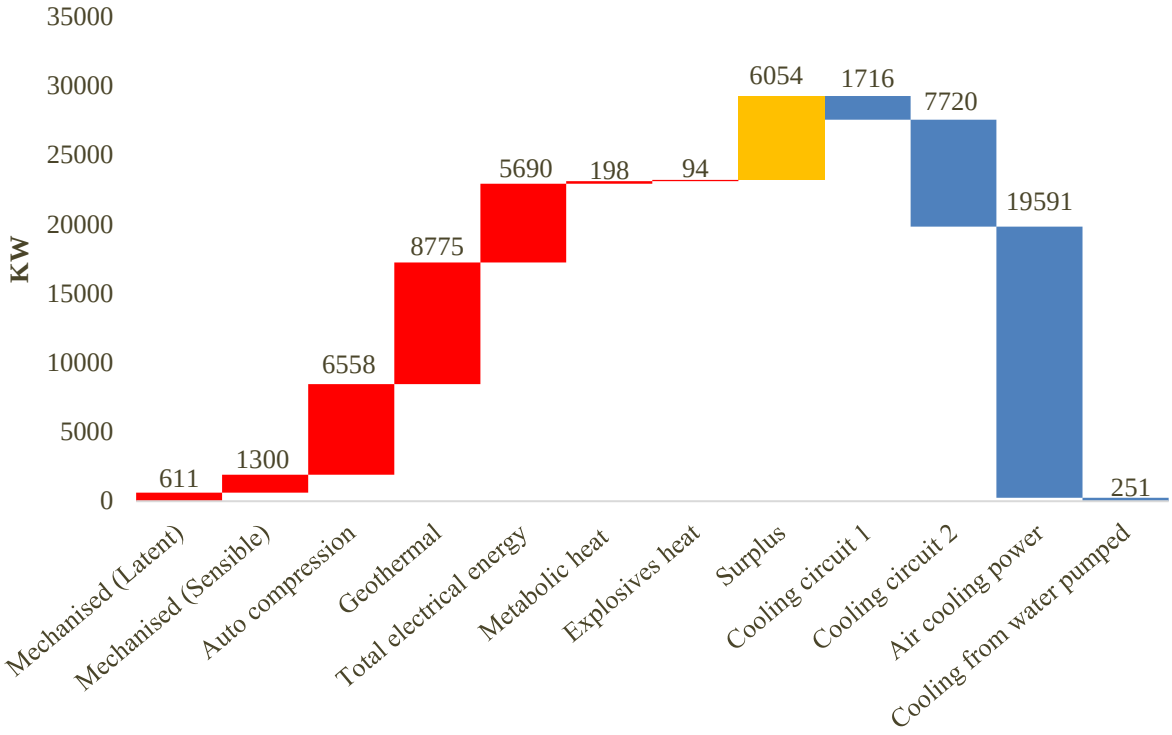

Figure 4-5: Dynamic heat load breakdown

In Figure 4-5 the surplus cooling supplied can, therefore, be interpreted as the quantified system inefficiency which amounts to approximately 70% inefficiency with regards to supplied cooling. This inefficiency is comprised of as the combination of air leakages, or positional efficiency of secondary cooling units.

Monitoring equipment was also fitted to crucial equipment to indicate any system changes which might give rise to a change in the mine's heat load. Figure 4-6 illustrates the system characteristic curve of the surface fan.

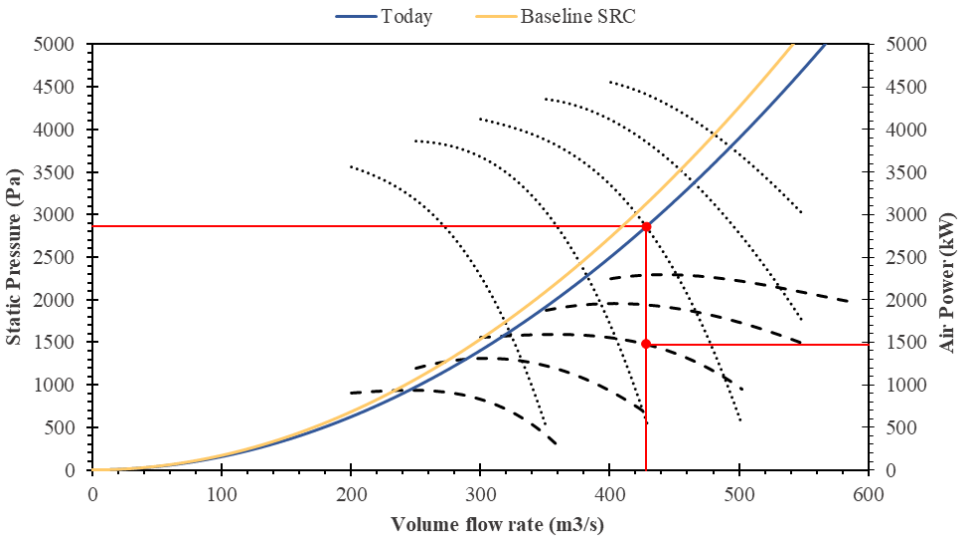

Figure 4-6: Dynamic surface fan system characteristic curve

Through monitoring key infrastructure as is shown in Figure 4-6, allows the ventilation engineer to better understand the performance of such components as well as detect and quantify any changed occurring on the system.

Currently, the Industry 4.0 technology is still being phased in and level 2 and level 3 data is planned for the new financial year which will enable evaluation in more detail such as real-time heat load component breakdown per level or workplace. This will highlight problematic areas as well as give valuable insight into the dynamic nature of the system and the various interdependencies.

4.4. Conclusion

Introducing Industry 4.0 technology to mine ventilation will greatly assist the evaluation of the dynamic nature of mines' thermodynamics. It is, however, important that this roll-out is planned and structured in accordance with a DIKW model approach which has proven in the past to have substantial benefits.

From this approach, an improved understanding can be derived from the required cooling as well as how the cooling infrastructure can be optimised with regards to planned maintenance and utilisation.

This study has highlighted the need for the use of Industry 4.0 technology with regards to heat load monitoring and illustrated that apart from gaining wisdom into the dynamic nature of the daily heat load profile.

5

CHAPTER 5

Conclusions and recommendations

"Take the attitude of a student, never be too big to ask questions, never know too much to learn something new."

Og Mandino[5]

[5] Brainy Quote, https://www.brainyquote.com/quotes/og_mandino_134856, [2019/11/10]

5. CONCLUSIONS AND RECOMMENDATIONS

5.1. Summary

This section aims to conclude the main findings of this study and will give special focus to the novel contributions set out during Chapter 1 of this study.

5.2. Novel contributions

5.2.1. Heat load determination using an energy balance

From the results obtained in Chapter 3 it was shown that through using an energy balance approach to determine heat loads in deep-level mines, effective and accurate results can be obtained. These results adhere to the laws of thermodynamics by accounting for all the forms of energy through applying a well-known concept such as energy balance together with actual measurements.

The approach was evaluated in three case studies and closely resembled the values obtained from the more time-consuming approach of constructing a ventilation simulation model. It was also shown that, for specific cases, the typical industry approach of using heat-prediction graphs can be used. However, care should be taken to apply this approach for mines falling outside the empirical data set of such graphs.

5.2.2. Current and future increase in mine mechanisation

The results obtained through using the energy balance approach for a mechanised mine showed that conventional heat-prediction graphs will misrepresent the various sources of heat. As the utilisation of mechanised machinery increases, so will the misrepresentation.

5.2.3. Impact of seasonal changes on mine heat loads

The seasonal impact was evaluated according to the dynamic ambient conditions. The influences of these conditions were used to derive a dynamic secondary cooling demand profile. For instances where secondary cooling was located underground, these dynamic demand profiles were constructed through using a simulation model to approximate the ambient conditions' impact on the secondary cooling circuits underground.

5.2.4. Industry 4.0 adoption in mine ventilation

The importance and impact if applying Industry 4.0 technology to a mine's ventilation networks were discussed and illustrated. Valuable insight can be gained from this approach, and clear and even more accurate heat load determination can be achieved. A roll-out strategy was developed and obtained results shown when implementing such a strategy.

Applying such technology to the thermodynamic cycles of a mine will assist in identifying key shortfalls, as well as assist in evaluating the thermal flywheel effects for various ambient conditions.

From the discussed novel contributions, and results in Chapter 3, it is clear that the initial hypothesis held true which anticipated discrepancies between the current heat load planning approach and that of an energy balance approach.

5.3. Recommendations for future work

5.3.1. Heat source benchmarking and nature of mining

Through evaluating various mines, it can be explored what the heat-source breakdown is proportionate to each mine's production. This will assist in identifying shortfalls within specific mines that need to be addressed.

5.3.2. Cooling efficiency

More focus should be placed on the overall cooling efficiency with respect to the actual cooling supplied to the active working area. This efficiency should form part of a guideline to assist mine planners to know when cooling infrastructure needs to be relocated to improve positional efficiency.

5.3.3. Thermal flywheel

The effects and nature of the thermal flywheel need to be explored in more depth and quantified by using simulation modelling packages. This parameter should be evaluated in more depth during ambient seasonal changes.

5.3.4. Industry 4.0

There is a need to incorporate Industry 4.0 technology, such as real-time monitoring devices, into simulation packages to enable accurate and real-time simulations.

5.3.5. Uncertainty study

It will be insightful to investigate the uncertainty of each of the heat load components and measurements taken to investigate the uncertainty of conducting heat load studies, e.g. Monte Carlo or sequential perturbation analyses.

5.4. Final conclusion

Two case studies were evaluated using the developed energy balance approach. Both case studies were simulated to validate the results since it differed from the well-known industry approach of using heat-prediction graphs. The energy balance approach and simulation models correlated well, whereas reasons were noted for the differences arising compared to the heat-prediction graphs.

The main reasons were concluded to be that of these mines not adhering to the typical grid pattern mining structure, which formed the empirical data set of the heat-prediction graphs. It was also noted that mines that are more heavily mechanised are misrepresented when using heat-prediction graphs and that various heat sources might be erroneously quantified doing so.

The energy balance approach therefore provides for a practical yet accurate approach to quantify deep-level mine heat loads.

BIBLIOGRAPHY

[1] How a Handful of Countries Control the Earth's Most Precious Materials, [Online]. Available: https://www.fastcompany.com/1694164/how-handful-countries-control-earths-most-precious-materials. [Accessed: 09-Jun-2019].

[2] World mining data 2018 iron and ferro alloy metals non-ferrous metals precious metals industrial minerals mineral fuels International Organizing Committee for the World Mining Congresses, .

[3] **Neingo, P. N.** and **Tholana, T.** 2016. Trends in productivity in the South African gold mining industry, *J. South. African Inst. Min. Metall.*, vol. 116, no. 2, pp. 283–290.

[4] **Gold Fields** 2019. Integrated Annual Review 2018, no. Icmm, pp. 1–166.

[5] What mining still means for South Africa - IRR - DOCUMENTS | Politicsweb, [Online]. Available: https://www.politicsweb.co.za/documents/what-mining-still-means-for-south-africa--irr. [Accessed: 09-Jun-2019].

[6] **Chamber of Mines** 2017. Mine SA 2017 Facts & Figures Pocketbook, *Chamb. Mines*.

[7] **Michal, K.** and **Rossouw, A.** 2018. SA Mine 2018.

[8] SA gold slump continues as annual production falls by 19.5% | Fin24, [Online]. Available: https://www.fin24.com/Economy/sa-gold-slump-continues-as-annual-production-falls-by-195-20190613. [Accessed: 09-Nov-2019].

[9] **Brune, J. F.** 2010. Extracting the science : a century of mining research, Society for Mining, Metallurgy, and Exploration.

[10] The world's deepest gold mine is in South Africa - Business Insider, [Online]. Available: http://www.businessinsider.com/the-worlds-deepest-gold-mine-is-in-south-africa-2016-12?IR=T. [Accessed: 13-May-2018].

[11] **Ryan, A.** and **Euler, D. S.** Jul. 2017. Heat stress management in underground mines, *Int. J. Min. Sci. Technol.*, vol. 27, no. 4, pp. 651–655.

[12] **Donoghue, A. M.** 2004. In-depth reviews: Occupational health hazards in mining: an overview.

[13] **Glazer, J. L.** 2005. Management of Heatstroke and Heat Exhaustion, *Am. Acad. Fam. Physicians.*, vol. 71, p. 8.

[14] **Mcpherson, M. J.** 2012. Subsurface Ventilation and Environmental Engineering, 2nd ed., Springer Science & Business Media.

[15] **Donoghue, A. M.**, **Sinclair, M. J.**, and **Bates, G. P.** Mar. 2000. Heat exhaustion in a deep underground metalliferous mine., *Occup. Environ. Med.*, vol. 57, no. 3, pp. 165–74.

[16] **Mine Health and Safety Coucil** 1996. Mine Health and Safety Act No. 29 of 1996 and Regulations, p. 587.

[17] **Stewart, J. M.** 1981. Heat transfer and limiting physiological criteria as a basis for the setting of heat stress limits*, *J. South. African Inst. Min. Metall.*, vol. 81, no. 8, pp. 239–251.

[18] **Wyndham, C. H.**, **Allan, A. M.**, **Bredell, G. A. G.**, and **Andrew, R.** 1967. Assessing the Heat Stress and Establishing the Limits for Work in a Hot Mine, *Brit. 7. Ind. Med*, vol. 967.

[19] **R.C.W. Webber, R.M. Franz, W.M. Marx, P. C. S.** 2003. A review of local and international heat stress indices Background to the investigation, *J. South. African Inst. Min. Metall.*, vol. 103, no. 5, pp. 313–323.

[20] **Zondi, M.** 2018. Mine Health and Safety Inspectorate - Annual Report 2017/2018.

[21] Section 54s cost SA mines R4.8bn in 2015, and 2016 may be worse - Miningmx, [Online]. Available: https://www.miningmx.com/opinion/columnists/27866-stoppages-lop-r4-8bn-off-2015-revenue-2016-worse/. [Accessed: 06-Jun-2019].

[22] **Hemp, R., Deglon, P.** 1979. A Heat Balance in a Section of a Mine, *J. Mine Vent. Soc. South Africa*, no. 12, pp. 148–156.

[23] **J. Burrows, R. Hemp, W. Holding, R. . S.** 1989. Planning ventilation and refrigeration requirements, Ventilation and occupational environment engineering in mines- Chapter 38, 3rd ed., Johannesburg, South Africa: Mine Ventilation Society of Southg Africa.

[24] **Moorecraft, H.** 2019. Heat load mangement program. Interview, Pretoria, South Africa.

[25] **Duckworth, I. J.**, **Mousset-Jones, P.**, and **Advisor, T.** 1993. A Heat Balance Study for a Mechanized Cut-and-Fill Stope.

[26] **Bluhm, S.** et al. 2003. Mine Ventilation Society of South Africa. Managing the Basics Conference.

[27] **S. Bluhm** and **M. Biffi** Variations in ultra-deep, narrow reef stoping configurations and the effects on cooling and ventilation.

[28] **Africa, M. V. S. of S.** 2014. VOEEM_Rough_Planning_and_ROT (Chapter 38), pp. 784–805.

[29] **Mack, M.G., Starfield, A. M.** 1985. The Computation of Heat Loads in Mine Airways Using the Concept of Equivalent Wetness, in *Proceedings 2nd US Mine Ventilation Symposium*, pp. 421–422.

[30] **Ouedemi, M.A., Deliac, E.P., Cassini, P.** 1985. Modeling and Prediction of Climatic Conditions in a Deep Level Development Heading, in *Proceedings 2nd US Mine Ventilation Symposium*.

[31] **Amano, K.**, **Sakai, K.**, and **Hiamatsu, Y.** 1986. A Calculation System using a PC for the Design of Underground Ventilation and Air Conditioning, *Int. J. Rock Mech. Mining, Sci. Geomech.*, vol. 19, pp. 31–38.

[32] **McPherson, M. J.** 1986. The analysis and simulation of heat flow into underground airways, *Int.*

J. Min. Geol. Eng., vol. 4, no. 3, pp. 165–195.

[33] **S.J. Bluhm; N.A. Alexander; T.W March; P. Bottomley; F. von Glehn** 1986. The measurement of heat load in deep level stope in Klerksdorp Goldfields, *Mine Vent. Soc. South Africa*, vol. 39, no. 10, pp. 129–140.

[34] **Hemp, R.** 1989. Sources of heat in mines, Ventilation and Occupational Environment Engineering in Mines, 3rd ed., Johannesburg: Mine Ventilation Society of South Africa.

[35] **Roy, T. R.** and **Singh, B.** 1991. Computer Simulation of Transient Climate Conditions in Underground Airways, *Mining, Sci. Technol.*, vol. 13, no. 3, pp. 395–402.

[36] **Wagner, H.** 2013. The management of heat flow in deep mines, *Min. Rep.*, vol. 149, no. 2, pp. 88–100.

[37] **Roghanchi, P.**, **Kocsis, K. C.**, **Danko, G.**, and **Powell, A.** 2017. Underground climatic monitoring and modeling: Are we missing something?, *Qual. - Access to Success*, vol. 18, no. January, pp. 133–139.

[38] **Nell, D.**, **Maré, P.**, and **Mathews, E.** 2019. Industry 4.0 roll-out strategy for dynamic mine heat load management, *SAIJE*.

[39] **Çengel, Y. A.** and **Boles, M. A.** 2006. Thermodynamics - An engineering approach, Fifth., .

[40] **Wiles, G. G.** and **Phil, D.** Wet-bulb temperature gradients in horizontal airways, *J. South African Inst. Min. Metall.*, vol. 59, no. 7, pp. 339–359.

[41] **Starfield, A. M.** 1966. Tables for the flow of heat into a rock tunnel with different surface transfer coefficients, *J. South. AFRICAN Inst. Min. Metall.*, vol. 66, no. 12, p. 692.

[42] **Bottomley, P.**, **von Glehn, F.**, and **Matthews, M.** 1987. Predicting and reducing stope heat flow in South African gold mines, in *Proceedings 3rd U.S. Mine Ventilation Symposium*.

[43] **Van der Walt, J.** and **Whillier, A.** 1979. Heat pick-up from the rock in gold mines: the water-rock thermal balance and the thermal efficiency of production, *J. Mine Vent. Soc. South Africa*, vol. 32, no. 7, pp. 125–144.

[44] **Van der bijl, J.** and **Kleingeld, M.** 2007. Sustainable DSM on deep mine refrigeration systems - A novel approach, North-West University.

[45] **AFRICA, M. C. S.** 2017. Modernisation : towards the mine of tomorrow.

[46] **Nixon, C. A.**, **Gilliest, A. D. S.**, and **Howes, M. J.** 1992. Analysis of heat sources in a large mechanised development end at Mount Isa Mine, Proceedings Fifth Int, Mine Ventilation Congress.

[47] **Brake, D. J.** and **Bates, G. P.** 2002. Limiting metabolic rate (Thermal Work Limit) as an index of thermal stress, *Appl. Occup. Environ. Hyg.*, vol. 17, no. 3, pp. 176–186.

[48] **Van Rensburg, J. P.**, **Marx, H. E.**, **Van Der Walt, W. H.**, **Schutte, P. C.**, and **Kielblock, A. J.**

1991. Estimated metabolic rates associated with underground mining tasks: conventional and mechanised mining operations, Johannsburg: Chamber of mines of South Africa.

[49] **RCW Webber-Youngman** 2005. An integrated approach towards the optimization of ventilation, air cooling and pumping requirements for hot mines, North-West University.

[50] **Bluhm, S. J.**, **Marx, W. M.**, **Von Glehn, F. H.**, and **Biffi, M.** 2001. Vuma mine ventilation software, *J. Mine Vent. Soc. South Africa*, vol. 54, no. 3.

[51] **Ramani, R. V** 2006. Editors : Jan M . Mutmansky, 11th ed., PENNSYLVANIA: Taylor & Francis Group.

[52] **Wiley, S. C.** 2015. Digital commons @ montana tech optimization of the quantity of heated/refrigerated air required for ventilating underground mines with ventilation-on-request systems.

[53] **Maré, P.** and **Marais, P. J. H.** 2017. Novel simulations for energy management of mine cooling systems, no. May, pp. 1–264.

[54] **Arndt, D. C.** Jul. 2006. Integrated dynamic simulation of large thermal systems.

[55] **Gold, H.** 2018. Mineral Resources and Reserves By Operation Target 1.

[56] **Waples, D. W.** and **Waples, J. S.** 2004. A review and evaluation of specific heat capacities of rocks, minerals, and subsurface fluids. Part 2: Fluids and porous rocks, *Nat. Resour. Res.*, vol. 13, no. 2, pp. 123–130.

[57] **Mossop, S. C.** and **Gafner, G.** Oct. 1951. The thermal constants of some rocks from the orange free state, *J. Chem. Metall. Min. Soc. South Africa*, vol. 52, no. 4, pp. 61–73.

[58] **Owen, M. S.** 2013. Ashrae Handbook Fundamentals, 1791 Tullie Circle, N.E., Atlanta, GA 30329: ASHRAE.

[59] **Deloitte** 2018. The Future of Mining in Africa. Navigating a Revolution., pp. 1–24.

[60] **Sishi, M. N.** 2017. Implementation of Industry 4 . 0 technologies in the mining industry – a case study By October 2017, no. October.

[61] **Pretorius, J. G.**, **Mathews, M. J.**, **Maré, P.**, **Kleingeld, M.**, and **van Rensburg, J.** 2019. Implementing a DIKW model on a deep mine cooling system, *Int. J. Min. Sci. Technol.*, vol. 29, no. 2, pp. 319–326.

[62] **Rowley, J.** 2007. The wisdom hierarchy: representations of the DIKW hierarchy, *J. Inf. Sci.*, vol. 33, no. 2, pp. 163–180.

[63] **Ahsan, S.** and **Shah, A.** Data, Information, Knowledge, Wisdom: A Doubly Linked Chain?

[64] **Goch, D.C. and Patterson, H. S.** The heat flow into tunnels, *J. Chem. Metall. Min. Soc. South Africa*, vol. 41, pp. 117–128.

[65] **De, Y.** and **Lambrechts, V. '** The estimation of ventilation air temperatures in deep mines, *J. Chem. Metall. Min. Soc. South Africa*, vol. 50, no. 8, pp. 184–198.

[66] **Beck, A., Jaeger, J. C.** and **Newstead, G.** 1956. The measurement of the thermal conductivity of rocks by observations on boreholes, *Aust. J. Phys.*, vol. 9, no. 2, pp. 286–295.

[67] **Wiles, G. G.** and **Quilliam, J. H.** 1959. Some temperature gradients observed in specially selected underground airways, *J. South African Inst. Min. Metall.*, vol. 59, no. 7, pp. 360–368.

[68] **Starfield, A. M.** 1966. The computation of temperature increases in wet and dry airways, *J. Mine Vent. Soc. South Africa*, vol. 19, no. 10, pp. 157–165.

[69] **Jaeger, J.C., Chamalaun, T.** 1966. Heat Flow in an Infinite Region Bounded Internally by a Circular Cylinder with Forced Convection at the Surface, *Aust. J. Phys.*, vol. 19, pp. 475–488.

[70] **Lambrechts, J. de V.** 1967. Prediction of web-bulb temperature gradients in mine airways, *J. South. African Inst. Min. Metall.*, vol. 67, no. 11, pp. 595–610.

[71] **Starfield, A. M.** and **Dickson, A. J.** 1967. A study of heat transfer and moisture pick-up in mine airways, *J. South. African Inst. Min. Metall.*, vol. 68, no. 5, pp. 211–234.

[72] **Starfield, A. M.** 1969. A rapid method of calculating temperature increases along mine airways, *J. South. African Inst. Min. Metall.*, vol. 70, no. 4, pp. 77–83.

[73] **Ramsden, R.** 1975. Estimation of heat pick-up in mine airways, Johannesburg, South Africa.

[74] **Whillier, A., Ramsden, R.** 1976. Sources of Heat in Deep Mines and the Use of Mine Service Water for Cooling.

[75] **Gibson, K.** 1976. The computer simulation of climatic conditions in underground mines, University of Nottingham.

[76] **Vost, K. R.** 1977. Rapid changes of air temperature in underground airways, *J. South Am. Inst. Min. Metall.*, vol. 32, pp. 262–268.

[77] **Stewart JM.** 1981. Heat transfer and limiting physiological criteria as a basis for the setting of heat stress limits, *J. South. African Inst. Min. Metall.*, vol. 81, no. 8, pp. 239–251.

[78] **Amano, K.**, **Mizuta, Y.**, and **Hiramatsu, Y.** Feb. 1982. An improved method of predicting underground climate, *Int. J. Rock Mech. Min. Sci. Geomech. Abstr.*, vol. 19, no. 1, pp. 31–38.

[79] **Van Der Walt, J.**, **De Kock, E. M.**, **Eng, P.**, **Mith, L. K.**, and **Eng, C.** 1983. The analysis of ventilation requirements for mines.

[80] **Bluhm, S.J., Vost, K., Stewart, J. M.** 1983. Effect of Backfill on Heat Pick-up in a Stope.

[81] **Starfield, A.M, BLELOCHt, A. L.** 1983. A new method for the computation of heat and moisture transfer in a partly wet airway, *J. South African Inst. Min. Metall.*, pp. 263–269.

[82] **Sheer, T. J.** 1983. Investigations into the use of ice for cooling deep mines, in *In South African*

institution of refrigeration and air conditioning, p. 15.

[83] **Burton, R. C., et al.** 1984. Recirculation of air in the ventilation and cooling of deep gold mines, in *Proceedings third international mine ventilation congress*.

[84] **Smith, O.** 1982. Effects of a cooler underground environment on safety, labour and labour productivity, in *Third international mine ventilation congress*.

[85] **Hemp, R.** 1985. Air Temperature Increases in Airways, *J. Mine Vent. Soc. South Africa*, no. Jan, Feb, pp. 1–8, 13–20.

[86] **Sheer, T. J., D. del Castillo, and C. C.** 1986. Unconventional systems for removing heat from deep mines, *South African Mech Eng*, vol. 36, pp. 207–217.

[87] **Wagner, H.** 1986. The challenge of deep-level mining in South Africa.

[88] **McPherson, M. J.** and **Mousset-Jones, P.** 1986. The determination ofin situ rock thermal properties and the simulation of climate in an underground mine, *Int. J. Min. Geol. Eng.*, vol. 4, no. 3, pp. 197-216.

[89] **Gillies, A.D.S., Alexander, N. A.** 1986. The Heat Load in a Development End.

[90] **Hemp, R.** 1987. Air Temperature Increases in Airways - Further Work, *J. Mine Vent. Soc. South Africa*, vol. 40, no. 12, pp. 1–11.

[91] **Von Glehn, F.**, **Wernick, B.**, **Chorosz, G.**, and **Bluhm, S.** 1987. ENVIRON: A computer program for the simulation of cooling and ventilation systems on South African gold mines, in *Proceedings of the Twentieth International Symposium on the Application of Computers and Mathematics in the Mineral Industries*, vol. 1, pp. 319–330.

[92] **Matthews, M. K., H. N. Mccreadie, and T. C. M.** 1987. The measurement of heat flow in a backfilled stope, *J. Mine Vent. Soc. South Africa*, vol. 40, no. 11, pp. 142–148.

[93] **Moreby, R.** 1988. Thermodynamic Network Simulation Incorporating Airway Heat and Moisture Transfer, in *Proceedings 4th International Mine Ventilation Congress*, pp. 265–272.

[94] **Cheung, J.** 1988. A transient model to predict the weekly temperatures of the ventilation air in a partially wetted airway, *Int. J. Min. Geol. Eng.*, vol. 6, no. 4, p. 1988.

[95] **Howes, M. J.** 1988. Heat and Moisture Exchange in Mine Airways, in *Proceedings 4th International Mine Ventilation Congress*, pp. 257–264.

[96] **Danko, G.**, **Mousset-Jones, P.**, and **McPherson, M. J.** 1988. Air Temperature Calculation in Hot Airways: A Critique and New Solution.

[97] **Middleton, J. N.** 1991. A Comparison Between Heat Loads in Conventional and Trackless Mechanized Development Ends in Deep Gold Mines.

[98] **Pamgraphi, D. C.**, **Gupta, M. L.**, and **Baneijee, S. P.** 1991. An Empirical Study of Heat Flow and

Temperature Rise in Bord-and-Pillar Working in India, *Mining, Sci. Technol.*, vol. 12, no. 2, pp. 127–136.

[99] **Kielblock, A. J., and P. C. S.** 1991. Heat Stress Management–a comprehensive guideline, Johannesburg, South Africa.

[100] **Funnell, R. C., S. J. Bluhm, and T. J. S. 2001.** 2001. Optimisation of cooling resources in deep stopes, in *Proceedings 7th International Mine Ventilation Congress*.

[101] **Bluhm, S.** and **Biffi†, M.** 2001. Variations in ultra-deep, narrow reef stoping configurations and the effects on cooling and ventilation, *J. South African Inst. Min. Metall.*, vol. 101, no. 3, pp. 127–134.

[102] **Von Glehn, F. H.**, **Hemp, R.**, and **Funnell, R. C.** 2002. Numerical modelling of heat flow in mines, *S. Afr. J. Sci.*, vol. 98, no. 9–10, pp. 485–490.

[103] **Rawlins, C. A.** 2005. Diesel Power Vehicles, Pollution, and the Economic Balance Thereof.

[104] **Stinnette, J. D.**, **De Souza, E.**, and **Buchan, R. M.** 2013. Establishing total airflow requirements for underground metal/non-metal mines with tier iv diesel equipment.

[105] **S. Bluhm*, R. Moreby†, F. von Glehn*, and C. P.** 2014. Life-of-mine ventilation and refrigeration planning for Resolution Copper Mine, *J. South. African Inst. Min. Metall.*, vol. 114, no. 6, pp. 497–503.

[106] **Lukonde, P. M.** and **Chileshe, P. R. K.** 2017. Mapping For Literature, Conceptual And Theoretical Framework And Methodology: Case Of Hot Deep Mining Ventilation Engineering Evaluation And Design, *Int. J. Sci. Technol. Res.*, vol. 6, no. 09, pp. 304–320.

APPENDIX A CRITICAL LITERATURE STUDY

Table A-1: Comprehensive literature review

#	Author	Title	Source	Date	Findings/Shortcomings	Ref.
1	Goch, D.C. Patterson, H.A.	The heat flow into tunnels	Journal Article	1940	In this paper Goch and Patterson expanded on works concerning integrals conducted by Nicholson, Carslaw and Jaeger as well as Smith in the early 19 hundred. In the article, they supply heat flow time-dependent tables for ease of use assuming uniform cross-section, uniform rock properties as well as approximate undergrounds drives as cylindrical in nature.	[64]
2	Lambrechts de V., J.	The estimation of ventilation air temperatures in deep mines	Journal Article	1950	Derived a rule of thumb to estimate wet-bulb temperature increases of airflow in haulages, stopes and vertical shafts. Purely empirical based on mines in the Witwatersrand area.	[65]
3	Beck, A., Jaeger, J.C.	The measurement of the thermal conductivity of rocks by observations on boreholes	Journal Article	1954	Developed a probe with a heater and thermal measurement section to insert into boreholes to measure the rock thermal conductivity value	[66]
4	Wiles, G.G.	Wet-bulb temperature gradients in horizontal airways	Journal Article	1959	Derived a theoretical model to estimate wet-bulb temperatures by applying experimental constants. Dependant on many parameters.	[40]
5	Wiles, G.G. Quilliam, J.H.	Some temperatures observed in specifically selected underground airways	Journal Article	1959	Validated the theoretical model derived by G.G Wiles in 1959	[67]
6	Starfield, A.M.	The computation of temperature increases in wet and dry airways	Journal Article	1966	Heat and moisture pick-up in mine airways	[68]
7	Jaeger, J.C. Chamalaun, T.	Heat flow in an infinite region bounded internally by a circular cylinder with forced convection at the surface	Journal Article	1966	Supplies numerical values for the surface temperature of a region bound by a cylindrical volume. Also supplies approximation for these values.	[69]
8	Lambrechts de V., J.	Prediction of wet-bulb temperature gradients in mine airways	Journal Article	1967	Correlating T_Wb to parameters such as VRT, airway wetness, air velocity and haulage distance. It was noted that dry-bulb temperatures play a minor role whereas airflow velocity plays an inverse role. It was also noted that it is virtually impossible to have a purely scientific approach since there is a drastic fluctuation of heat as a result of constant ambient changes.	[70]
9	Starfield, A.M. Dickson, A.J.	A study of heat transfer and moisture pick-up in mine airways	Journal Article	1967	The latent impact is drastic when the wet-bulb depression is great. Dry haulages are advantages, especially long haulages. The model considers an airway in cross-section as a square void in an infinite extent of rock. The hanging wall and sidewalls are assumed dry while the footwall is assumed wet, the degree of wetness being determined by a wetness factor. The temperatures in the rock surrounding the airway are calculated at successive time intervals by a finite difference solution of the heat conduction equation. Heat and moisture transfer from rock to air is assumed to depend on the rock surface temperatures and the heat and moisture content of the air. Not for everyday use, requires computer modelling.	[71]
10	Starfield, A.M.	A rapid method of calculating temperature increases along mine airways	Journal Article	1969	Previous research is done by using a computer model to allow ease of interpolation	[72]
11	Ramsden, R.	Estimation of heat pick-up in mine airways	Report	1975	It is stated that the equation developed by Ramsden predicted heat flow values to within 1.7% of the measured results, over the tunnel length	[73]
12	Whillier, A. Ramsden, R.	Sources of heat in deep mines and the use of mine service water for cooling	Conference proceedings	1976	Showed close correlation to the face area heat load obtained by empirical results.	[74]
13	Gibson, K.	The computer simulation of climatic conditions in underground mines	Thesis / Dissertation	1976	Gibson's technique solves the radial heat equation using Laplace transforms to produce an integral involving four Bessel functions. This provides a dimensionless temperature gradient.	[75]

14	Vost, K.R.	Rapid changes of air temperature in underground airways	Journal Article	1977	Investigated the theoretical and empirical methods to predict air temperature gradients in underground airways. He states that most theoretical methods for the prediction of air-temperature gradients in underground airways assume that the temperature of the air entering either remains constant or has only slow seasonal variation. Vost measured large changes in temperature, caused by changes in 13 atmospheric conditions on the surface, which were measured over a fourteen-day period in the air entering a horizontal airway. The changes in average temperature between successive days at the surface and at depth were calculated and linear correlations conducted. The experiments showed that changes in atmospheric conditions at surface can produce rapid variations in wet-bulb temperature at depth in a shaft and provide one example of the penetration of these changes 3400 m from surface. This approach limits heat flow from circular tunnels and will lead to some errors when applied to stope sections although as found the thesis by Ian John Duckworth, it can be applied with reasonable success.	[76]
15	Hemp, R. Deglon, P.	A heat balance in a section of a mine	Conference proceedings	1979	However, all three of these publications fail to correlate heat flow data with a specific stope, instead reflecting measurements taken over a section of a mine. During these studies, it was assumed that the heat released during blasting was absorbed in the rock and gradually released since no heat spike was monitored on the return airside.	[22]
16	Stewart, J.M.	Heat transfer and limiting physiological criteria as a basis for the setting of heat stress limits	Journal Article	1981	Conducted work in South Africa on the fundamentals of human heat stress and determined the metabolic heat production for men He determined that the heat production for a man varies from 118 W for a winch operator to 468 W for a man shovelling rock. For the purposes of the study, an average metabolic heat production figure of 250 W was applied to the crew to determine the overall heat load resulting from the men in the stope.	[77]
17	Amano, K. Mizuta, Y. Hiamatsu, Y.	An improved method of predicting underground climate	Journal Article	1982	A computerised model was developed which used the moisture content of the air to account for the wetness factor of the airway. The aim was to improve climate prediction in underground haulages.	[78]
18	Van der Walt, J. De Kock, E. M. Mith, L. K.	The analysis of ventilation requirements for mines	Journal Article	1983	Developed a methodology for calculating/estimating mine cooling requirements. Does not directly discuss the physical calculations required although the study focusses on the steps to be taken to quantify each source of heat.	[79]
19	Bluhm, S.J. Vost, K. Stewart, J.M.	Effect of backfill on heat pick-up in a stope	Journal Article	1983	Investigated the effect of backfill on heat pick-up in stopes. With reasonable accuracy, the heat produced by the backfill in stoped could be predicted.	[80]
20	Starfield, A.M Blelocht, A.L.	A new method for the computation of heat and moisture transfer in a partly wet airway	Journal Article	1983	Includes the quasi-steady state solution for solving heat flow in a radial plane. Only based on circular haulages. This model involves a quasi-steady state approach an is incorporated into a computer model to improve mine airway heat transfer accuracy and calculation sped.	[81]
21	Sheer T.J.	Investigations into the use of ice for cooling deep mines	Conference proceedings	1983	The study focused on the practicality and scope for using ice as a form of cooling in comparison to traditional chilled service water.	[82]
22	Burton R.C. Plenderleith W Stewart, J.M. Pretorious, B. Holding, W.	Recirculation of air in the ventilation and cooling of deep gold mines	Conference proceedings	1984	Discusses recirculation in the mining environment and differentiates between controlled and uncontrolled recirculation.	[83]
23	Smith, O.	Effects of a cooler underground environment on safety, labour and labour productivity	Conference proceedings	1984	Quantified the impact on productivity when supplying a cooler working environment	[84]
24	Mack, M.G. Starfield, A.M.	The computation of heat loads in mine airways using the concept of equivalent wetness	Conference proceedings	1985	The study concluded that the moisture and heat exchange can be calculated with relative ease when assuming airways can be approximated as a circular hole as well as uniform conditions exist for both moisture and temperature around such hole.	[29]

25	Hemp, R.	Air temperature increases in airways	Journal Article	1985	Illustrated how previous circular wet tunnels approaches developed to estimate heat flow can be adapted for square tunnels with wet footwalls.	[85]
26	Ouedemi, M.A. Deliac, E.P. Cassini, P.	Modelling and prediction of climatic conditions in a deep level development heading	Conference proceedings	1985	The work mainly focused on development heading which at the time was viewed complex in nature to evaluate. Heat exchange models were derived for these headings.	[30]
27	Sheer, T.J. del Castillo, D. Csatary, C.J.L.	Unconventional systems for removing heat from mines	Conference proceedings	1986	Looked at using alternative methods such as ice being supplied from the surface for secondary cooling.	[86]
28	Amano, K. Sakai, K. Hiamatsu, Y.	A calculation system using a pc for the design of underground ventilation and air conditioning	Journal Article	1986	This was an improvement of the previous work conducted in 1982 and utilised a personal computer's computational capabilities for underground design criteria with regards to ventilation and refrigeration.	[31]
29	Wagner, H.	The challenge of deep-level mining in South Africa	Journal Article	1986	Discussed all the limiting factors faced by mining as it extends extend to new depths. Argues that as mechanisation increases, problems will worsen. The study is outdated, and more recent figures need to be investigated.	[87]
30	McPherson, M.J.	The analysis and simulation of heat flow into underground airways	Journal Article	1986	This study focusses on time-variant heat flow and uses a simulation program called CLIMSIM. This enables the prediction of climatic changes in underground systems.	[32]
31	McPherson, M.J. Mousset-Jones, P.	The determination of in-situ rock thermal properties and the simulation of climate in an underground mine	Journal Article	1986	This article focused on additional applications of the CLIMSIM simulation model and quantified the accuracy through actual measurements.	[88]
32	Bluhm, S.J. Alexander, N.A. March, T.W Bottomley, P. von Glehn, F.	The measurement of heat loads in a deep level stope in the Klerksdorp goldfield	Journal Article	1986	Al parameters were measured and using the energy balance the heat flow from the rock was estimated. This estimation came close to the theoretical estimation from Whillier and Ramsden. This study focused on a specific stope and not the whole mine in general. When investigating the whole mine the various heat sources will represent in different ratios.	[33]
33	Gillies, A.D.S. Alexander, N.A.	The heat load in a development end	Report	1986	Results were given for comprehensive empirical study conducted on heat flow from a development end. Results were compared to prediction models and good correlations were evident especially compared to models from Ramsden in 1975 as well as the initial work conducted by Goch and Patterson.	[89]
34	Bottomley, P. von Glehn, F. Matthews, M.	Predicting and reducing stope heat flow in South African gold mines	Conference proceedings	1987	Conducted similar work to that of Bluhm in 1986 where the heat load is theoretically calculated and practically measured on deep-level mine stopes.	[42]
35	Hemp, R.	Air temperature increases in airways - further work	Journal Article	1987	This paper was an extension of the work conducted by Hemp in 1985 which was refined.	[90]
36	Von Glehn, FH; Wernick, BJ; Chorosz, G; Bluhm, SJ	ENVIRON: A computer program for the simulation of cooling and ventilation systems on South African gold mines	Report	1987	The paper discussed a new simulation program called Environ. This program is divided into two main sections namely heat flow and airflow simulation for network analysis	[91]
37	Matthews M.K. McCreadie, H.N. March, T.C.W	The measurement of heat flow in a backfilled stope	Journal Article	1987	Supplies experimental data into heat flow from backfill in stopes	[92]
38	Moreby, R.	Thermodynamic network simulation incorporating airway heat and moisture transfer	Conference proceedings	1988	A program is used which accounts for compressibility of air when predicting heat flow. This allows the user to specify surface conditions when simulating underground conditions.	[93]
39	Cheung, J.	A transient model to predict the weekly temperatures of the ventilation air in a partly wetted airway	Report	1988	Cheung predicted weekly temperatures based on changes to the ventilating air. This caters for a more dynamic approach since this I surely a fluctuation parameter.	[94]
40	Howes, M.J.	Heat and moisture exchange in mine airways	Conference proceedings	1988	A non-uniform boundary approach is developed in this study which allows for a more in-depth and unique scenario evaluation in a mine.	[95]

41	Danko, G. Mousset-Jones, P. McPherson, M.J.	Air temperature calculation in hot airways: A critique and new solution	Journal Article	1988	Sensible and latent heat transfer in an airway developed for a homogeneous infinite solid.	[96]
42	Burrows, J. Hemp, R. Holding, W. Stroh, R.M	Planning ventilation and refrigeration requirements, Ventilation and occupational environment engineering in mines- Chapter 38	Book	1989	Supplies rule of thumbs to estimate ventilation quantities. Estimating heat production from graphs based on extensive empirical results to be used for rough planning purposes. These charts are region-specific as well as cater for a full production conventional mine.	[23]
43	Hemp, R. Lancaster, F.H.	Sources of heat in mines	Book	1989	It was found that wet surfaces increase heat flow rate with 52%. Various methods were compared to calculating the wet-bulb temperature gradient. Discusses each heat source in mines. Hot fissure water and the resultant heat flow due to convection was not accounted for – mentions little calculations exist for this.	[34]
44	Middleton, J.N.	A comparison between heat loads in conventional and trackless mechanized development ends in deep gold mines	Report	1991	Results showed that most of the heat was evident during the loading cycles. It was also concluded that locomotives add considerably less heat (7.5%) compare to LHD's when evaluating the movement of the same amount of rock.	[97]
45	Pamgraphi, D.C. Gupta, M.L. Baneijee, S.P.	An empirical study of heat flow and temperature rise in board-and-pillar working in India	Journal Article	1991	Significant contributing variables to heat flow are identified from statistical evaluation	[98]
46	Roy, T.R. Singh, B.	Computer simulation of transient climate conditions in underground airways	Journal Article	1991	A program called CLIMA is discussed which can be used to solve underground heat transfer whilst accounting for changes in air conditions/parameters.	[35]
47	Kielblock, A.J. Schutte, P.C.	Heat stress management, a comprehensive guideline	Report	1991	Evaluated the effect on worker performance as a result of environmental conditions	[99]
48	McPherson, M.J.	Subsurface ventilation and environmental engineering	Book	1993	Argues that using an empirical approach for heat production can be very misleading when one of the many conditions change under which the study was performed. There is not an easy method developed for actual practical use on-site to determine the heat load of a mine. Although all the theory is readily communicated, a clear approach discussion is not evident.	[14]
49	Duckworth, I.J. Mousset-Jones, P.	A heat balance study for a mechanized cut-and-fill stope	Thesis / Dissertation	1993	Practical exercise to evaluate the heat in a stoping area through measuring all the heat contributing sources confirming previous developed theoretical models to be accurate. The study was conducted on a specific workplace and mine setup. There was difficulty in establishing credible measurements in some cases. As usual, irregular mining activity and production priority negatively influences the study at certain stages	[25]
50	Bluhm, S.J. von Glehn, F.H. Marx, W.M. Biffi, M.	VUMA mine ventilation software	Journal Article	2001	Paper discussed the use and advantages of the VUMA simulation software	[50]
51	Funnell, R.C. Bluhm, S.J. Sheer, T.J.	Optimisation of cooling resources in deep stopes	Conference proceedings	2001	The study discusses the use of chilled service water and the positional efficiency thereof.	[100]
52	Bluhm, S.J. Biffi, M.	Variations in ultra-deep, narrow reef stoping configurations and the effects on cooling and ventilation	Journal Article	2001	Paper evaluates various stoping differences and how these differences impact heat loads in working areas. Does not provide a direct guide for estimating heat loads in these workings.	[101]
53	Von Glehn, F.H. Hemp, R. Funnell, R.C.	Numerical modelling of heat flow in mines	Journal Article	2002	Focus is placed on numerical modelling of heat flow in stopes and dams using simulation software	[102]

54	Webber, R.C.W. Franz, R.M. Marx, W.M. Schutte, P.C.	A review of local and international heat stress indices Background to the investigation	Journal Article	2003	A combination of heat stress indices is to be used when mining at extreme depths. It is recommended that air cooling power be used during the design of ultra-deep mines and that wet-bulb temperatures serve as the monitoring parameter of adequate ventilation.	[19]
55	Webber, R.C.W.	An integrated approach towards the optimization of ventilation, air cooling and pumping requirements for hot mines	Thesis / Dissertation	2005	The study investigates the potential optimization in current operations with regards to energy consumption in ventilation, refrigeration and dewatering. The study does not focus on estimating mine heat loads. Although the study provides insight into the specific case study it is outdated.	[49]
56	Rawlins, C A	Diesel power vehicles, pollution, and the economic balance thereof	Report	2005	The study focusses on the increasing demand for ventilation through the growing impact of mine mechanisation. Study focus more the on pressure placed on diluting the contaminants that it focused on addressing the addition of heat	[103]
57	Horst, W.	The management of heat flow in deep mines	Journal Article	2013	Concludes that 75% of heat transfer is due to rock heat flux. Systematically discuss the calculation of heat loads. Illustrates the advantages of heat load and water usage when using ice slurry mixtures. The study mainly builds on previous work. Makes use of the Willier approach to calculate heat loads.	[36]
58	Stinnette, J D De Souza, E Buchan, R.M	Establishing total airflow requirements for underground metal/non-metal mines with tier iv diesel equipment	Thesis / Dissertation	2013	Despite emission limits being lowered by US EPA Tier IV and EURO Stage 4 regulations, the minimum ventilation requirements cannot change	[104]
59	S. Bluhm*, R. Moreby†, F. von Glehn*, and C. Pascoe	Life-of-mine ventilation and refrigeration planning for resolution copper mine	Journal Article	2014	Investigated possible solution for addressing the high heat load scenario for a specific case study.	[105]
60	Wiley, S.C.	Optimization of the quantity of mines with ventilation-on-request for ventilating underground heated/refrigerated air required systems	Thesis / Dissertation	2015	The study aims to provide a detailed method for estimating mine heat loads through a developed solver. Method is labour intensive. Latent heat not accounted for resulting in constant air humidity. The case study was based on a mine which is considerably shallower than typical South African deep-level mines.	[52]
61	Anderson, R. De Souza, E.	Heat stress management in underground mines	Journal Article	2017	Heat monitoring program with heat management strategies. Engineering solutions to heat control. Relies on real-time monitoring equipment. Did not focus on the accuracy of simulation modelling. Based on swallow potash mine.	[11]
62	Lukonde, P.M. Chileshe. P.R.K.	Mapping for literature, conceptual and theoretical framework and methodology: case of hot deep mining ventilation engineering evaluation and design	Journal Article	2017	Highlights key findings from literature with regards to heat and heat flow in a mine. Discusses specific heat increase due to mechanisation of mining. Some of the findings look misleading with regards to low heat load contribution for auto-compression. Focus on new workings and not holistic mine heat load	[106]
63	Roghanchi, P. Kocsis, K.C Danko, G. Powel, A.	Underground climatic monitoring and climatic modelling: Are we missing something	Journal Article	2017	Looks at the role of continuous monitoring of key ventilation parameters and the use thereof in modelling software	[37]

APPENDIX B HEAT PRODUCTION GRAPHS

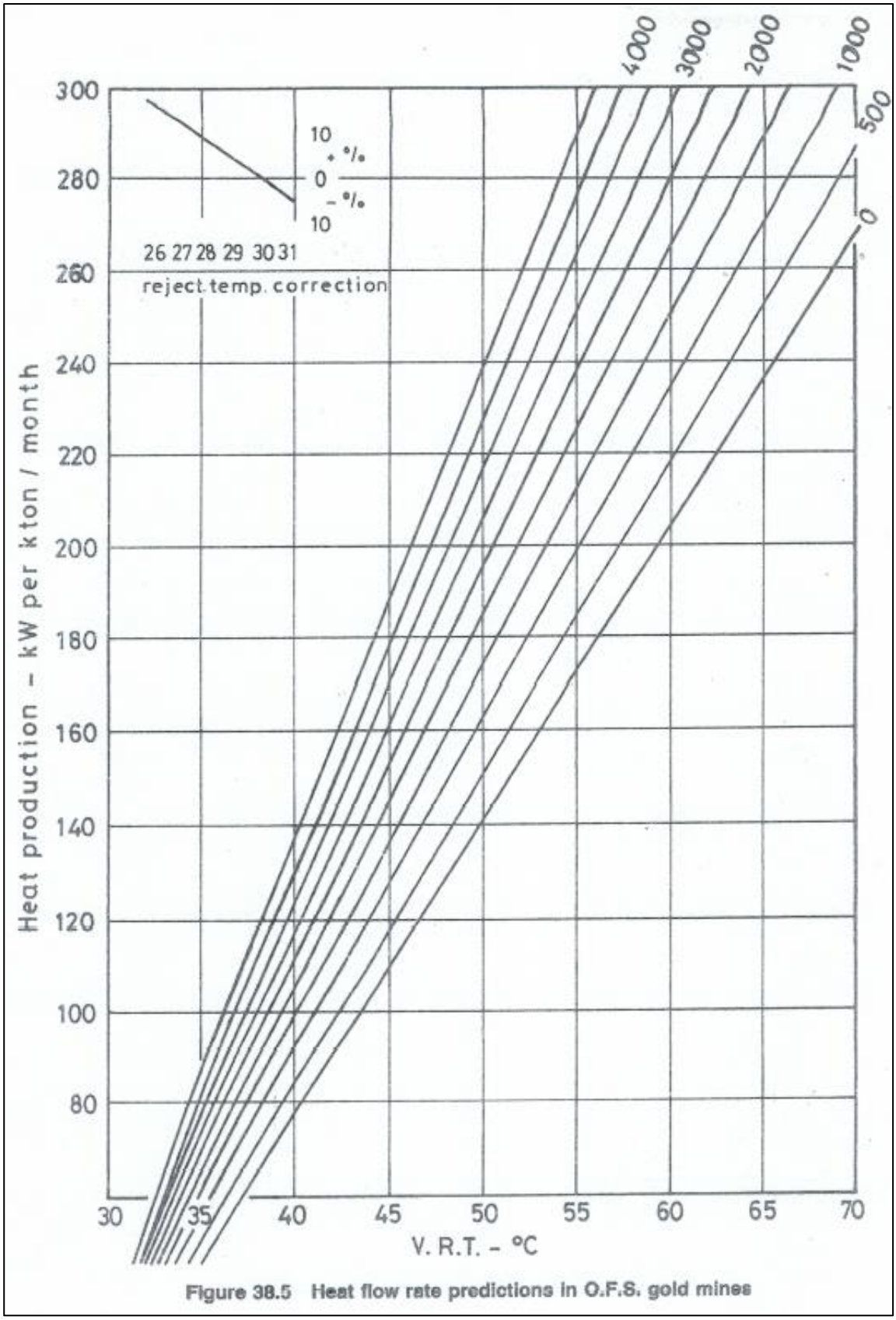

Figure B-1: Heat flow rate prediction in the Free State gold mines [23]

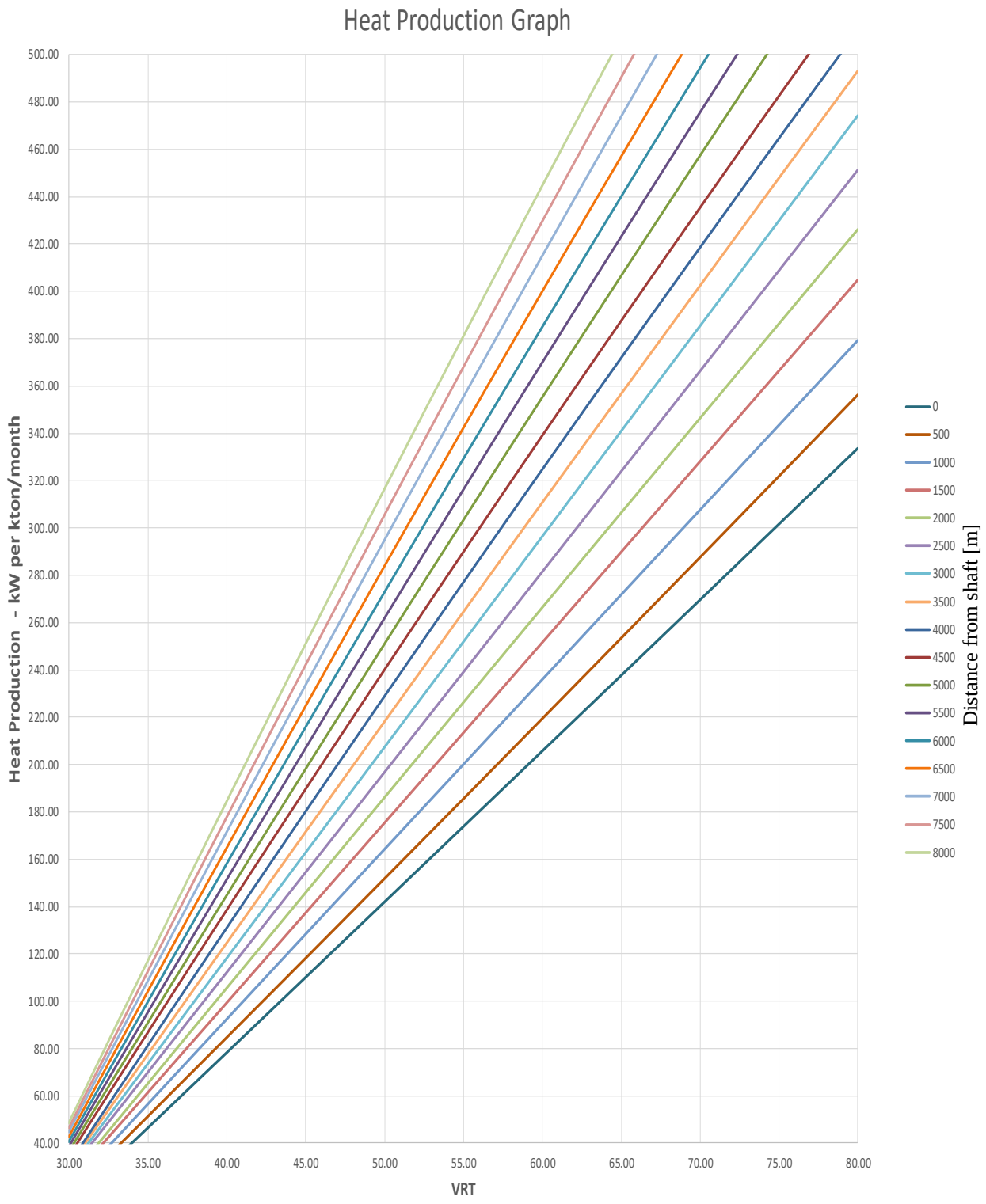

Figure B-2: Extrapolated heat production graph

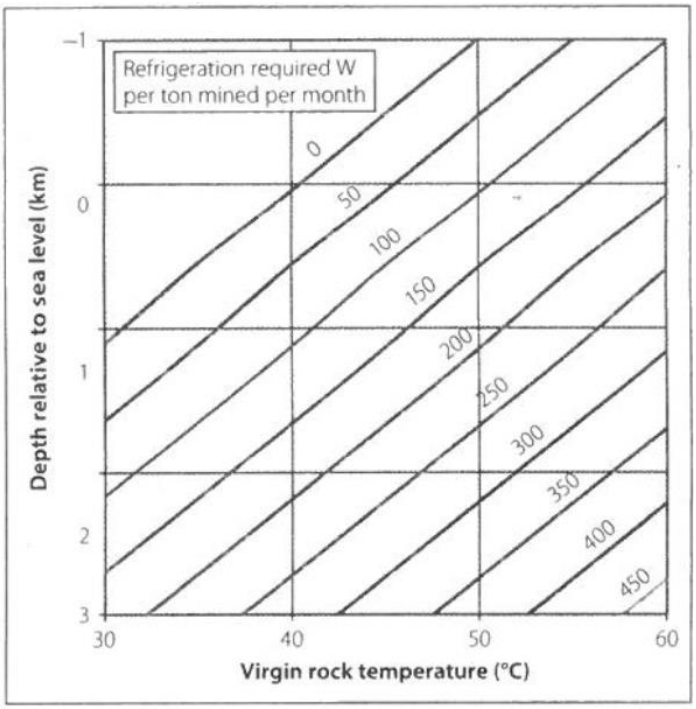

Figure B-3: Method for estimating refrigeration requirements [23]

APPENDIX C INPUTS FOR ENERGY BALANCE APPROACH

Table C-1: Energy balance heat load approach input parameters

No.	Parameter	Unit	Reference
3	Collar depth	m	Mine planning department, surveyors
4	Tonnes	kg	Mine planning department
7	Hoisting depth	m	Mine planning department, surveyors
8	Average tip height	m	Mine planning department, surveyors
9	Average mining depth	m	Mine planning department, surveyors
10	Conveyor start depth	m	Mine planning department, surveyors
11	Conveyor end depth	m	Mine planning department, surveyors
16	Mean mining depth VRT	C	Mine planning department
17	Total airflow downcasted	kg/s	Mine ventilation department, surveys
19	Dry-Bulb Temperature (Surface)	C	Weather station, surveys
20	Wet-Bulb Temperature (Surface)	C	Weather station, surveys
21	Barometric Pressure (Surface)	kPa	Weather station, surveys
22	Airflow through surface BAC	kg/s	Mine ventilation department, surveys
23	Surface BAC duty	kW	Mine ventilation department, surveys
24	Dry-Bulb Temperature (Surface BAC)	C	The engineering department, surveys
25	Wet-Bulb Temperature (Surface BAC)	C	The engineering department, surveys
26	Barometric Pressure (Surface BAC)	kPa	The engineering department, surveys
27	Dry-Bulb Temperature (Reject)	C	Mine ventilation department, surveys
28	Wet-Bulb Temperature (Reject)	C	Mine ventilation department, surveys
29	Barometric Pressure (Reject)	kPa	Mine ventilation department, surveys
30	Reject depth	m	Mine planning department
31	Dry-Bulb Temperature (Reject Goal)	C	Mine ventilation department, surveys
32	Wet-Bulb Temperature (Reject Goal)	C	Mine ventilation department, surveys
33	Surface FP evaporator duty	kW	The engineering department, surveys, SCADA
40	Underground FP evaporator duty	kW	The engineering department, surveys, SCADA
41	Underground motor power	kW	The engineering department, surveys
43	Average monthly diesel consumption	ℓ	The engineering department, surveys
44	Diesel utilisation	H	Engineering department, surveys
45	Average electric load underground	kW	The engineering department, surveys
46	Water pumped to surface	ℓ/s	The engineering department, surveys, SCADA
47	Water temperature in	C	The engineering department, surveys, SCADA
48	Water temperature out	C	The engineering department, surveys, SCADA

49	Employees (Miners)	-	Human resources
50	Average metabolic heat rate	W	Literature
51	Explosives used	kg/monthly	Mine planning
53	Rock density	kg/m3	Mine rock engineers
54	Fissure flow	l/s	Mining department, SCADA
55	Fissure water inlet temperature	C	Mining department, surveys
56	Fissure water outlet temperature	C	Mining department, surveys
58	Pumping depth	2301	Mine planning department, surveyors

APPENDIX D MODELLING FUNDAMANETALS

Heat flux calculation procedure for dry surfaces [14]

Inputs:

- Airway dimensions $[m]$
- Coefficient of friction $f\ \left(=\ Atkinsons\ friction\frac{factor}{0.6}\right)$
- Age of airway $t\ (seconds)$
- Airflow $Q\ [m^3/s]$
- Mean dry-bulb temperature θ_d [°C]
- Mean wet-bulb temperature θ_w [°C]
- Mean barometric pressure $[kPa]$
- Rock thermal conductivity $k_r\ [W/(m°C])$
- Rock density $\rho_r\ [kg/(m^3])$
- Rock specific heat $C_r\ [J/(kg°C])$
- Rock diffusivity $\alpha_r\ [m^2/(s])$
- Virgin rock temperature VRT [°C]
- Thermal conductivity of air $k_a\ [W/(m°C])$

Outputs:

1. Basic calculation
   - 1.1. Airway dimensions $A\ [m^2]$
   - 1.2. Perimeter of airway $per\ [m]$
   - 1.3. Hydraulic mean diameter $d_h = 4A/per\ \ [m]$
   - 1.4. Effective radius $r_a = \frac{per}{2\pi}\ [m]$
   - 1.5. Reynolds number $R_e\ [-]$
   - 1.6. Moisture content of air $X\ \left[\frac{kg}{per}kg\ dry\ air\right]$
   - 1.7. Mean radiation path length $L\ [m]$
2. Nusselt number $N_u = \frac{0.35fR_e}{\frac{1+1.592\left(15.217fR_e{}^{0.2}-1\right)}{R_e{}^{0.125}}}$
3. Determine heat transfer coefficient
   - 3.1. Convective coefficient $h_c = k_a\frac{N_u}{d_h}$
   - 3.2. Radiative coefficient $h_r = 22.68 \times 10^{-8}(273.15\ +\ \theta_d)^3\ \left[\frac{W}{m^2°C}\right]$
   - 3.3. Absortion fraction $a_b = 0.104\ln(147XL)\ [-]$
   - 3.4. Overall heat transfer coefficient $h = h_c + a_b h_r\ \left[\frac{W}{m^2°C}\right]$
4. Biot number $B = hr_a/k_r\ \ [-]$
5. Fourier number $F_0 =\ \alpha_r t/r_a{}^2[-]$
6. Temperature gradient G
7. Heat flux $q = h\frac{G}{B(VRT-\theta_d)}$
8. Heat energy $\frac{q\times per\times airway\ length}{1000}$

Heat flux calculation procedure for wet surfaces [14]

Inputs:

- Airway dimensions $[m]$
- Coefficient of friction $f\ \left(=\ Atkinsons\ friction\frac{factor}{0.6}\right)$
- Age of airway $t\ (seconds)$
- Airflow $Q\ [m^3/s]$
- Mean dry-bulb temperature θ_d [°C]
- Mean wet-bulb temperature θ_w [°C]
- Mean barometric pressure $P\ [kPa]$
- Rock thermal conductivity $k_r\ [W/(m°C])$
- Rock density $\rho_r\ [kg/(m^3])$
- Rock specific heat $C_r\ [J/(kg°C])$
- Rock diffusivity $\alpha_r\ [m^2/(s])$
- Virgin rock temperature VRT [°C]
- Thermal conductivity of air $k_a\ [W/(m°C])$
- Wet surface temperature θ_{ws} [°C]

Outputs:

2. Basic calculation
   - 8.1. Airway dimensions $A\ [m^2]$
   - 8.2. Perimeter of airway $per\ [m]$
   - 8.3. Hydraulic mean diameter $d_h = 4A/per\ [m]$
   - 8.4. Effective radius $r_a = \frac{per}{2\pi}\ [m]$
   - 8.5. Reynolds number $R_e\ [-]$
   - 8.6. Moisture content of air $X\ \left[\frac{kg}{per}kg\ dry\ air\right]$
   - 8.7. Mean radiation path length $L\ [m]$
9. Nusselt number $N_u = \frac{0.35fR_e}{\frac{1+1.592\left(15.217fR_e{}^{0.2}-1\right)}{R_e{}^{0.125}}}$
10. Determine heat transfer coefficient
    - 10.1. Convective coefficient $h_c = k_a\frac{N_u}{d_h}$
    - 10.2. Radiative coefficient $h_r = 22.68\times10^{-8}(273.15\ +\ \theta_d)^3\ \left[\frac{W}{m^{2\circ}C}\right]$
    - 10.3. Absorption fraction $a_b = 0.104\ln(147XL)\ [-]$
    - 10.4. Overall heat transfer coefficient $h = h_c + a_b h_r\ \left[\frac{W}{m^{2\circ}C}\right]$
11. Biot number $B = hr_a/k_r\ [-]$
12. Fourier number $F_0 =\ \alpha_r t/r_a{}^2[-]$
13. Temperature gradient G
14. Heat flux $q = h\frac{G}{B-G}(VRT-\theta_{ws})\ \left[W\frac{}{m}^2\right]$
15. Sensible heat $q_{sen}\ = h\ (\theta_{ws}\ -\ \theta_d)$

16. Latent heat $q_{lat} = 0.0007h\, L_{ws} \frac{e_{ws}-e}{P}$

16.1. Saturated vapour pressure for air $e_{sat,air} = 610.6 \exp\left(\frac{17.27\theta_w}{237.3+\theta_w}\right)\ [Pa]$

16.2. Saturated moisture content $X_{sat,air} = 0.622\ \left(\frac{e_{sat,air}}{P-e_{sat,air}}\right)\left[\frac{kg}{kg}dry\ air\right]$

16.3. Latent heat of evap at wet-bulb temperature $L_{w,air} = (2502.5 - 2.386\theta_w)1000\ \left[\frac{J}{kg}\right]$

16.4. Sigma heat $S_{air} = L_{w,air}X_{sat,air} + 1005\theta_w\ \left[\frac{J}{kg}dry\ air\right]$

16.5. Actual moisture content $X_{air} = S - 1005\theta_w/\left(\left[\!\left[(L]\!\right]_{w,air} + 1884(\theta_d - \theta_w)\right)\left[\frac{kg}{kg}dry\ air\right]$

16.6. Actual vapour pressure $e_{air} = PX/(0.622 + X)[Pa]$

16.7. Saturated vapour pressure for water $e_{ws} = 610.6 \exp\left(\frac{17.27\theta_{ws}}{237.3+\theta_{ws}}\right)[Pa]$

16.8. Latent heat of evap at θ_{ws} $L_{w,air} = (2502.5 - 2.386\theta_{ws})1000\ \left[\frac{J}{kg}\right]$

17. Heat balance $q = q_{sen} + q_L$

18. Error correction $E = q - (q_{sen} + q_L)\ [E \to 0]$

19. Heat energy $\frac{q \times per \times airway\ length}{1000}$

APPENDIX E CALCULATED ENERGY BALANCE RESULTS

Case study 2

Table E-1: Auto-compression (Case study 2)

Ref	Elevation entry [m]	Elevation exit [m]	Air mass flow [kg/s]	Enthalpy change [kJ/kg]	Auto-compression [kW]
A-D	0	1126.9	350	11	3861.3
D-E	1126.9	1218.9	330.7	0.9	297.8
E-F	1218.9	1279.9	326.2	0.6	194.8
F-G	1279.9	1462.9	322.7	1.8	578.1
G-H	1462.9	1523.9	313.6	0.6	187.2
H-I	1523.9	1584.9	306.2	0.6	182.9
I-J	1584.9	1645.9	300.8	0.6	179.6
J-K	1645.9	1766.9	294.8	1.2	349.2
K-L	1766.9	1827.9	284.8	0.6	170.1
M-N	1827.9	1919.9	248.8	0.9	224.1
N-O	1919.9	2010.9	205.8	0.9	183.3
O-P	2010.9	2102.9	191.3	0.9	172.3
P-Q	2102.9	2163.9	138.3	0.6	82.6
Q-R	2163.9	2224.9	123.8	0.6	73.9
R-S	2224.9	2285.9	74.8	0.6	44.7
Total					**6782**

Table E-2: Potential gain from electrical equipment (Case study 2)

Parameter	Amount [kg/s]	Height gain [m]	Potential energy gain [kW]
Water pumped to the surface	27.4	2301	630
Rock transported on conveyor	8	396	29
Total			**659**

Table E-3: Equipment to be excluded from effective electrical heat load (Case study 2)

Electric equipment	Design duty [kW]	Qty.	Utilisation [h]	Total design duty [kW]	Duty @ utilisation [kW]
Mining fans (75 kW)	75	8	24	600	600
Mining fans (45 kW)	45	2	24	90	90
FP Motors	732	2	12	1464	673
Total					**1 363**

Table E-4: Effective electrical heat load (Case study 2)

Parameter	Value [kW]
Total electric load supplied	4376
Potential gain	659
Excluded equipment	1 363
Effective electrical heat load	**2 353**

Table E-5: Mechanised heat load (Case study 2)

Parameter	Unit	Value
Total diesel consumption	$\ell/month$	37
Calorific value of diesel	MJ/kg	45.6
Diesel density	kg/m^3	0.85
Daily average	kW	1576
Vapour ratio	-	5
Heat evaporation of water	kJ/kg	*2450*
Combustion efficiency	%	0.95
Multiplication factor	-	2
Latent heat of diesel	kW	9
Total mechanised heat load	$\boldsymbol{kW}$	**29.4**

Table E-6: Metabolic heat rate (Case study 2)

Parameter	Unit	Value
Employees	$[-]$	740
Average metabolic rate	$[W]$	0.25
Metabolic heat load	$[\boldsymbol{kW}]$	**185**

Table E-7: Explosives heat load (Case study 2)

Parameter	Unit	Value
Explosives used (Monthly)	$[kg]$	15 000
Heat produced per kilogram	$[MJ/kg]$	4030
Blast frequency	$[\boldsymbol{hours}]$	24
Explosives heat load	$[\boldsymbol{kW}]$	**23**

Table E-8: Rock properties used for simulation [14, 56, 57]

Parameter	Unit	Value
Predominant rock type	-	Quartzite
Rock density	kg/m^3	2756
Thermal conductivity	$W/m/℃$	6.2
Specific heat capacity	$J/kg/℃$	850
VRT gradient	℃	$19 + 14.6 * Depth/1000$

APPENDIX F SAJIE PUBLICATION

Mr. Diaan Nell:

Congratulations, your submission Optimising deep-level mine heat load profiles have now also been accepted for inclusion in the special edition of SAJIE (South African Journal of Industrial Engineering).

Reviewers could rate certain elements of your paper, and the average rating from all reviews were taken and ranked. The editor then did a final check for suitability. This paper satisfied the ranking cut-off as well as the SAJIE suitability check.

You need to confirm whether you would like this to appear in the special edition. It is expected that the special edition will appear at the end of November 2019.

The conditions are as follows:
1. You need to register, attend and present at the SAIIE Nexxxt conference - if not, your paper will be withdrawn from SAJIE.
2. You acknowledge that this paper is withdrawn from the conference proceedings. Your presentation will still appear in the program with a note to say that it will be published in the special edition.
3. The Organising Committee will reload your paper on your behalf in the SAJIE on-line system with a SAJIE30/3 identifier.
4. You do not have to pay submission fees but must pay the publication fees.
5. You need to support the technical editing process, because there are strict deadlines to get the special edition published end October or early November.

Please "Reply All" to this email confirming your decision so that the editorial team (Prof Corne Schutte and Stephan Snyman) will be copied.

Thank you and looking forward to your participation in this event and special edition.

Regards

Corne & Stephan

South African Journal of Industrial Engineering XXXX

INDUSTRY 4.0 ROLL-OUT STRATEGY FOR DYNAMIC MINE HEAT LOAD MANAGEMENT

D. Nell[1*#], E.H. Mathews[1] & P. Maré[1†]

ARTICLE INFO

Article details
Presented at the 30th annual conference of the Southern African Institute for Industrial Engineering (SAIIE), held from 30 September - 2 October 2019 in Port Elizabeth, South Africa

Available online XX

Contact details
* Corresponding author
dnell@rems2.com

Author affiliations
1 Faculty of Engineering, North-West University, CRCED-Pretoria, Pretoria, South Africa

\# Author was enrolled as a doctoral student at the North-West University's Centre for Research and Continued Engineering Development (CRCED) in Pretoria, South Africa

† Post-doctoral student at the North-West University's Centre for Research and Continued Engineering Development (CRCED) in Pretoria, South Africa

DOI
http://dx.doi.org/10.7166/XX-X-XXXX

ABSTRACT

Deep-level mining is under severe financial pressure from several unique challenges. One of these is maintaining acceptable underground temperatures for humans to work in while achieving demanding production targets. As mines regularly reach new depths, additional heat is added to the system, contributing to this problem. Accurate mine heat load studies are therefore required to ensure that heat sources are actively evaluated, managed, and mitigated through adequate cooling practices. However, present heat load models are based on design parameters that cater for worst-case scenarios. Most of these models are also based on outdated empirical data taken at a time when mining differed from the present. Industry 4.0 technologies provide potential optimisation benefits when integrated with new heat load models to ensure effective monitoring, and consequently dynamic management, of heat sources. The roll-out strategy presented in this article will serve as a real alternative to earlier and outdated heat load prediction models.

OPSOMMING

Diep goud myne is onder ernstige finansiële druk weens verskeie unieke uitdagings. Een daarvan is die handhawing van aanvaarbare ondergrondse temperature vir mense om in te werk, terwyl dit veeleisende produksieteikens najaag. Aangesien myne gereeld nuwe dieptes bereik, word additionele hitte bygevoeg tot die probleem. Daar is dus noukeurige studies oor myn hittelading nodig om te verseker dat hittebronne aktief geëvalueer, bestuur en aangespreek word deur voldoende verkoelingspraktyke. Huidige modelle vir hittelas studies is egter gebaseer op ontwerp parameters wat voorsiening maak vir die slegste situasie. Die meeste van hierdie modelle is ook gebaseer op verouderde empiriese data wat wat verskil van huidige mynbou praktyke. "Industry 4.0"-tegnologieë bied potensiële optimeringsvoordele wanneer dit geïntegreer word met hittelas modelle. Dit verseker effektiewe monitering en gevolglik dinamiese bestuur van hittebronne. Die uitrolstrategie wat in hierdie artikel aangebied word, dien as 'n werklike alternatief vir vorige verouderde hittelas modelle.

1 INTRODUCTION

South Africa's gold mining industry is under severe pressure, resulting in a declining production trend, as shown in Figure 1. This decline in production leads to reduced revenue, causing substantial strain on the country's economy, and negatively impacts various downstream activities.

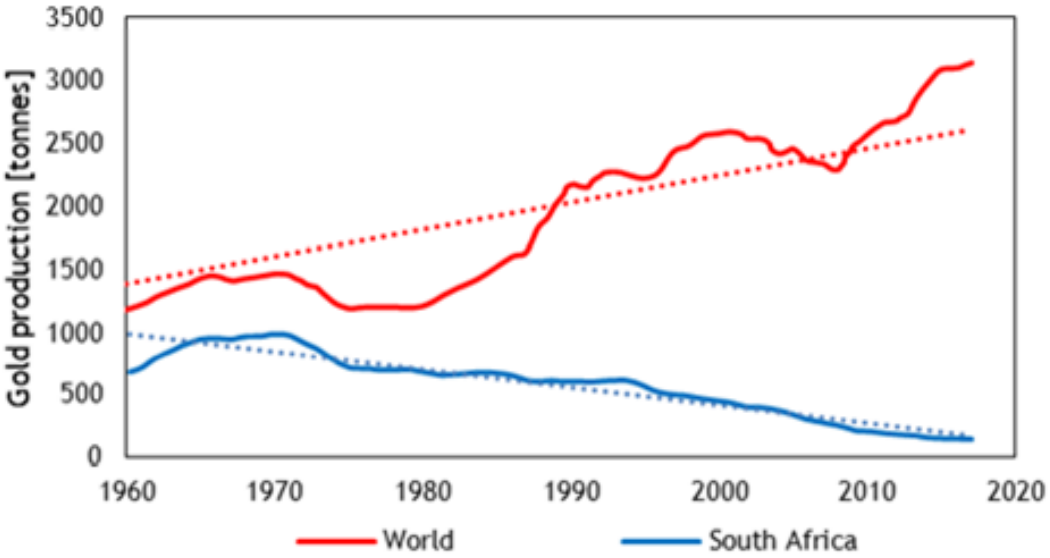

Figure 1: Local vs global gold production since 1960 [1]

Despite this negative climate facing the industry, a considerable number of gold ore deposits are still available in South Africa [2]. Figure 2 illustrates that South Africa still holds the number three ranking in mineable gold reserves, which highlights the role yet to be played by this struggling industry.

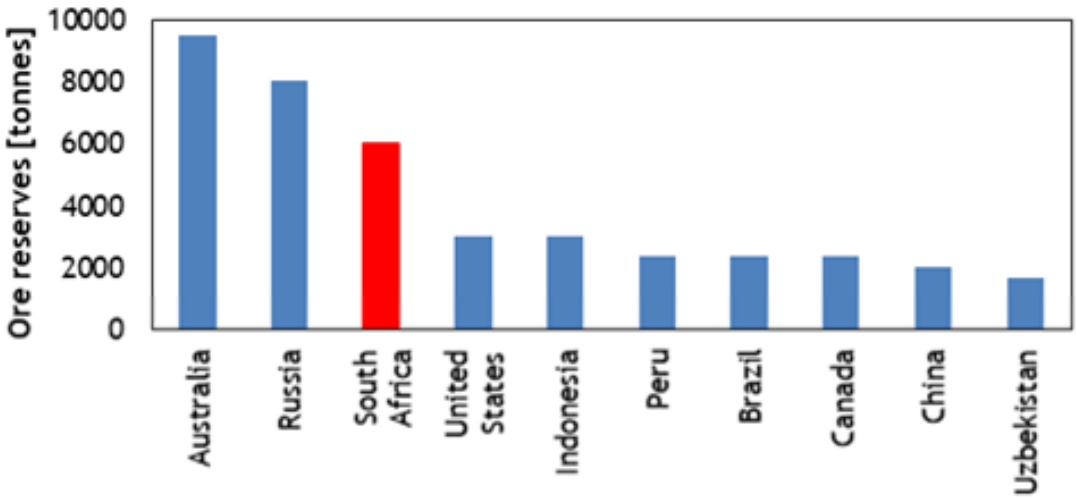

Figure 2: Gold ore reserves per country [2]

The South African gold industry is unfortunately strained by a variety of challenges, ranging from technical to socio-economic. One of these challenges is the increasing depth of South African gold mines, which are among the deepest in the world. These increased depths lead to new challenges that directly impact operational efficiency [3].

One such example is that of increased cases of environmental conditions that exceed legal limits and that lead to a direct loss of production [4, 5]. Ensuring that adequate cooling is supplied and used becomes a daily task in most of these mines.

To address and mitigate the rise in heat, heat load studies are performed to ensure that enough cooling is supplied to all active workings and planned workings [6]. At most mining operations these heat load studies are static in nature, and are conducted on an annual basis [7]. These studies are then used during the strategic life-of-mine planning to cater for any required capital expenditure on cooling requirements [6].

In an article issued by Deloitte [8] and in a case study performed on a uranium mine [9], it is clear that, with Industry 4.0 on the horizon, the South African mining industry is yet to discover how this new technological front will form part of its day-to-day operations. Facing many social challenges, the adoption of this new technology needs to be a guided process in which the value is realised down to the level of the miner. This will ensure that these technological advances serve as a real alternative to earlier and outdated approaches.

To guide this integration process of new technological advances, a model tailored for the mining industry with regard to ventilation needs to be implemented [10]. One such approach will be that of a data-information-knowledge-wisdom (DIKW) model, as illustrated in Figure 3.

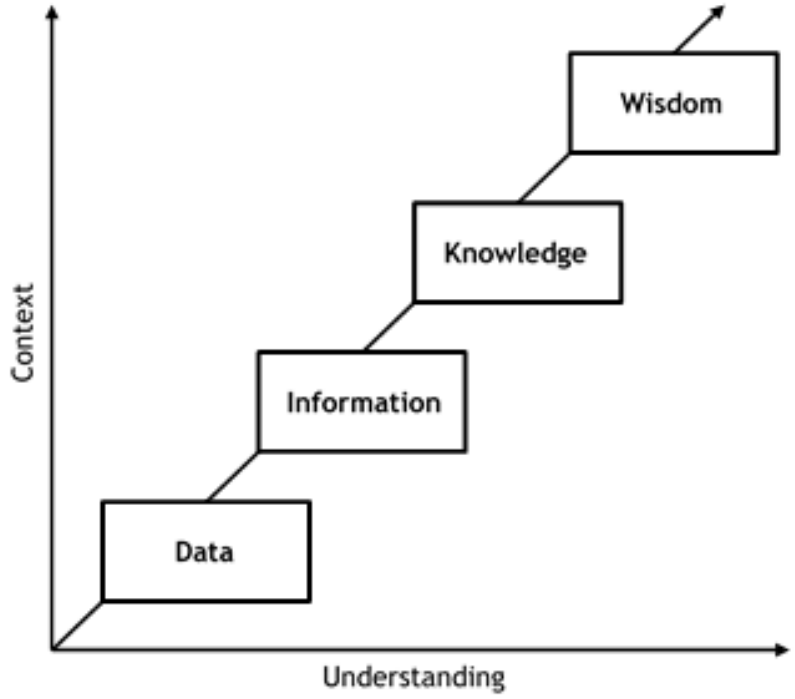

Figure 3: DIKW model [11, 12]

Figure 3 highlights that, to understand fully and appreciate the complete context of a problem, data needs to be translated into wisdom, which will deliver actionable steps to address the problem.

In a study conducted by Pretorius *et al*. [10], it was proven that significant improvements were realised by implementing an effective DIKW reporting platform on the cooling circuit of a mine. In much the same fashion, substantial benefits can be realised in understanding and reporting on daily heat sources to allow management to have an improved understanding of the nature of the heat sources and how to mitigate their effects.

The methodology in the next section will elaborate on how this model can be used as a roll-out strategy for the mining industry.

2 METHODOLOGY

The methodology focused on implementing the DIKW model with the aim of obtaining wisdom from the system that can lead to clear and actionable daily tasks. The method is therefore divided into the four pillars of the DIKW model, highlighted in Figure 3 [12].

2.1 Data

A wide variety of technologies is available on the market that is specifically designed to monitor/analyse the ventilation network of a complex system such as a mine. These technologies assist to monitor the system continuously, leading to an improved understanding of how various sub-systems interact with one another and which systems are sensitive to specific changes.
To understand where these technologies need to be implemented, it is important first to understand the basic ventilation network layout of a mine. Figure 4 illustrates such a layout, indicating the location of bulk air coolers (BACs) and return airways (RAWs).

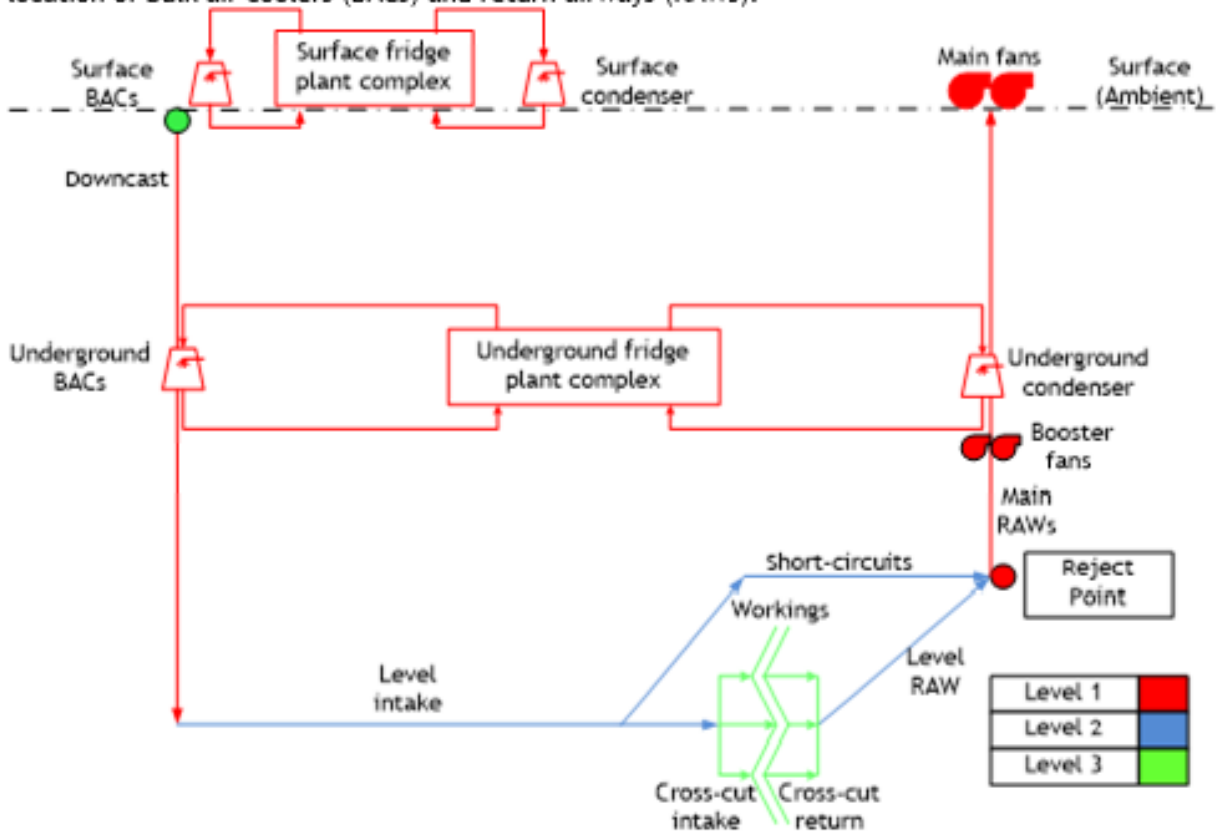

Figure 4: Basic mine ventilation flow diagram [13]

From Figure 4 it is evident that numerous components play a role in the ventilation network of a mine. The figure also shows that the heat pickup from the shaft inlet (green dot) to the point of reject (red dot) is essentially the heat experienced by the employees in the working area (also known as 'stopes').

Collecting data at different levels of detail for the various components will lead to improved insight. Monitoring these components will enable effective daily network analysis. These various levels of detail are summarised below in Table 1, and illustrated in Figure 4 above.

Table 1: Data acquisition detail level

Level	Description	Data Points
Level 1	Aims at holistically evaluating the mine. It gives valuable insight into global problems and highlights system constraints, such as inadequate cooling infrastructure. This data level approach can, therefore, be implemented to verify that the current infrastructure is adequate. This will also give valuable insight into the thermodynamic damping effect (thermal flywheel) and the expected response rate of such damping.	Ambient air conditions, fridge plants, BACs, main return airway, intakes airways and main fans

Level 2	Focuses on specific mining levels. This approach is specifically useful to determine how the intensity of mining processes is distributed, and where additional infrastructure needs to be introduced. Applying this level of data collection will highlight places with sub-standard supply conditions.	Level returns, level intakes, level-specific cooling
Level 3	Focuses on specific workplaces and gives valuable insight into daily activities and task concentration. This also assists to monitor the efficiency of ventilation appliances.	Cross-cut intakes/return airways, fridge plants, mobile coolers, etc.

At each of the mentioned data points, forms of energy need to be measured as they cross the specific boundary. In most instances, the main form of energy will be heat transported in the air, and it is crucial that the psychrometric properties of the air are measured [14]. In instances where heat is transferred from boundaries other than air (e.g., return water from the BAC), the energy content needs to be monitored.
In most instances, mines implement supervisory control and data acquisition (SCADA) systems without using such systems to their full potential [10]. Ideally, having a mine comply with all three of these levels will enable a precise heat source breakdown, and cater for the specific needs at each working section. However, implementing such a system can be a costly and timeous undertaking, and should rather be phased in gradually.

In cases where such an instrumentation roll-out is restricted by limited capital, key points can be instrumented and used in conjunction with dynamic thermal modelling software [13]. These models bridge the gap between the unknown and the immeasurable and give valuable insight into daily operational constraints.

As part of this phase-in-plan, it should also be taken into account that, as the level of detail increases, the demand for maintaining and implementing such a system will also increase. Consequently, the required and dedicated manpower should also be allowed for.

2.2 Information

As indicated by the second step in the DIKW model, the acquired data needs to be translated into useful information. This is done using an energy balance for the specific levels by accounting for all the forms of energy. This balance will ensure that the energy content in the measurement boundary is accurately characterised. This step has been extensively researched in the past, and various heat load prediction models have been developed [13, 14].

In most instances, mines in South Africa are fairly well-established and, together with the availability of Industry 4.0 technology, these heat sources can be actively measured rather than predicted. Figure 5 elaborates on the various heat sources/sinks in the mining industry.

2.3 Knowledge

The daily heat load profile can be constructed automatically to reflect better the dynamic nature of the system. This profile will capture the spike in mining intensity as well as the effect of the ambient conditions.

This is achieved by identifying key performance indicators (KPIs) and translating these parameters into a daily automated reporting system. All relevant role-players receive these reports and can action tasks based on dynamic system changes. These KPIs will include:

- System resistance curves of the key fan systems to assist in monitoring changes
- Fan use and mechanical condition monitoring
- Air properties of level intakes/returns (quantity and quality)
- Heat load component breakdown to monitor changes in components, such as mechanised equipment, geothermal heat exposure, etc.
- Dynamic heat load balance to track supplied cooling compared with the heat load

2.4 Wisdom

The final step is to translate knowledge into actionable wisdom. The derived knowledge will enable wisdom to be applied to the system and the interdependencies of the system to be understood. This will entail some of the following:

- The dynamic heat load profile can be used to structure the planned maintenance of the refrigeration circuits to ensure that the required cooling is always supplied while maintaining infrastructure.
- Planning can be optimised by adding the required infrastructure to address a cooling shortfall and so to achieve the planned reject temperature (return temperature from the workings). The capital and operating costs involved for such infrastructure can be accurately determined from the cooling shortfall to optimise costs.
- From the dynamic heat load profile, the current cooling infrastructure can also be planned to advance alongside mining activity to prevent a situation where mining exceeds the supply scope of the refrigeration system.

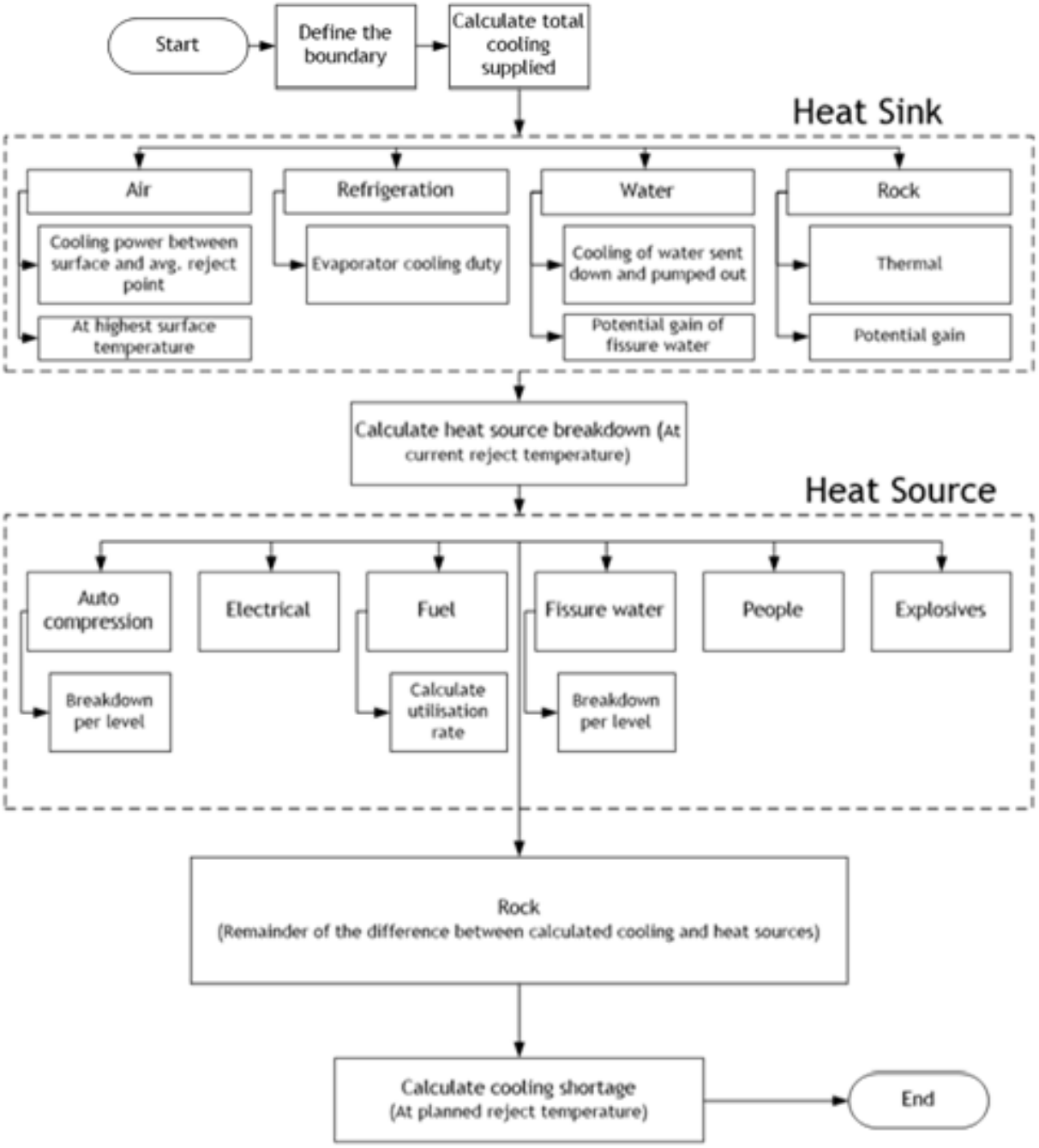

Figure 5: Heat load energy balance approach [14-16]

- The profiles will give insight into over-concentrated mining activity and assist the manager in distributing these activities more effectively, leading to reduced concentration-induced heat spikes throughout the mine.
- Problem identification will be accelerated greatly through active monitoring. In cases where fall-of-ground, ventilation appliance damage, or any other form of ventilation alteration occurs, the daily monitoring will enable a quick response to these occurrences.

The system architecture described will form the backbone of implementing a ventilation-on-demand system. This will be the final optimisation step in the mine of the future to ensure that localised mining begins at optimal efficiency levels.

3 RESULTS & DISCUSSION

The mine under investigation has partially adopted Industry 4.0 technologies with the aim of monitoring at a level similar to that of level 1, as discussed in Table 1. The results were therefore constructed through recorded data and audited data that were translated into an automatic report that was generated daily. The report could then be sent to all involved parties to inform them of any key system changes. The main findings are shared below, based on the holistic energy balance approach.

Figure 6 illustrates the daily heat load profile and the supplied cooling. This is illustrated at the current reject temperature of 32.5°C wet-bulb.

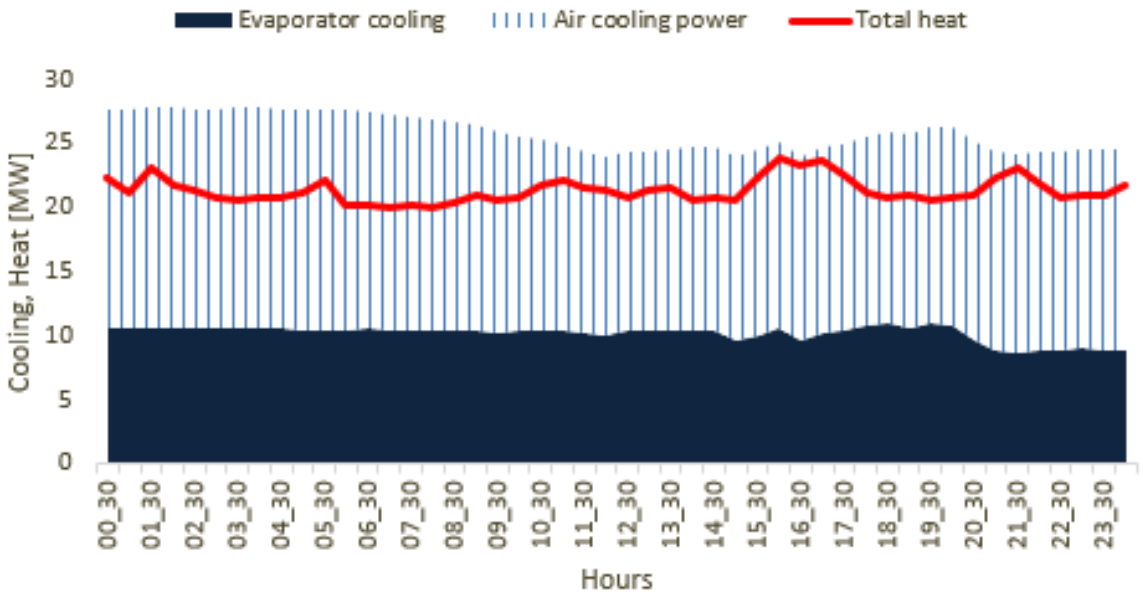

Figure 6: Dynamic heat load – current conditions

From Figure 6 it is evident that enough cooling is supplied for the calculated heat load. However, the mine used for this case study is extremely hot. This serves as a first level indication that, although the secondary cooling infrastructure might be sufficient, large ventilation system inefficiencies exist that need to be investigated.

The next step was plotting the heat load breakdown for the day. This breakdown of all the heat sources and the supplied cooling is monitored and automatically generated. Figure 7 illustrates this breakdown.

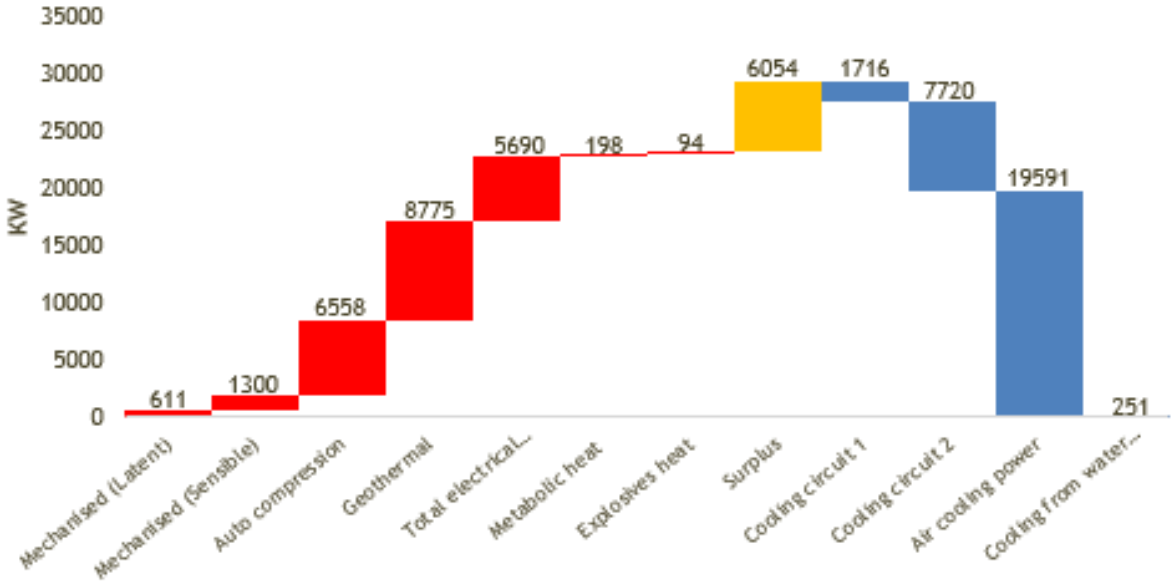

Figure 7: Dynamic heat load breakdown

In Figure 7 the breakdown of each source can be seen and compared on a daily basis to evaluate system changes. The surplus cooling supplied can be interpreted as the system inefficiency, which amounts to about 70 per cent of supplied cooling. This inefficiency consists of a combination of air leakages, or the positional inefficiency of secondary cooling units.

Monitoring equipment was also fitted to crucial equipment to indicate any system changes that might give rise to a change in the mine's heat load. Figure 8 illustrates the system characteristic curve of the surface fan.

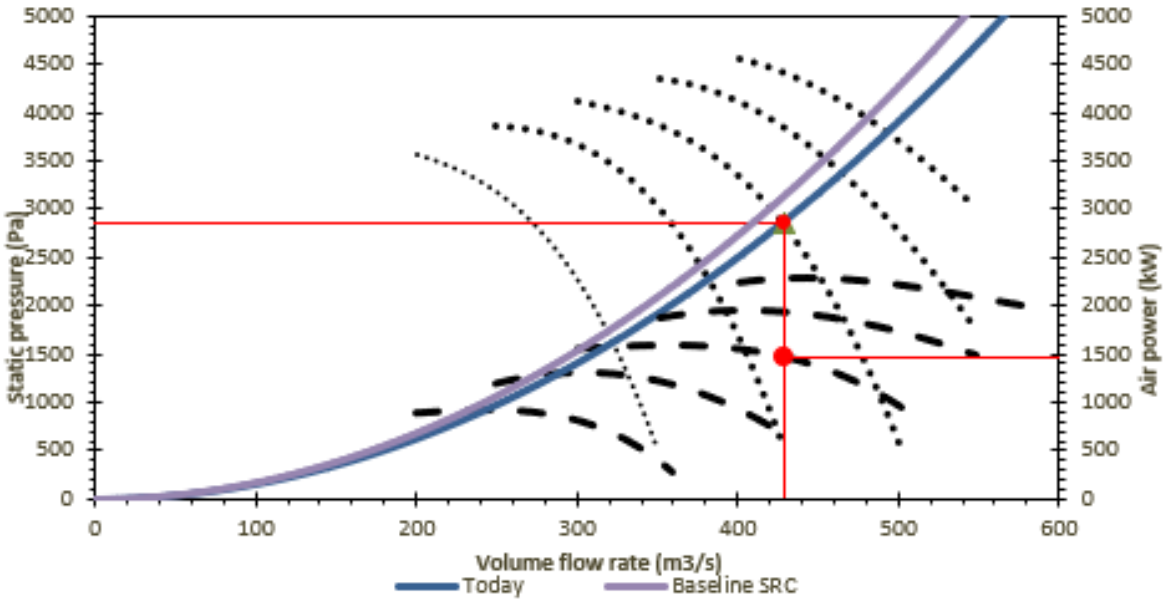

Figure 8: Dynamic surface fan system characteristic curve

Monitoring key infrastructure through the information shown in Figure 8 allows the ventilation engineer to understand better the performance of such components, and to detect and quantify any changes occurring in the system. The resistance improvement was the result of key system changes made; these can be seen in Figure 8 by the movement of the blue system resistance line.

Currently, Industry 4.0 technology is still being phased in, and level 2 and level 3 data are planned for the new financial year, which will enable evaluation in more detail. This will highlight

problematic areas and give valuable insight into the dynamic nature of the system and the various interdependencies.

4 CONCLUSION

Introducing Industry 4.0 technology to mine ventilation will greatly assist the evaluation of the dynamic nature of mines' thermodynamics. It is important, however, that this roll-out is planned and structured in accordance with a DIKW model approach, which has proven in the past to have substantial benefits.

From this approach, the key components of a mine – such as various heat sources – can be easily and frequently evaluated. This will lead to an improved understanding of such heat sources, and whether cooling strategies are effectively applied.

This study has highlighted the need for the use of Industry 4.0 technology to monitor heat load and has illustrated that data can be translated into wisdom by evaluating the dynamic nature of the daily heat load profiles.

REFERENCES

[1] Chamber of Mines 2017. Mine SA 2017 Facts & Figures Pocketbook, *Chamb. Mines*.
[2] Janisch, P. R. 1986. Gold in South Africa, *J. S. Afr. Ins. Min. Met.*, vol. 86, no. 8, pp. 273-316.
[3] Neingo, P. N. and Tholana, T. 2016. Trends in productivity in the South African gold mining industry, *J. South. African Inst. Min. Metall.*, vol. 116, no. 2, pp. 283-290.
[4] Section 54s cost SA mines R4.8bn in 2015, and 2016 may be worse - Miningmx, [Online]. Available: https://www.miningmx.com/opinion/columnists/27866-stoppages-lop-r4-8bn-off-2015-revenue-2016-worse/. [Accessed: 06-Jun-2019].
[5] Zondi, M. 2018. Mine Health and Safety Inspectorate - Annual Report 2017/2018.
[6] J. Burrows, R. Hemp, W. Holding, R. . S. 1982. Ventilation and occupational environment engineering in mines, .
[7] Moorecraft, H. 2019. Heat load mangement program. .
[8] Deloitte 2018. The Future of Mining in Africa. Navigating a Revolution., pp. 1-24.
[9] Sishi, M. N. 2017. Implementation of Industry 4 . 0 technologies in the mining industry - a case study By October 2017, no. October.
[10] Pretorius, J. G., Mathews, M. J., Maré, P., Kleingeld, M., and van Rensburg, J. 2019. Implementing a DIKW model on a deep mine cooling system, *Int. J. Min. Sci. Technol.*, vol. 29, no. 2, pp. 319-326.
[11] Rowley, J. 2007. The wisdom hierarchy: representations of the DIKW hierarchy, *J. Inf. Sci.*, vol. 33, no. 2, pp. 163-180.
[12] Ahsan, S. and Shah, A. Data, Information, Knowledge, Wisdom: A Doubly Linked Chain?
[13] McPherson, M. J. 1993. Subsurface ventilation systems, *Subsurf. Vent. Environ. Eng.*, pp. 91-133.
[14] Hemp, R. 1989. Sources of heat in mines, Ventilation and Occupational Environment Engineering in Mines, 3rd Edition, Prof. J.J.L. du Plessis, Mine Ventilation Society of Southg Africa, 2014, 407-439 .
[15] Duckworth, I. J., Mousset-Jones, P., and Advisor, T. 1993. A Heat Balance Study for a Mechanized Cut-and-Fill Stope.
[16] S.J. Bluhm; N.A. Alexander; T.W March; P. Bottomley; F. van Glehn 1986. The Measurement of heat load in Deep level Stope in Klerksdorp Goldfields, *Mine Vent. Soc. South Africa*, vol. 39, no. 10, pp. 129-140.

APPENDIX G Process Toolbox

Process toolbox (PTB) is a one-dimensional Computational Fluid Dynamics (CFD) code solving complex thermo-hydraulic networks. The code includes incompressible (water), compressible (air) and two-phase fluids (steam). Semi empirical component models are linked to pressure nodes/boundaries to form complex flow networks.

PTB enables the user to drag and drop a wide variety of components on a 3D Graphical User Interface (GUI) and allows the development of complex flow networks to scale. The user can easily navigate on the 3D interface. Figure G-1 illustrates the 3D platform as well as some of the available pre-configured components, which is easily accessible from the built-in library.

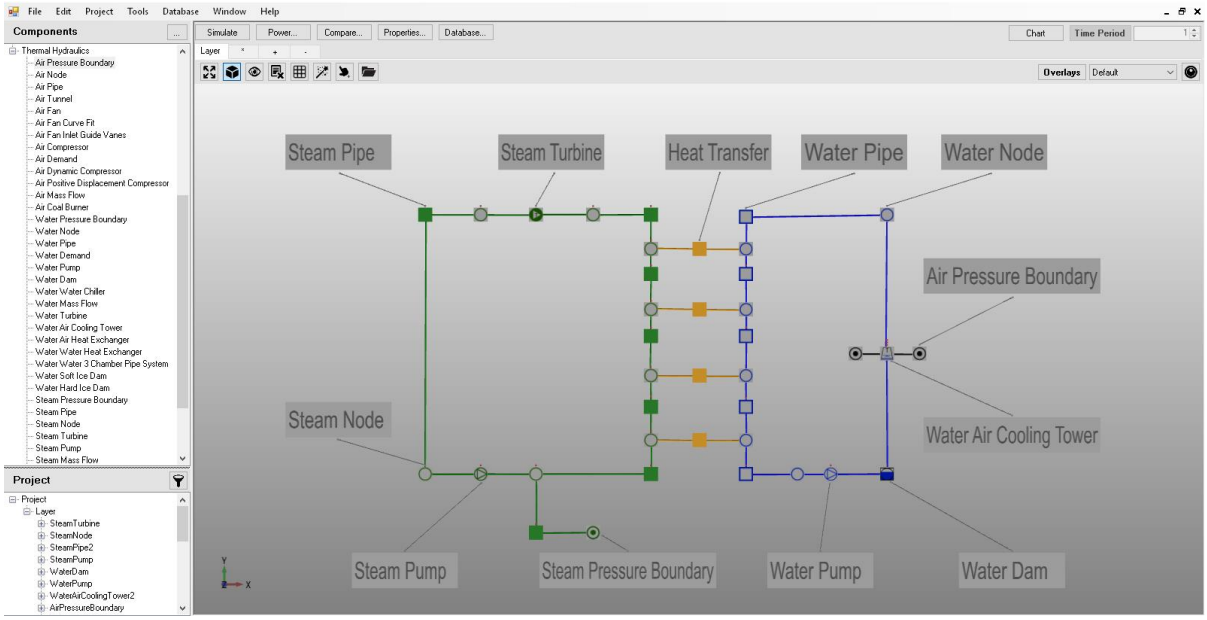

Figure G-1: PTB 3D Graphical User Interface

The code solves energy, mass and momentum for steady-state and transient solutions for any number of time periods and period size. Transient flow is solved with a quasi-steady-state semi-implicit algorithm where the pressure matrix is linearized to guarantee convergence for every time step (no iterations required). This method improves simulation stability and results in reduced simulation time. Energy is solved for each time step with transient explicit functions (no iterations and matrix solver required) that again improves stability and decrease simulation time.

All the thermo-hydraulic properties (pressure, temperature, enthalpy, quality) in the network are calculated in the pressure nodes and pressure boundaries. The component models are responsible for flow resistance, heat transfer, mass transfer and work calculations on the fluids. The component models receive fluid inlet conditions from the upstream nodes, execute the required calculations and transfer the outlet conditions to the downstream nodes.

Each component and node/boundary have a user input interface to specify its operational envelope and a user output interface to view the calculated outputs. Typical user interface inputs and outputs of the water pump component are displayed in the figures below.

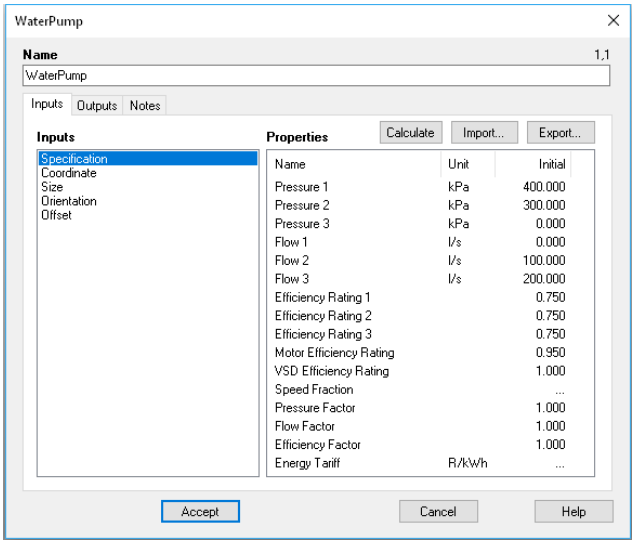

Figure 2: Water Pump User Input Interface

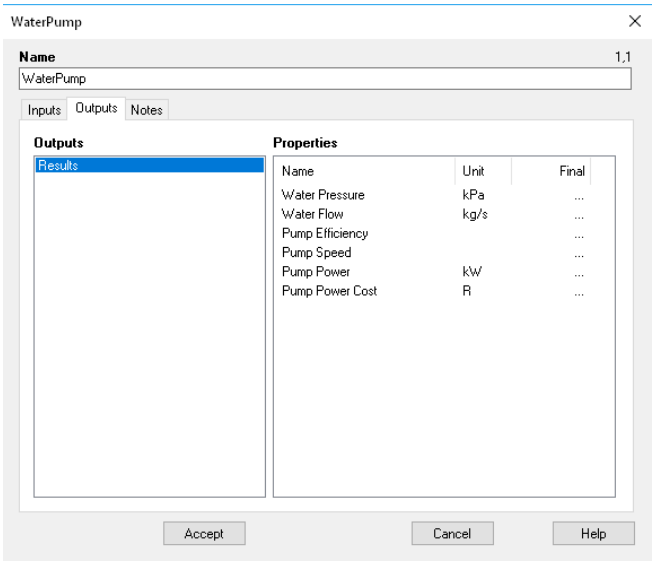

Figure 3: Water Pump User Output Interface

The code of all the component models are a combination of fundamental principles and empirical parameters. The empirical parameters taken from system measurements allows for more accurate component characterisation and therefore improved simulation results. All the component models utilise explicit functions, therefore no iterations are required during component calculations. This again improves the simulation stability and reduces simulation time.

The following component models are currently included in PTB:

Table G-1: Process ToolBox (PTB) - Available components

Air components	Water components	Water/Air Components	Steam Components	General Components
Air Pressure Boundary	Water Pressure Boundary	Water-Air Cooling Tower	Steam Pressure Boundary	PI Controller
Air Node	Water Node	Water-Air Heat Exchanger	Steam Node	Step Controller
Air Pipe	Water Pipe		Steam Pipe	Heat Transfer
Air Tunnel	Water Pump		Steam Pump	
Air Fan	Water Dam		Steam Turbine	
Air Compressor	Water Soft Ice Dam		Steam Mass Flow	
Air Demand	Water Hard Ice Dam			
Air Mass Flow	Water Chiller			
Air Coal Burner	Water Mass Flow			
	Water Turbine			
	Water-Water Heat Exchanger			
	Water 3CPS			

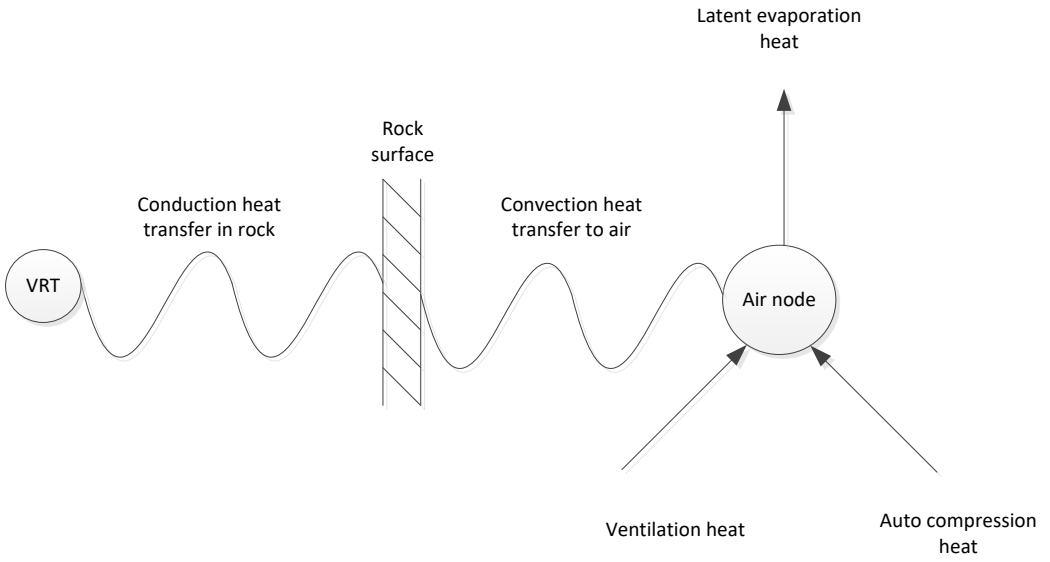

Figure G-2: PTB heat transfer solver schematic

The air tunnel component is discretised in 10 separate air nodes each solving for the parameters shown in Figure G-2 which illustrates one such air node. The conduction heat transfer coefficient is a function of the haulage age and the rock properties. The Dittus Boelter correlation is used to calculate the convective heat transfer coefficient [58]. An energy balance is then conducted to simultaneously solve for the air node temperature and rock surface temperature.

APPENDIX H Sensitivity analysis

Figure H-1 and Figure H-2 illustrates the sensitivity of the key parameters used for calculating the respective heat loads in case study one and case study 2. From these figures it is evident that the wet bulb temperature, place a significant role and should be taken with great care.

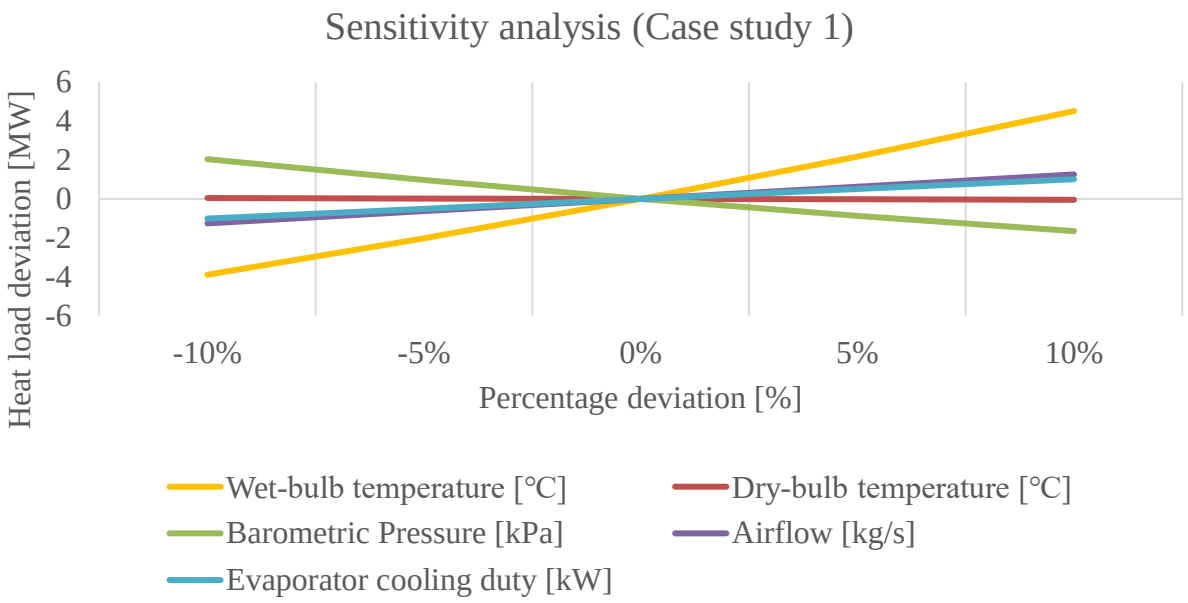

Figure H-1: Case study 1 sensitivity analysis

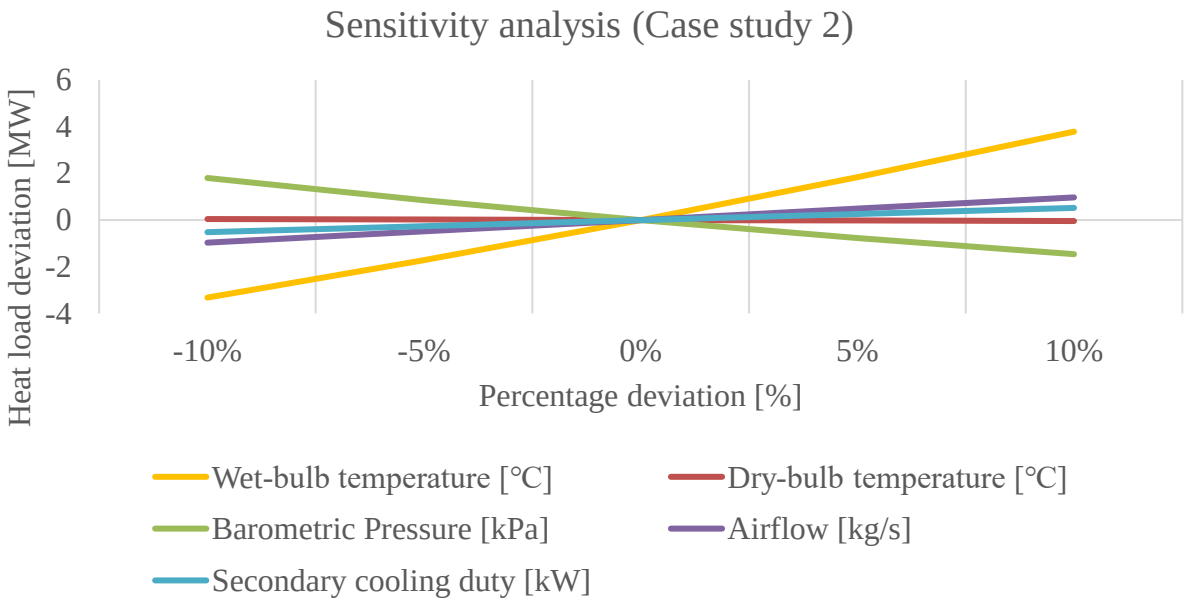

Figure H-2: Case study 2 sensitivity analysis

However, it is also noted that it would be highly unlike to make a wet bulb temperature reading error in excess of 3℃. To ensure that such errors are kept to a minimum, multiple readings should be taken and cross-referenced with other parties as was done in this study. Also, in the case of electronic monitoring devices, the accuracy should be frequently verified through manual readings and if required, calibrated accordingly.

From the methodologies discussed in this study, namely the energy balance approach and the well-known industry approach, similar measuring techniques are applied. Therefore, should such measurement errors occur it will impact the outcome of both the above-mentioned approaches.